

Polyolefin Elastomers: A Study on Crosslinking, Blends and Composites

Polyolefinové elastomery: studie síťování, směsí a kompozitů

Doctoral Dissertation

Submitted

by

Rajesh Theravalappil, M.Sc.

 Tomas Bata University in Zlín
Faculty of Technology

March 2012

*Thesis Submitted for Fulfillment of PhD Degree
In*

Doctoral study program: P2808 Chemistry and Materials Technology

2808V006 Technology of Macromolecular Compounds

Supervisor: Assoc. Prof. Petr Svoboda

CONTENTS

ABSTRACT	4
ABSTRAKT	6
ACKNOWLEDGEMENTS	8
LIST OF PUBLICATIONS	9
1. INTRODUCTION	
1.1 Thermoplastic elastomers (TPEs)	10
1.1.1 Polyethylene/poly (α -olefin) copolymers	14
1.2 Polymer blends	14
1.3 Conducting polymer composites (CPC)	16
1.3.1 Conduction mechanism and percolation theory	17
1.4 Crosslinking of polymers	19
1.4.1. Effects of crosslinking	20
2. OBJECTIVE OF THE THESIS AND BRIEF SUMMARY	21
3. CLOSING REMARKS	
3.1 Conclusions	24
3.2 Contribution to science and practice	25
3.3 Scope for future studies	25
4. REFERENCES	26
5. PAPER 1	32
6. PAPER 2	39
7. PAPER 3	65
8. PAPER 4	88
CURRICULUM VITAE	119

ABSTRACT

Thermoplastic elastomers (TPEs) are materials with processability of thermoplastics while possessing the elastic properties of conventional vulcanized elastomers. Polyolefin elastomers (POEs) prepared by the copolymerization of ethylene with various comonomers like propylene, butene, hexane and octene possess low density and considerably good elasticity. They are being used very widely in almost all fields that are touching the human life such as medical, electrical, electronics, automotive and personal care products. Ethylene-octene copolymer (EOC) is a member of POE group with excellent compatibility with most of other olefins and good processability together with very good elastic properties and high filler acceptance. Due to these attractive properties, EOC has been selected for our studies for modification through blending, composite preparation and crosslinking.

Blending of different polymers helps us to prepare new polymeric materials with favorable properties depending on our requirement. Polymer blends can simultaneously have many advantageous properties of different polymers like processability of thermoplastics and elastic property of an elastomer, through proper selection of composition. We have used EOC to improve the elastic properties of polypropylene (PP). It has been observed that with the incorporation of EOC, elasticity of PP has been improved considerably and the morphological studies of these blends also were very useful in understanding of achieved improvements. Through residual strain experiments, it has been observed that these blends have good elastic properties when the PP content is low (0-30 wt.%). Other mechanical properties of these blends also were studied.

Nowadays, conducting polymer composites (CPCs) receive increasing attention due to their importance in the electrical and electronics fields. CPCs of ethylene-octene copolymer using three different kinds of fillers (expandable graphite, carbon fibres (CF), multiwall carbon nanotubes (MWCNT) and their electrical and thermal conductivities along with their mechanical properties were evaluated. Percolation threshold for expandable graphite composites has been observed at 16 vol.% while it was at 8 vol.% for MWCNT and 5 vol.% for CF composites showing the importance of filler dimensions on percolation threshold. The same trend was visible in the case of thermal conductivity also. While being a conducting filler, above 40 wt.% level, expandable graphite acts as an eco-friendly halogen-free flame retardant also. Even at high filler loadings, shore-A hardness

values that denote the softness or rubbery nature of materials did not increase excessively. This is pointing towards the candidature of these composites as pressure or strain sensors. Electrical and thermal conductivities of composites with CF and MWCNT fillers were improved considerably even with low filler levels while their thermal stabilities were also increased. Apart from this, they even acted as reinforcing fillers as they helped in improving tensile modulus of composites considerably. These results strengthen the claim that CF and MWCNT fillers have multiple roles to act in their composites.

The process of cross-linking enables us to expand the application range (e.g. higher temperatures) of polymers. Peroxide crosslinking is economically favorable and has been widely used in the industry these days. Peroxide crosslinking of EOC has been carried out and creep and elastic properties at temperatures above EOC's melting temperature (T_m) has been analyzed. As the peroxide content increases, gel content which is a measure of crosslinking density was found to be increased. This improvement in extent of crosslinking was reflected in the increased creep resistance also. It was noticed that the crosslinked EOC has undergone increased creep flow at higher temperatures (120 and 200 °C) compared to 70 °C showing the remarkable effect of temperature on creep behavior. Stress also has shown a visible effect on creep as creep flow increased notably with stress from 0.077 to 0.210 MPa. Creep compliance slope values calculated from the creep compliance versus time curves showed a strong dependence on peroxide content and temperature at which creep experiment has been carried out. We could conclude that with increasing temperature, creep is more prominent especially at low peroxide levels. It was also noted that crosslink density has a major effect on storage modulus and $\tan(\delta)$ especially at high temperatures showing increased elasticity.

Key words:

Polyolefin elastomers, Blends, Elastic properties, Conducting fillers, Electrical and Thermal Conductivities, Peroxide Crosslinking, Mechanical Properties, Creep.

ABSTRAKT

Termoplastické elastomery (TPE) jsou materiály se zpracovatelností termoplastů, které mají elastické vlastnosti konvenčních vulkanizovaných elastomerů. Polyolefinové elastomery (POE) připravené kopolymerací etylenu s různými ko-monomery jako propylen, butylen, hexen a okten mají nízkou hustotu a značně dobrou elasticitu. Jsou využívány velmi široce téměř ve všech oblastech, které se dotýkají lidského života, jako např. lékařské, elektrické, elektronické, automobilové a produkty pro osobní péči. Etylen-oktenový kopolymer (EOC) je člen POE skupiny s vynikající kompatibilitou s většinou jiných olefinů a dobrou zpracovatelností spolu s velmi dobrými elastickými vlastnostmi a schopností být vysoce plněn. Díky těmto přitažlivým vlastnostem byl EOC vybrán pro naše studium pro modifikace mícháním, přípravou kompozitů a síťováním.

Mísení různých polymerů nám pomáhá připravit nové polymerní materiály s příznivými vlastnostmi závisujícími na našich požadavcích. Polymerní směsi mohou mít současně mnoho výhodných vlastností různých polymerů jako např. zpracovatelnost termoplastů a elastické vlastnosti elastomeru prostřednictvím vhodného výběru složení. Použili jsme EOC k vylepšení elastických vlastností polypropylenu (PP). Bylo pozorováno, že začleněním EOC do PP se elasticita PP značně zlepšila a studium morfologie těchto směsí bylo užitečné pro porozumění dosažených vylepšení. Za pomoci experimentů zkoumajících zbytkové protažení bylo zjištěno, že směsi měly dobré elastické vlastnosti, když byl obsah PP nízký (0-30 hm.%). Další mechanické vlastnosti těchto směsí byly také studovány.

V dnešní době získávají elektricky vodivé kompozity (CPC) rostoucí pozornost kvůli jejich důležitosti v oblastech elektrotechniky i elektroniky. Byly zkoumány elektrické a tepelné vodivosti a mechanické vlastnosti u vodivých kompozitů na bázi etylen-oktenového kopolymeru se třemi různými plnivy: rozvinutelný grafit, uhlíková vlákna (CF), uhlíkové nanotrubičky s mnoha stěnami (MWCNT). Perkolační práh u kompozitů s rozvinutelným grafitem byl pozorován přibližně pro obsah plniva 16 obj. %, zatímco pro MWCNT to bylo 8 obj. % a pro CF dokonce jen 5 obj. %, což ukazuje na důležitost rozměrů pro perkolační práh. Stejný trend byl viditelný v případě tepelné vodivosti. Rozvinutelný grafit má funkci elektricky vodivého plniva a zároveň nad úrovní 40 hm. % funguje také jako ekologicky přátelský retardér hoření, který neobsahuje halogeny. I při vysokém obsahu plniva se hodnoty Shore-A tvrdosti (které ukazují na měkkost nebo

kaučukovitost) příliš nezvýšily. Toto ukazuje na možnou kandidaturu těchto kompozitů jakožto tlakových nebo deformačních senzorů. Elektrická i tepelná vodivost kompozitů s CF a MWCNT plnivou byla výrazně zlepšena, a to dokonce i při nízkých úrovních plnění. Tepelná stabilita byla zlepšena také. Kromě toho tyto plniva účinkovaly jako ztužující plniva, protože značně pomohly ve zlepšení modulu pružnosti v tahu. Tyto výsledky posilují tvrzení, že CF a MWCNT plniva mají více rolí, které hrají v kompozitech.

Proces síťování nám umožňuje rozšířit rozsah uplatnění polymerů (např. pro vyšší teploty). Síťování peroxidy je ekonomicky výhodné a je v této době široce používáno v průmyslu. V této práci bylo provedeno peroxidové zesíťování EOC, a pak byly změřeny kríp a elastické vlastnosti nad teplotou tání (T_m) kopolymeru. S rostoucím obsahem peroxidu rostl i obsah gelu, který je měřítkem síťové hustoty. Toto zlepšení zesíťováním se odrazilo také ve zlepšené odolnosti proti krípu. Zesíťovaný EOC vykazoval vyšší kríp při vyšších teplotách (120 a 200 °C) ve srovnání s 70 °C, což ukazuje na významný vliv teploty na kríповé chování. Ukázalo se, že napětí má také značný vliv na kríp, když byl zaznamenán značně vyšší kríp při zvyšování napětí z 0,077 na 0,210 MPa. Hodnoty směrnice kríповé poddajnosti vypočítané z grafu závislosti kríповé poddajnosti na čase ukázaly silnou závislost na obsahu peroxidu a teplotě, při které byl kríповý experiment proveden. Můžeme učinit závěr, že s rostoucí teplotou je kríp výraznější zvláště pak při nízkých úrovních peroxidu. Bylo rovněž zaznamenáno, že hustota zesíťování má významný vliv na modul pružnosti a $\tan(\delta)$, zvláště za vyšších teplot, což ukazuje na vyšší elasticitu.

Klíčová slova:

Polyolefinové elastomery, směsi, elastické vlastnosti, vodivá plniva, elektrická a tepelná vodivost, síťování peroxidem, mechanické vlastnosti, kríp.

ACKNOWLEDGEMENTS

First and foremost, I express my sincere thanks to my supervisor *Associate Professor Petr Svoboda*, Department of Polymer Engineering, Faculty of Technology, Tomas Bata University in Zlin, Czech Republic, for giving me the opportunity to work with him and for his valuable guidance and constant support during the entire period of my stay in TBU.

I gratefully acknowledge Assoc. Prof. Jarmila Vilcakova for her advice and crucial contribution which helped me a lot to carry out some experiments. I am indebted to my colleagues, members of Faculty of Technology and other friends for their co-operation extended to me during my study. I take this opportunity to pay my gratitude to Mr. Pavol Priekala, Alpha Demoroom, TBU for his kind co-operation and technical support.

I would like to express my love and gratitude to my beloved wife, Mrs. Sameepa for her understanding and endless love, throughout the duration of my studies.

Lastly, I would like to thank my dearest mother, brother and other family members for all their love, encouragement and support in all my pursuits.

LIST OF PUBLICATIONS

1. Petr Svoboda, **Rajesh Theravalappil**, Dagmar Svobodova, Pavel Mokrejs, Karel Kolomaznik, Keisuke Mori, Toshiaki Ougizawa, Takashi Inoue; Elastic properties of polypropylene/ethylene-octene copolymer blends, *Polymer Testing*, Volume 29 (6), 2010, 742-748.
Impact Factor: 2.016
2. **Rajesh Theravalappil**, Petr Svoboda, Sameepa Poongavalappil and Dagmar Svobodova; Creep and dynamic mechanical analysis studies of peroxide cross-linked ethylene-octene copolymer (accepted for publication in *Macromolecular Materials and Engineering*). DOI: 10.1002/mame.201100289.
Impact Factor: 1.916
3. Petr Svoboda, **Rajesh Theravalappil**, Sameepa Poongavalappil, Jarmila Vilcakova, Dagmar Svobodova, Pavel Mokrejs, Antonin Blaha; A study on electrical and thermal conductivities of ethylene-octene copolymer/expandable graphite composites (accepted for publication in *Polymer Engineering & Science*). DOI 10.1002/pen.22192.
Impact Factor: 1.296
4. **Rajesh Theravalappil**, Petr Svoboda, Sameepa Poongavalappil, Jarmila Vilcakova, Dagmar Svobodova, Petr Slobodian, Robert Olejnik, Simona Mrkvickova; Multiple roles of multiwall carbon nanotubes (MWCNT) and carbon fibers (CF) in their composites with ethylene-octene copolymer (submitted to *Carbon* in January 2012).

1. INTRODUCTION

1.1 Thermoplastic elastomers (TPEs)

One class of materials that have high growth potential and applicability in the current polymer market is that of thermoplastic elastomers (TPEs). The rise of thermoplastic elastomers in the market was in the late 1950s, with the introduction of thermoplastic polyurethane (TPU). In 1965, the company Shell developed and introduced commercial styrene diene block copolymer, Kraton. In 1970s, commercial copolyester and blends of polypropylene (PP) and ethylene-propylene-diene monomer (EPDM) rubber gave a boost to the growth of this field. During this period, it was realized that TPEs would have a bright and promising future in both the rubber and the plastic industries. As a consequence of the extensive research efforts devoted toward their development and commercialization, the 1980s witnessed the growth of TPE to maturity.

TPEs can be defined as a class of polymers, which combine the service properties of elastomers with the processing properties of thermoplastics. TPEs consist of two structural units: (1) amorphous segment that is soft in nature and has a low glass-transition temperature (T_g) and (2) a crystalline and/or hard segment with high T_g that acts as physical cross-link for the soft segments. These two segments, i.e., soft and hard segments, must be thermodynamically incompatible to each other at service temperature to prevent the interpenetration of the segments. Therefore, a TPE possesses biphasic morphological structure. The hard segments that act as physical cross-links are thermally labile, and this allows TPEs to soften and flow under shear force at elevated temperature as in the case of true thermoplastics. TPEs bridge the gap between conventional rubbers and thermoplastics [1].

Thermoplastic elastomers possess hardness in between that of thermoset rubbers and hard thermoplastics.

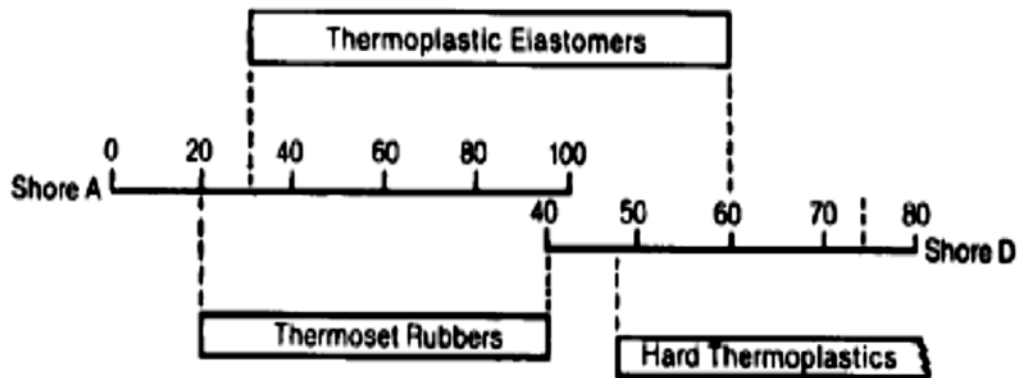


Figure 1.1 Hardness behavior of TPEs [2].

General classification of TPEs based on their chemistry and morphology is,

1. Block Copolymers
 - a. Styrenic block copolymers
 - b. Thermoplastic copolyesters (COPE)
 - c. Thermoplastic polyurethanes (TPU)
 - d. Thermoplastic polyamides (COPA)
2. Blends and elastomeric alloys
 - a. Elastomeric rubber-plastic blends
 - b. Thermoplastic vulcanizates (TPVs)
 - c. Melt processable rubber
3. Crystalline-amorphous block copolymers
4. Ionomers
 - a. Sulfonated-EPDM rubber (S-EPDM)
 - b. Zn or Na salt of ethylene acrylic acids
5. Miscellaneous

Thermoplastic elastomers can perform as a rubber material. They also have the ability to be reprocessed when heated above the melt transition temperature. A TPE has the behavior below the melt temperature of being elastic like a thermoset rubber. The source of this behavior varies with the chemistry and structure of the various TPE materials as will be discussed. This ability to be reprocessed addresses the recyclability limitation of thermoset rubbers, thus there is little scrap when processing thermoplastic elastomers. This gives TPEs an important economic advantage. Also unneeded TPE articles can be remelted and reprocessed to recover the scrap material. Normally this is done by grinding the articles to make a TPE crumb that is mixed with virgin TPE during processing. This TPE capability provides an important environmental impact, as well as an economic impact. The dual capability of elastomeric properties and recyclability are achieved using one of several approaches to prepare the TPE [1].

From the above-mentioned classes, we can broadly look into the morphology of some types of TPEs. In the case of a block copolymer, the rigid crystalline regions act as virtual crosslinks with the flexible rubbery blocks providing the overall flexibility of these copolymers. The rubber and plastic polymers need to be somewhat incompatible with each other so that separate phases are formed in the case of rubber/plastic blends. A TPV is a blend of thermoplastic with fully crosslinked, i.e., vulcanized, rubber. The thermoplastic is the continuous phase and the crosslinked rubber is a dispersed particulate phase. TPVs are prepared by dynamic vulcanization. A schematic representation of these TPE types is shown in Figure 2.

Each of these achieves the elastic performance characteristic of a rubber in different fashions. A significant portion of the molecular make-up contributes to the elastomer-like performance in one phase. Another portion of the molecular make-up contributes a phase with thermoplastic properties. The dual phase nature combined

with the chemistry of the polymer dictate the performance capabilities of the TPE [3].

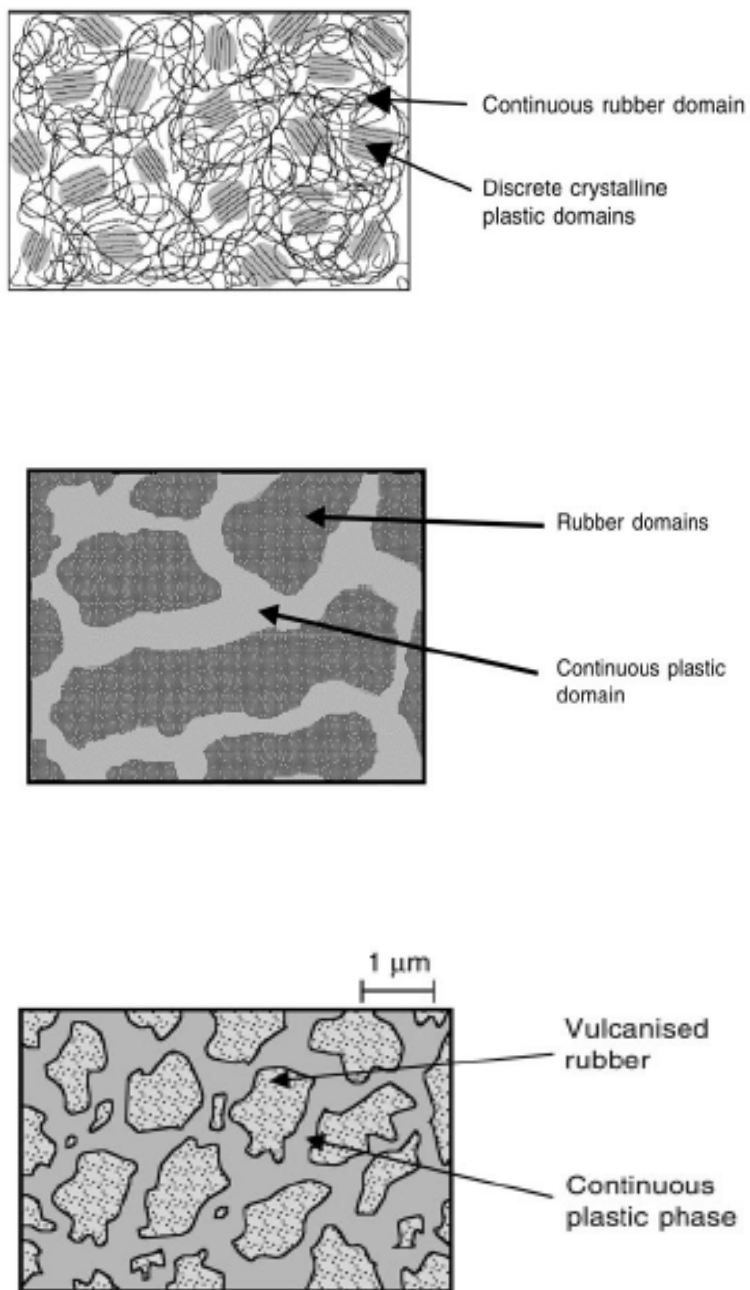


Figure 1.2 Morphology of (a) block copolymer, (b) rubber/plastic blend and (c) thermoplastic vulcanizate [3].

1.1.1 Polyethylene/poly (α -olefin) copolymers

Copolymers of ethylene with higher α -olefins have been synthesized using Ziegler-Natta catalysts. Higher contents of 1-butene and 1-hexene give crystalline, low modulus polymers that are similar to ethylene-propylene copolymers in that the ethylene crystallinity provides the mechanism for thermoplastic processing. The polymers have been called plastomers because they have properties that can range from low-density polyethylene-like materials to TPEs with many of characteristics of plasticized PVC.

The commercial ethylene- α -olefin copolymers produced using metallocene catalysts are characterized by narrow molecular weight and compositional distributions. This results from the catalysts having a single type of polymerization site. The low T_g of the polymer (~ 55 °C) and relatively low T_m (50-90 °C) result in rapid crystallization rates so that final properties are rapidly achieved and thermoplastic processing is easily carried out. Because of their easy processing, good physical properties and chemical inertness of polyolefins, plastomers of this type are expected to provide very useful TPEs with a range of rubber-like properties [4].

1.2 Polymer blends

Only homopolymers cannot fulfill all requirements of applications due to some of their unwanted or inferior properties. Blending two or more polymers in the right composition with right choice of homopolymers is the best way to overcome this situation. For this, homopolymers are selected in such a way that superior properties of one polymer should not be diminished by the addition of the other.

Polymer blends can be divided mainly into two groups: miscible and immiscible. Miscible blends are homogeneous and stable; however they are few in number. Their properties tend to be in between that of the two individual polymers.

Most of the polymer blends are immiscible and their properties are mainly depend on their phase morphologies which are decided by their viscosity, interfacial tension and processing methods [5-6].

Melt blending is a method for preparing blends of immiscible polymers and has a great academic as well as industrial importance. It is possible to overcome the unwanted properties or disadvantages of polymer through blending with a right choice of another polymer. Toughening of brittle polymers using an elastomer is a best example in this case and the toughening efficiency is highly dependent on the content, particle size, and architecture of elastomer, as well as the interactions between phases determining the mechanical properties of the polymer blends [7]. There is a widespread interest in developing materials systems and structures with existing polymers as in the form of blends or multi-layers to meet the demands of a particular application. The combination of the individual properties of different polymers is often aimed for in specific applications [8]. The blend morphology and the phase dimensions determine the ultimate properties of the blend. It is reported that the final blend morphology in binary/ternary blends depends on filler size, sequence of mixing, viscosity of the polymer matrix, along with other factors [9].

There are two kinds of benefits related to polymer blends. One is material related and the other manufacturer related. The material-related benefits are [10],

- (i) Providing materials with full set of desired properties at the lowest price.
- (ii) Extending the engineering resins' performance.
- (iii) Improving specific properties, viz. impact strength or solvent resistance.
- (iv) Offering the means for industrial and/or municipal plastics waste recycling.

Blending also benefits the manufacturer by offering:

- (i) Improved processability, product uniformity, and scrap reduction.
- (ii) Quick formulation changes.

- (iii) Plant flexibility and high productivity.
- (iv) Reduction of the number of grades that need to be manufactured and stored.
- (v) Inherent recyclability.

Polypropylene (PP) is one of the most widely used engineering polymers because of its good mechanical and thermal properties, chemical resistance, and easy processing features. To date, elastomer-toughened PP blends are one of the most successful systems. Elastomers can be ethylene-propylene copolymer (EPR), ethylene-propylene diene monomer (EPDM) and ethylene vinyl acetate. More recently, poly (ethylene-octene) (EOC) was used as the impact modifier for PP, and the results show that EOC presented good toughening efficiency and better processability than EPDM in toughening PP. When compared with conventional EPR or EPDM, EOC exhibits the advantage of mechanical properties when blended with PP [7].

1.3 Conducting polymer composites (CPC)

Nowadays, conductive polymeric composites (CPC) have been extensively studied because of their potential applications in light emitting devices, batteries, electromagnetic shielding, antistatic and corrosion resistant coatings, sensors and other functional applications. Also they possess many desirable properties like high strength, light weight, design and processing advantages etc [11-14]. A number of researchers have studied the conductivity and other related properties of composites using various fillers. Commonly used fillers in the CPCs are carbon black [15-17], single wall (SWCNT) [18-20] and multiwall carbon nanotubes (MWCNT) [21-23]), carbon fiber [24-28], graphite [29-34] and metal powders [35-38]. ShROUT et al. explored the possibility of conducting composites containing borides, silicides and carbides of some metals as fillers in polyethylene and epoxy resin matrices [39]. MoSALA et al. compared the thermal and electrical conductivities of SWCNT and MWCNT composites using epoxy resin matrix [40]. Expandable graphite fillers are well known as eco-friendly halogen-free flame retardant, simultaneously being

conducting fillers as well. The advantage of carbon fillers over metal powders is that only very low amount of filler is enough to achieve good conductivity so that total weight of the composite can be reduced.

1.3.1 Conduction mechanism and percolation theory

Polymer composites consist of at least two components, a polymer matrix and a filler. The filler can be an inorganic powder such as a metal or a ceramic, or an organic material such as carbon (carbon black or a fullerene) or an intrinsically conducting polymer. The conductivity depends critically on the volume content of the filler. For very low filler fractions, the mean distance between conducting particles is large and the conductance is limited by the polymer matrix, which has typically a conductivity in the order of $10^{-15} \Omega^{-1} \text{ cm}^{-1}$. When a sufficient amount of filler is loaded, the filler particles get closer and form linkages, which result in an initial conducting path through the whole material. The corresponding filler content is called a percolation threshold. In this concentration range, the conductivity can change drastically by several orders of magnitude for small variations of the filler content. Finally, at high loading of the filler, the increasing number of conducting paths form a three-dimensional network. In this range the conductivity is high and less sensitive to small changes in volume fraction. In order to create a well conducting polymer composite, the filler's conductivity has to be much higher than that of the matrix.

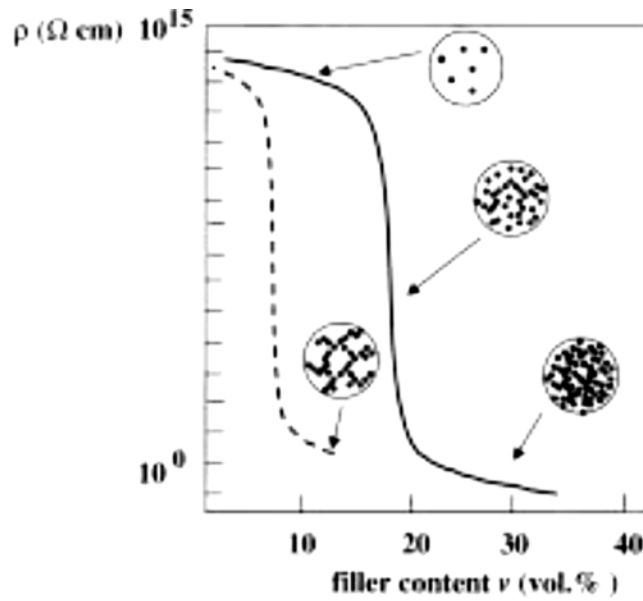


Figure 1.3 Schematic sketch of the resistivity of a composite as a function of filler concentration, showing percolation behavior.

Percolation theory gives a phenomenological description of the conductivity of a system near to a metal-insulator transition. Excellent introductions are given by Scher and Zallen [41].

In model percolation studies one starts with a large, preferably infinite regular periodic lattice. A site of this lattice is then assigned at random with a probability P . All sites are bonded to adjacent sites by a conductive bond. At a critical probability P_c an infinite conducting cluster is first formed in the infinite lattice. This means that at an initial percolating path through the material the conductivity σ of the lattice changes from insulating to an infinite value. Above P_c the conductivity is found to increase as

$$\sigma(P) \propto (P - P_c)^n \quad (1)$$

with a parameter n between 1.65 and 2 for three dimensional lattices. P_c is called as the critical or percolation threshold. The percolation behavior can be influenced by the shape of the filler. Fibers show, for example, a percolation threshold of only several percent. Additionally, geometry and dimension of the regarded composite sample, as for example, the distance of external electrodes have to be considered.

1.4 Crosslinking of polymers

Crosslinking process involves the formation of chemical bonds (crosslinks) between adjacent molecular chains to form a three-dimensional network. There exist several methods to produce crosslinked polymers, such as chemical methods, using mainly sulfur (for unsaturated polymers) [42] peroxides [43-47] or silanes [48-52] and high-energy irradiations such as electron beam or γ -beam [53-57] techniques. In recent years, crosslinked polymers have been widely explored for a number of industrial applications requiring withstanding high-temperature environments. Examples of such applications include wire and cable coating, heat shrinkable materials, hot water tubing, and steam-resistant food packaging.

Thermochemical crosslinking involving organic peroxides is most widely used for its controlled decomposition rate, minimal side products, and economical process. Peroxide is incorporated into the polymer, at the time of mixing, below the activation temperature of the peroxide. The crosslinkable polymer will later be molded and shaped and then cured under pressure and temperature. Suitable peroxide has to be selected to give fast crosslinking without precuring in the mixing chamber; hence, dicumyl peroxide (DCP) is widely used for this purpose [58].

Peroxide crosslinking follows a well-known free radical mechanism. In the first stage, the “initiation,” peroxide undergoes homolytic fission to give rise to free radical formation. This operation is carried out at high temperatures. Free radicals formed are very reactive chemical species which initiate “propagation” reactions. Only the formation of two types of macroradicals is presented. The formed macroradicals can recombine - “termination” reactions- thus leading to crosslinked structures. Other secondary reactions that can occur in crosslinking with peroxide are those with H transfer or scission/degradation reactions with formation of aldehydes, carboxylic acids, ketones, vinyl groups, etc. Peroxide crosslinking have both advantages and disadvantages. The process of incorporation is simple but the disadvantages are blooming and unpleasant smell [59-60].

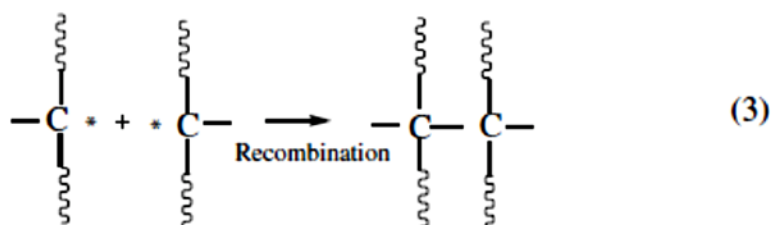
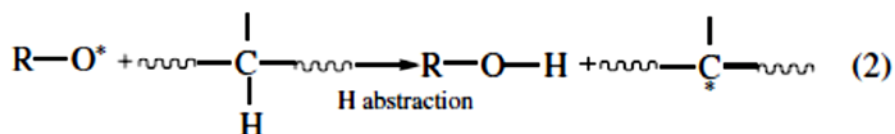
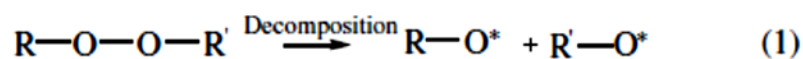


Figure 1.4 Scheme of peroxide initiated crosslinking reaction [59].

1.4.1 Effect of crosslinking

Primary effect of crosslinking is the formation of three-dimensional network of polymer chains. This network enables them to achieve improved mechanical properties, especially elastic properties, thermal stability and chemical resistance. Another important advantage of crosslinking is that it enables the polymers to work at elevated temperatures above their melting temperatures. As a result of crosslinking, we can get polymers with a wide range of applications. Many researchers studied the effect of different kinds of crosslinking techniques on improvement of mechanical and thermal properties of blends and composites of various polymers [61-67].

2. OBJECTIVE OF THE THESIS AND BRIEF SUMMARY

Prime emphasis of this thesis was given to the modification of polyolefin elastomers namely ethylene-octene copolymer with excellent elastic properties having commercial importance. This modification was carried out in three different ways in order to meet different requirements such as melt blending, composite preparation and crosslinking. The main tasks of this thesis are:

- Preparation of PP/EOC blends via melt blending with an intention of improving elastic properties of PP accompanied by morphological analysis.
- Preparation of EOC/expandable graphite conducting polymer composite and their electrical and thermal studies and flammability studies thereafter.
- Crosslinking of EOC via peroxide crosslinking method using DCP and evaluation of elastic and creep properties at elevated temperatures.
- Finally, to study the electrical and thermal conductivities along with the thermal and mechanical properties of EOC composites with carbon fibres and multiwall carbon nanotube fillers.

Paper 1 deals with preparation of PP/EOC blends followed by the evaluation of their properties. Blends were prepared by the melt blending of these two individual polymers in a Haake Minilab mixing machine at 200 °C for 5 min with a mixing speed of 50 rpm. Composition of blends was varied by changing the PP content from 0 to 100 wt.%. Elastic properties of these blends were evaluated by the tensile stress-strain test conducted in hysteresis mode at a crosshead speed of 10 mm min⁻¹. In this test, samples were stretched to fixed elongations (100, 200 and 300%) and allowed to go back to the initial position at the same speed. The residual strain values, which are obtained directly from the curve are the measure of elasticity, were noted and compared. Other tensile properties like tensile modulus, elongation at break and stress at break were also measured. Values of M100 and M300, which are

industrially important, were also noted. Morphology of these blends has been studied using TEM and found very significant developments which correlate with their observed elastic and mechanical properties. It was observed by the DSC analysis that the EOC crystals (only 7 wt.%) act as tie points for amorphous chains (93 wt.%). Good elastic properties were observed when the PP content is low (0-30 wt.%) and the tensile modulus values were found to be increasing with PP content.

In *Paper 2*, modification of EOC matrix by preparing expandable graphite composites is illustrated, followed by evaluation of electrical and thermal conductivities and flame retardancy properties. It was observed that percolation threshold for EOC/expandable graphite filler composites was observed to be at 16 vol. % (30 wt.%). In the case of AC conductivity, frequency had an increasing effect while permittivity had an inverse effect. Thermal conductivity(λ) values for pure EOC matrix and 50 wt.% composite observed to be 0.196 and 0.676 $\text{Wm}^{-1}\text{K}^{-1}$ are correspondingly; an increase of about 245% has been observed. At filler loading above 40 wt.%, expandable graphite acts as an environmentally friendly halogen-free flame retardant also. Shore-A hardness of these composites even at high filler levels did not rise markedly which shows the rubbery nature or softness of these composites and they can find potential application in the field of sensors.

Peroxide crosslinking of EOC using dicumyl peroxide was carried out and its effect on properties at elevated temperatures was studied. This is the subject of *Paper 3*. DCP along with Irganox 1010 antioxidant was first mixed with EOC using a Brabender mixing machine at 100 °C for 10 min at a mixing speed of 50 rpm. These mixed compounds then crosslinked at 170 °C in a compression molding machine and sheets were prepared out of them, simultaneously. These sheets were used for the evaluation of mechanical and elastic properties at temperature above T_m of virgin EOC (50 °C). Peroxide content had a positive effect on gel content and showed that crosslinking increased with DCP content. Residual strain has been

measured at 70 °C and found that with an increase in peroxide level, elasticity improves. Creep is very important mechanical property as far as the long term application of polymers under stress is concerned. After crosslinking, creep resistance of DCP-crosslinked EOC has found improved. Temperature and stress during creep have an inverse effect on creep resistance.

Paper 4 deals with the study of electrical and thermal conductivities and mechanical and thermal properties of EOC composites prepared by incorporating CF and MWCNT fillers. Increase in filler content resulted in increase in electrical conductivities with percolation behavior. Percolation threshold for CF-composites was observed at 5 vol. % and for MWCNT-composites at 8 vol.% respectively. Also, it has been observed that, length and diameter of fillers play an important role in the conductivity of composites. CF-composites showed a higher conductivity than the MWCNT one at all filler levels above percolation and frequencies. Thermal conductivity also has been found to be increasing with filler loading level. Thermal stability of these composites has improved much with increase in filler level. Filler content has a remarkable influence on mechanical properties such as tensile modulus. Altogether, multiple roles of CF and MWCNT fillers in their composites with EOC matrix has been proved through their increased conductivity and thermal stability together with improved mechanical properties.

3. CLOSING REMARKS

3.1. Conclusions

From the present thesis which dealt with the modification of polyolefin elastomers, following concluding points can be drawn:

- Elasticity of PP has been improved by addition of EOC into it and the best elasticity was observed when PP content was low (0-30 wt.%). Large numbers of amorphous chains (93%) are held together by a small amount of lamellar crystals that act as tie points.
- Electrical and thermal conductivities of EOC/expandable graphite composites were highly influenced by the filler content. Percolation threshold was observed at about 16 vol. % of graphite loading. Above 40 wt.% level, expandable graphite also served as flame retarding filler. Only a slight increase in Shore-A hardness shows the softness/rubbery nature of these composites even at high levels of graphite loading pointing towards their potential applicability as strain/pressure sensors.
- Peroxide crosslinking has enabled ethylene-octene copolymer to achieve a good crosslinking which has been reflected in increased creep resistance even at high temperatures well above T_m . Elastic properties at high temperatures also were improved by crosslinking.
- EOC composites with CF and MWCNT fillers show improved electrical and thermal conductivities even with low filler loadings. Aspect ratio of fillers plays an important role in the conductivities and other properties of the composites. Thermal stability and mechanical properties of composites were also found improved with increase in CF and MWCNT level proving their multiple roles in their composites.

3.2. Contribution to science and practice

The outcome of the present doctoral study throws light towards the industrial importance of polyolefinic elastomers. Modifications of these copolymers through blending, composite preparation and crosslinking enable them to widen their range of application. Blending with other polymers could result in a new polymer system with improved elastic and impact properties while conducting composites with comparatively low hardness values could find application as pressure or strain sensors. Another important finding of this doctoral thesis is the improvement in creep and elastic properties at high temperatures above the T_m of EOC making it a competitive candidate to be used at elevated temperatures. The above-mentioned findings can lead to formulations of new application-oriented products.

3.3. Scope for future studies

From the results obtained out of the present work, following suggestions can be proposed for future studies.

- Preparation of thermoplastic vulcanizates via dynamic vulcanization to achieve new materials with improved properties.
- Study of effect of pressure or strain on electrical and thermal conductivity of conducting polymer composites made out of EOC to find suitable application as pressure/strain sensors.
- Study of effect of temperature on conductivity.
- Crosslinking of other EOCs containing various comonomer contents and study of their influence on properties.

REFERENCES

- [1] BHOWMICK, A.K. *Current Topics in Elastomers Research*, Florida: Taylor & Francis Group, LLC, 2008. ISBN 13-978-0-8493-7317-6.
- [2] HARPER, C.A. *Handbook of Plastics, Elastomers and Composites*, New York: McGraw-Hill, 2002. ISBN 978-0070266933.
- [3] KEAR, K.E. *Developments in Thermoplastic Elastomers*, Shropshire: Rapra Review Reports, 2003. ISBN 1-85957-433-5.
- [4] HOLDEN, G., KRICHELDORF, H.R., QUIRK, R.P. *Thermoplastic Elastomers*, Cincinnati: Hanser Gardner Publications, 2004. ISBN 1569903646.
- [5] ISAYEV, A.I., PALSULE, S. *Encyclopedia of Polymer Blends: Vol. 2 - Processing*, Weinheim: Wiley-VCH Verlag & Co., 2011. ISBN 3527319301.
- [6] NWABUNMA, D., KYU, T. *Polyolefin Blends*, New York: Wiley-Blackwell, 2008. ISBN 0471790583.
- [7] TANG, W.H., TANG, J., YUAN, H.L., JIN, R.G. Crystallization Behavior and Mechanical Properties of Polypropylene Random Copolymer/Poly(Ethylene-Octene) Blends. *J. Appl. Polym. Sci.* 2011, vol. 122, no. 1, p. 461-468.
- [8] OZEN, I., RUSTAL, C., DIRNBERGER, K., FRITZ, H.G., EISENBACH, C.D. Modification of Surface Properties of Polypropylene Films by Blending with Poly(Ethylene-B-Ethylene Oxide) and Its Application. *Polym. Bull.* 2012, vol. 68, no. 2, p. 575-595.
- [9] ALI, I., ELLEITHY, R., AL-ZAHRANI, S.M., MOHSIN, M.E.A. Viscoelastic, Thermal, and Morphological Analysis of HDPE/EVA/CaCO₃ Ternary Blends. *Polym. Bull.* 2011, vol. 67, no. 9, p. 1961-1978.
- [10] UTRACKI, L.A. *Polymer Blends Handbook*, Dordrecht: Kluwer Academic Publishers, 2002. ISBN 1-4020-1110-5.
- [11] CHO, H.B., TOKOI, Y., TANAKA, S., SUEMATSU, H., SUZUKI, T., JIANG, W.H., NIIHARA, K., NAKAYAMA, T. Modification of BN Nanosheets and Their Thermal Conducting Properties in Nanocomposite Film with Polysiloxane According to the Orientation of BN. *Compos. Sci. Technol.* 2011, vol. 71, no. 8, p. 1046-1052.
- [12] DU, X.S., XIAO, M., MENG, Y.Z. Synthesis and Characterization of Polyaniline/Graphite Conducting Nanocomposites. *J. Polym. Sci. Pol. Phys.* 2004, vol. 42, no. 10, p. 1972-1978.

- [13] GUPTA, A., CHOUDHARY, V. Effect of Multiwall Carbon Nanotubes on Thermomechanical and Electrical Properties of Poly(Trimethylene Terephthalate). *J. Appl. Polym. Sci.* 2012, vol. 123, no. 3, p. 1548-1556.
- [14] MALINAUSKAS, A. Chemical Deposition of Conducting Polymers. *Polymer* 2001, vol. 42, no. 9, p. 3957-3972.
- [15] FLANDIN, L., CHANG, A., NAZARENKO, S., HILTNER, A., BAER, E. Effect of Strain on the Properties of an Ethylene-Octene Elastomer with Conductive Carbon Fillers. *J. Appl. Polym. Sci.* 2000, vol. 76, no. 6, p. 894-905.
- [16] YIN, Q., LI, A.J., WANG, W.Q., XIA, L.G., WANG, Y.M. Study on the Electrical and Mechanical Properties of Phenol Formaldehyde Resin/Graphite Composite for Bipolar Plate. *J. Power Sources* 2007, vol. 165, no. 2, p. 717-721.
- [17] CUI, L.M., ZHANG, Y., ZHANG, Y.X., ZHANG, X.F., ZHOU, W. Electrical Properties and Conductive Mechanisms of Immiscible Polypropylene/Novolac Blends Filled with Carbon Black. *Eur. Polym. J.* 2007, vol. 43, no. 12, p. 5097-5106.
- [18] HORNBOSTEL, B., POTSCHEKE, P., KOTZ, J., ROTH, S. Single-Walled Carbon Nanotubes/Polycarbonate Composites: Basic Electrical and Mechanical Properties. *Phys. Status Solidi B.* 2006, vol. 243, no. 13, p. 3445-3451.
- [19] KIM, H.J., KOIZHAIGANOVA, R.B., KARIM, M.R., LEE, G.H., VASUDEVAN, T., LEE, M.S. Synthesis and Characterization of Poly(3-Octylthiophene)/Single Wall Carbon Nanotube Composites for Photovoltaic Applications. *J. Appl. Polym. Sci.* 2010, vol. 118, no. 3, p. 1386-1394.
- [20] PAUL, R., MAITY, A., MITRA, A., KUMBHAKAR, P., MITRA, A.K. Synthesis and Study of Optical and Electrical Characteristics of a Hybrid Structure of Single Wall Carbon Nanotubes and Silver Nanoparticles. *J. Nanopart. Res.* 2011, vol. 13, no. 11, p. 5749-5757.
- [21] YANG, J.H., XU, T., LU, A., ZHANG, Q., TAN, H., FU, Q. Preparation and Properties of Poly (P-Phenylene Sulfide)/Multiwall Carbon Nanotube Composites Obtained by Melt Compounding. *Compos. Sci. Technol.* 2009, vol. 69, no. 2, p. 147-153.
- [22] LI, J., LUMPP, J.K., ANDREWS, R., JACQUES, D. Aspect Ratio and Loading Effects of Multiwall Carbon Nanotubes in Epoxy for Electrically Conductive Adhesives. *J. Adhes. Sci. Technol.* 2008, vol. 22, no. 14, p. 1659-1671.
- [23] PEDRONI, L.G., SOTO-OVIEDO, M.A., ROSOLEN, J.M., FELISBERTI, M.I., NOGUEIRA, A.F. Conductivity and Mechanical Properties of Composites Based on MWCNTs and Styrene-Butadiene-Styrene Block (TM) Copolymers. *J. Appl. Polym. Sci.* 2009, vol. 112, no. 6, p. 3241-3248.

- [24] CHOI, M.H., JEON, B.H., CHUNG, I.J. The Effect of Coupling Agent on Electrical and Mechanical Properties of Carbon Fiber/Phenolic Resin Composites. *Polymer* 2000, vol. 41, no. 9, p. 3243-3252.
- [25] FELLER, J.F., LINOSSIER, I., GROHENS, Y. Conductive Polymer Composites: Comparative Study of Poly(Ester)-Short Carbon Fibres and Poly(Epoxy)-Short Carbon Fibres Mechanical and Electrical Properties. *Mater. Lett.* 2002, vol. 57, no. 1, p. 64-71.
- [26] VILCAKOVA, J., SAHA, P., QUADRAT, O. Electrical Conductivity of Carbon Fibres/Polyester Resin Composites in the Percolation Threshold Region. *Eur. Polym. J.* 2002, vol. 38, no. 12, p. 2343-2347.
- [27] SAU, K.P., KHASTGIR, D., CHAKI, T.K. Electrical Conductivity of Carbon Black and Carbon Fibre Filled Silicone Rubber Composites. *Angew. Makromol. Chem.* 1998, vol. 258, no., p. 11-17.
- [28] ZHANG, C., YI, X.S., YUI, H., ASAI, S., SUMITA, M. Morphology and Electrical Properties of Short Carbon Fiber-Filled Polymer Blends: High-Density Polyethylene Poly(Methyl Methacrylate). *J. Appl. Polym. Sci.* 1998, vol. 69, no. 9, p. 1813-1819.
- [29] WENG, W.G., CHEN, G.H., WU, D.J., CHEN, X.F., LU, J.R., WANG, P.P. Fabrication and Characterization of Nylon 6/Foliated Graphite Electrically Conducting Nanocomposite. *J. Polym. Sci. Pol. Phys.* 2004, vol. 42, no. 15, p. 2844-2856.
- [30] CELZARD, A., MCRAE, E., MARECHE, J.F., FURDIN, G., DUFORT, M., DELEUZE, C. Composites Based on Micron-Sized Exfoliated Graphite Particles: Electrical Conduction, Critical Exponents and Anisotropy. *J. Phys. Chem. Solids* 1996, vol. 57, no. 6-8, p. 715-718.
- [31] SURESHA, B., SIDDARAMAIAH, KISHORE, SEETHARAMU, S., KUMARAN, P.S. Investigations on the Influence of Graphite Filler on Dry Sliding Wear and Abrasive Wear Behaviour of Carbon Fabric Reinforced Epoxy Composites. *Wear* 2009, vol. 267, no. 9-10, p. 1405-1414.
- [32] PANWAR, V., PARK, J.O., PARK, S.H., KUMAR, S., MEHRA, R.M. Electrical, Dielectric, and Electromagnetic Shielding Properties of Polypropylene-Graphite Composites. *J. Appl. Polym. Sci.* 2010, vol. 115, no. 3, p. 1306-1314.
- [33] JIN, J., LEESIRISAN, S., SONG, M. Electrical Conductivity of Ion-Doped Graphite/Polyethersulphone Composites. *Compos. Sci. Technol.* 2010, vol. 70, no. 10, p. 1544-1549.

- [34] SACHDEV, V.K., PATEL, K., BHATTACHARYA, S., TANDON, R.P. Electromagnetic Interference Shielding of Graphite/Acrylonitrile Butadiene Styrene Composites. *J. Appl. Polym. Sci.* 2011, vol. 120, no. 2, p. 1100-1105.
- [35] PINTO, G., MAAROUFI, A.K. Conducting Polymer Composites of Zinc-Filled Urea-Formaldehyde. *J. Appl. Polym. Sci.* 2005, vol. 96, no. 6, p. 2011-2015.
- [36] PINTO, G., JIMENEZ-MARTIN, A. Conducting Aluminum-Filled Nylon 6 Composites. *Polym. Composite.* 2001, vol. 22, no. 1, p. 65-70.
- [37] VILCAKOVA, J., SAHA, P., HAUSNEROVA, B., QUADRAT, O. Electrical Properties of Composites of Hard Metal Carbides in a Polymer Matrix. *Polym. Composite.* 2002, vol. 23, no. 5, p. 942-946.
- [38] YUAN, M., BROKKEN-ZIJP, J.C.M., HUIJBREGTS, L.J., DE WITH, G. Filler Size Effects on the Conductivity of Polymer Nanocomposites: Semiconductive Phthalocyanine Nanoparticles in Epoxy Matrices. *J. Polym. Sci. Pol. Phys.* 2008, vol. 46, no. 11, p. 1079-1093.
- [39] SHROUT, T.R., MOFFATT, D., HUEBNER, W. Composite PTCR Thermistors Utilizing Conducting Borides, Silicides and Carbide Powders. *J. Mater. Sci.* 1991, vol. 26, no. 1, p. 145-154.
- [40] MOISALA, A., LI, Q., KINLOCH, I.A., WINDLE, A.H. Thermal and Electrical Conductivity of Single- and Multi-Walled Carbon Nanotube-Epoxy Composites. *Compos. Sci. Technol.* 2006, vol. 66, no. 10, p. 1285-1288.
- [41] SCHER, H., ZALLEN, R. Critical Density in Percolation Processes. *J. Chem. Phys.* 1970, vol. 53, no. 9, p. 3759-3761.
- [42] COLEMAN, M.M., SHELTON, J.R., KOENIG, J.L. Sulfur Vulcanization of Hydrocarbon Diene Elastomers. *Ind. Eng. Chem. Prod. Res. Dev.* 1974, vol. 13, no. 3, p. 154-165.
- [43] MSAKNI, A., CHAUMONT, P., CASSAGNAU, P. Diffusion of the Dicumyl Peroxide in Molten Polymer Probed by Rheology. *Rheol. Acta* 2007, vol. 46, no. 7, p. 933-943.
- [44] MSAKNI, A., CHAUMONT, P., CASSAGNAU, P. Crosslinking of Ethylene-Octene Copolymers under Dynamic Conditions: A New Way to Access Polymeric Hyperbranched Structure. *Polym. Eng. Sci.* 2006, vol. 46, no. 11, p. 1530-1540.
- [45] JOHNSTON, R.T. Monte Carlo Simulation of the Peroxide Curing of Ethylene Elastomers. *Rubber Chem. Technol.* 2003, vol. 76, no. 1, p. 174-201.
- [46] SIRISINHA, K., MEKSAWAT, D. Comparison in Processability and Mechanical and Thermal Properties of Ethylene-Octene Copolymer Crosslinked by Different Techniques. *J. Appl. Polym. Sci.* 2004, vol. 93, no. 3, p. 1179-1185.

- [47] KOLESOV, I.S., RADUSCH, H.J. Multiple Shape-Memory Behavior and Thermal-Mechanical Properties of Peroxide Cross-Linked Blends of Linear and Short-Chain Branched Polyethylenes. *Express Polym. Lett.* 2008, vol. 2, no. 7, p. 461-473.
- [48] JIAO, C.M., WANG, Z.Z., GUI, Z., HU, Y. Silane Grafting and Crosslinking of Ethylene-Octene Copolymer. *Eur. Polym. J.* 2005, vol. 41, no. 6, p. 1204-1211.
- [49] SIRISINHA, K., MEKSAWAT, D. Preparation and Properties of Metallocene Ethylene Copolymer Crosslinked by Vinyltrimethoxysilane. *Polym. Int.* 2005, vol. 54, no. 7, p. 1014-1020.
- [50] ZHANG, G.Q., WANG, G.L., ZHANG, J., WEI, P., JIANG, P.K. Performance Evaluation of Silane Crosslinking of Metallocene-Based Polyethylene-Octene Elastomer. *J. Appl. Polym. Sci.* 2006, vol. 102, no. 5, p. 5057-5061.
- [51] GARNIER, L., DUQUESNE, S., CASETTA, M., LEWANDOWSKI, M., BOURBIGOT, S. Melt Spinning of Silane-Water Cross-Linked Polyethylene-Octene through a Reactive Extrusion Process. *React. Funct. Polym.* 2010, vol. 70, no. 10, p. 775-783.
- [52] SIRISINHA, K., MEKSAWAT, D. Changes in Properties of Silane-Water Crosslinked Metallocene Ethylene-Octene Copolymer after Prolonged Crosslinking Time. *J. Appl. Polym. Sci.* 2004, vol. 93, no. 2, p. 901-906.
- [53] PERRAUD, S., VALLAT, M.F., KUCZYNSKI, J. Radiation Crosslinking of Poly(Ethylene-Co-Octene) with Electron Beam Radiation. *Macromol. Mater. Eng.* 2003, vol. 288, no. 2, p. 117-123.
- [54] NICOLAS, J., VILLARREAL, N., GOBERNADO-MITRE, I., MERINO, J.C., PASTOR, J.M. Thermal Properties and SSA Fractionation of Metallocene Ethylene-Oct-1-ene Copolymers with High Comonomer Content Cross-Linked by Dicumyl Peroxide or Beta-Radiation. *Macromol. Chem. Physic.* 2003, vol. 204, no. 18, p. 2212-2221.
- [55] CARDENAS, M.A., VILLARREAL, N., GOBERNADO-MITRE, I., MERINO, J.C., PASTOR, J.M. Characterization of Electron Beam Irradiation Blends Based on Metallocene Ethylene-1-Octene Copolymer. *J. Polym. Sci. Pol. Phys.* 2007, vol. 45, no. 17, p. 2432-2440.
- [56] BHOWMICK, A.K., VIJAYABASKAR, V. Electron Beam Curing of Elastomers. *Rubber Chem. Technol.* 2006, vol. 79, no. 3, p. 402-428.
- [57] NICOLAS, J., RESSIA, J.A., VALLES, E.M., MERINO, J.C., PASTOR, J.M. Characterization of Metallocene Ethylene-1-Octene Copolymers with High Comonomer Content Cross-Linked by Dicumyl Peroxide or Beta-Radiation. *J. Appl. Polym. Sci.* 2009, vol. 112, no. 5, p. 2691-2700.

- [58] BORAH, J.S., NASKAR, K., CHAKI, T.K. Covulcanization of LLDPE/EMA Blends Using Dicumyl Peroxide. *J. Appl. Polym. Sci.* 2012, vol. 123, no. 1, p. 502-509.
- [59] STELESCU, M.D., MANAILA, E., CRACIUN, G., ZUGA, N. Crosslinking and Grafting Ethylene Vinyl Acetate Copolymer with Accelerated Electrons in the Presence of Polyfunctional Monomers. *Polym. Bull.* 2012, vol. 68, no. 1, p. 263-285.
- [60] RAJESHBABU, R., GOHS, U., NASKAR, K., THAKUR, V., WAGENKNECHT, U., HEINRICH, G. Preparation of Polypropylene (PP)/Ethylene Octene Copolymer (EOC) Thermoplastic Vulcanizates (TPVs) by High Energy Electron Reactive Processing. *Radiat. Phys. Chem.* 2011, vol. 80, no. 12, p. 1398-1405.
- [61] HWANG, I.T., JUNG, C.H., KUK, I.S., CHOI, J.H., NHO, Y.C. Electron Beam-Induced Crosslinking of Poly(Butylene Adipate-Co-Terephthalate). *Nucl. Instrum. Methods Phys. Res. Sect. B-Beam Interact. Mater. Atoms* 2010, vol. 268, no. 21, p. 3386-3389.
- [62] BASFAR, A.A., ALI, Z.I. Physico-Chemical Properties of Low Density Polyethylene and Ethylene Vinyl Acetate Composites Cross-Linked by Ionizing Radiation. *Radiat. Phys. Chem.* 2011, vol. 80, no. 2, p. 257-263.
- [63] PRAMANIK, N.K., HALDAR, R.S., BHARDWAJ, Y.K., SABHARWAL, S., NIYOGI, U.K., KHANDAL, R.K. Modification of Nylon 66 by Electron Beam Irradiation for Improved Properties and Superior Performances. *J. Appl. Polym. Sci.* 2011, vol. 122, no. 1, p. 193-202.
- [64] BENGTSSON, M., OKSMAN, K. Silane Crosslinked Wood Plastic Composites: Processing and Properties. *Compos. Sci. Technol.* 2006, vol. 66, no. 13, p. 2177-2186.
- [65] THERON, J.P., KNOETZE, J.H., SANDERSON, R.D., HUNTER, R., MEQUANINT, K., FRANZ, T., ZILLA, P., BEZUIDENHOUT, D. Modification, Crosslinking and Reactive Electrospinning of a Thermoplastic Medical Polyurethane for Vascular Graft Applications. *Acta Biomater.* 2010, vol. 6, no. 7, p. 2434-2447.
- [66] LEE, C.S., YOO, S.H., JHO, J.Y., CHOI, K., HWANG, T.W. Mechanical Properties of Ultra-High Molecular Weight Polyethylene Irradiated with Gamma Rays. *Macromol. Res.* 2004, vol. 12, no. 1, p. 112-118.
- [67] BOBOVITCH, A.L., UNIGOVSKI, Y., GUTMAN, E.M., KOLMAKOV, E., VYAZOVKIN, S. Viscoelastic Properties of Crosslinked LLDPE Films Biaxially Oriented at Temperatures Below Melting Point. *J. Appl. Polym. Sci.* 2007, vol. 103, no. 6, p. 3718-3723.

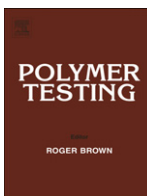
PAPER 1



ELSEVIER

Contents lists available at ScienceDirect

Polymer Testing

journal homepage: www.elsevier.com/locate/polytest

Material Properties

Elastic properties of polypropylene/ethylene–octene copolymer blends

Petr Svoboda^{a,*}, Rajesh Theravalappil^a, Dagmar Svobodova^a, Pavel Mokrejs^a,
Karel Kolomaznik^b, Keisuke Mori^c, Toshiaki Ougizawa^c, Takashi Inoue^d

^a Faculty of Technology, Tomas Bata University in Zlin, nam. TGM 275, 762 72 Zlin, Czech Republic

^b Faculty of Applied Informatics, Tomas Bata University in Zlin, Nad Stranemi 4511, 760 05 Zlin, Czech Republic

^c Department of Organic and Polymeric Materials, Tokyo Institute of Technology, 2-12-1-S8-33, Ookayama, Meguro-ku, Tokyo 152-8552, Japan

^d Department of Polymer Sci. & Eng., Yamagata University, Yonezawa 992-8510, Japan

ARTICLE INFO

Article history:

Received 23 April 2010

Accepted 30 May 2010

Keywords:

Polypropylene

Ethylene–octene copolymer

Elastic properties

TEM

Residual strain

DSC

ABSTRACT

Blends of polypropylene (PP) and ethylene–octene copolymer (EOC) across the whole composition range (10, 20, ..., 80, 90 wt.%) were investigated with focus on mechanical properties. Samples (0–50% of PP) were stretched in a tensile machine to given elongations (100, 200 and 300%) and then the crosshead returned to the initial position. The residual strain values were obtained from the hysteresis curves. These residual strain values were plotted as a function of applied strain and PP content. Stress at given elongation (M100 and M300) was also plotted as a function of PP content. At low PP content (0–20%), residual strain and stress at given elongation are close to those of pure EOC. A steeper increase in these values was observed for concentrations 20–50% of PP. Another set of experiments involved tensile testing to break (full range of concentrations). From these experiments, tensile modulus and stress at break were evaluated and plotted as a function of PP content. Modulus values were close to that of pure EOC in the range of 0–25% of PP. Then, the values start to increase almost linearly with increasing PP content. The mechanical properties of the blends were correlated with the structure observed by transmission electron microscopy (TEM). At 20% PP, there are PP particles with round shape uniformly dispersed in the EOC matrix. When the PP content increased to 30%, the shape of the PP particles changed to elongated. In the case of 40% of PP, the structure resembles a co-continuous one. Differential scanning calorimetry (DSC) revealed the nature of the excellent elastic behavior of EOC. EOC crystals at 7 wt% act as tie points for amorphous chains (physical cross-linking).

© 2010 Elsevier Ltd. All rights reserved.

1. Introduction

Polypropylene (PP) is one of the most versatile low cost commodity polymers. It has good chemical and moisture resistance, good ductility and stiffness and is easily processed. Although PP has seen widespread application, its limited impact strength, especially at lower temperature, due to its relatively high T_g is an obstacle to broader utilization as an engineering plastic. The impact properties of

PP can be considerably improved by incorporation of a rubbery phase. Accordingly, rubber-toughened PP blends with various impact modifiers have been studied, including ethylene–propylene rubber (EPR), ethylene–propylene–diene rubber (EPDM) and ethylene–propylene–styrene rubber (SEBS). Although a variety of elastomers have been studied, EPR and EPDM comprise the majority of commercialized impact modifiers, owing to their low cost. Recently, impact modification of PP, using metallocene-catalyzed ethylene–octene copolymer (EOC) has attracted attention. EOC provides more efficient impact modification than EPR, is more cost effective than EPDM and feeding of EOC pellets into the twin-screw extruder is easier than

* Corresponding author. Tel.: +420 576 031 335; fax: +420 577 210 172.
E-mail address: svoboda@ft.utb.cz (P. Svoboda).

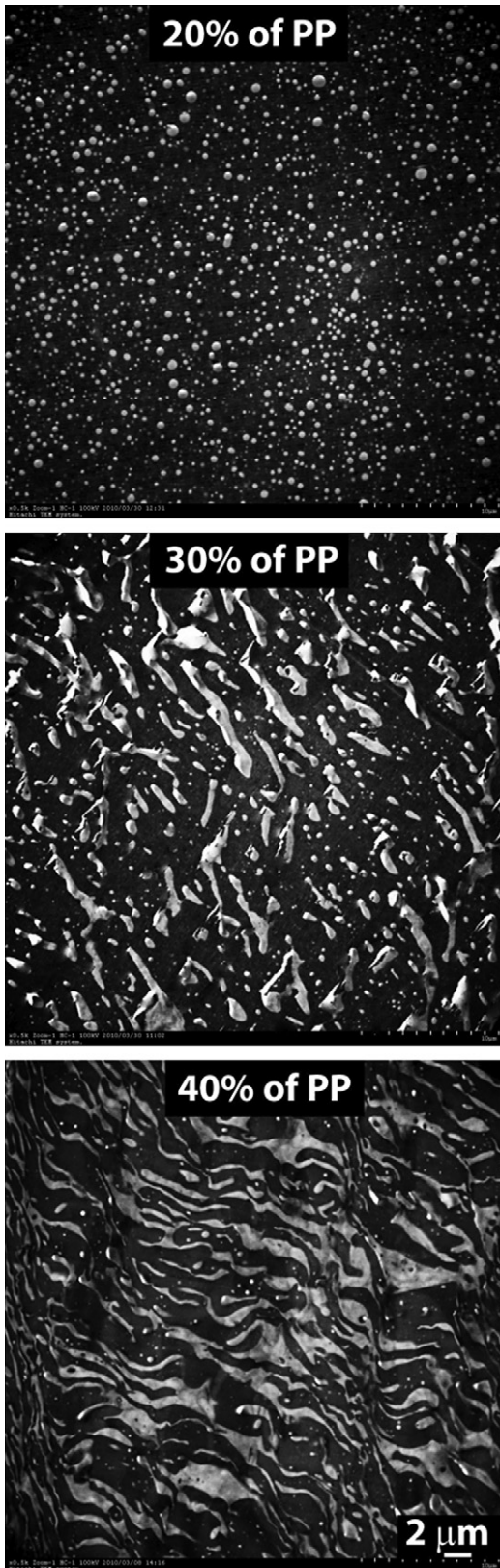


Fig. 1. TEM micrographs of EOC/PP blends with compositions 80/20, 70/30 and 60/40.

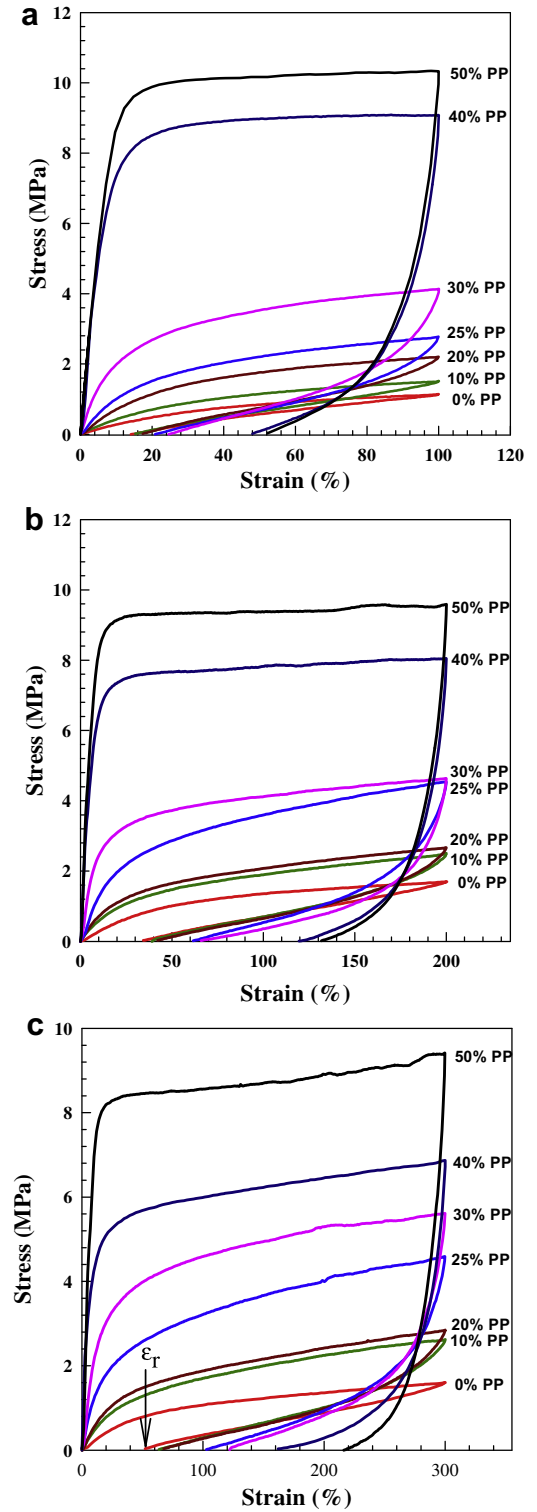


Fig. 2. Stress–strain curves of PP/EOC blends after: a) 100% elongation, b) 200% elongation and c) 300% elongation.

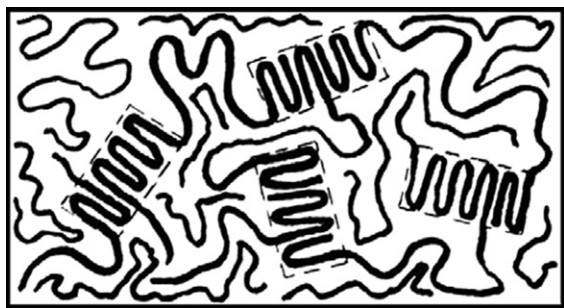


Fig. 3. Schematic diagram of the fragmented lamellar crystallites.

feeding EPDM bales. Consequently, the conventional EPR and EPDM impact modifiers are currently being substituted with newly developed EOC copolymers [1].

The development of Dow's INSITE™ constrained geometry catalyst technology (CGCT) has led to the polymerization of ultra-low-density ethylene–octene copolymers as well as copolymers with densities in the range of conventional LLDPEs. Copolymers with densities less than 0.90 g cm^{-3} synthesized with this technology constitute a unique class of thermoplastic elastomers. The grades of particular interest to the rubber industry are those with high comonomer content because this gives highly amorphous products with very low density. Materials with density lower than about 0.885 have been designated as “polyolefin elastomers” (POE). In 1993, DuPont Dow Elastomers introduced POEs under the brand name ENGAGE®. They are ethylene–octene copolymers produced via advanced INSITE™ catalyst and process technology designed to be processed like thermoplastics but can be compounded like elastomers. The exceptional performance of ENGAGE® is attributed to extraordinary control over polymer structure, molecular weight distribution, uniform comonomer composition and rheology. They are being considered for use in diverse applications such as in

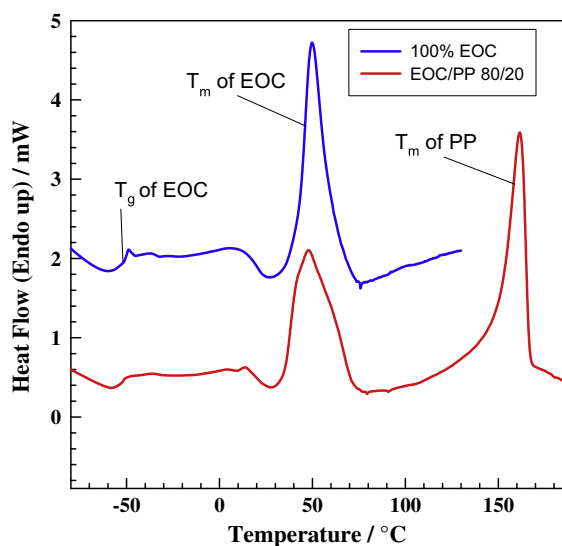


Fig. 4. DSC thermogram of pure EOC and EOC/PP (80/20) blend. Baseline was subtracted.

Table 1

Immediate residual strain and residual strain after 24 h for pure EOC.

Applied strain %	Immediate residual strain ϵ_r %	Residual strain after 24 h %
100	14.0	0.0
200	35.7	3.8
300	52.3	34.6

footwear applications and are a particularly good alternative for sealing applications due to their structural regularity and non-toxic composition. Foams made from these metallocene-based polyolefins (MPO) have been recently commercialized and are being considered for use in diverse applications as cushioning agents, gaskets, sealants, etc. [2].

Thermoplastic elastomers (TPEs) are known as materials showing the processing characteristics of thermoplastics and mechanical properties of vulcanized rubbers. They achieve such properties by a physical process—mixing of thermoplastic polymer and the elastomer together using high shear compounding equipment. The properties of these materials depend on the elastomer and thermoplastic polymer used, as well as on their ratio and miscibility [3,4]. PP/EOC blends have attracted interest from many research laboratories with focus on various aspects, e.g. rheology [5–10], crystallization [11–17], morphology [1,11,13,18–21], nanocomposites [22–28], mechanical properties [4,5,11,29,30] and thermal characterization [1,7,19]. We have focused on elastic properties of the PP/EOC blends. To our best knowledge, there has not been such a study published to date. This study has been performed as a first step in the development of a new type of TPE. The next step will be improvement of elastic properties by dynamic vulcanization (cross-linking of EOC phase).

2. Experimental

The isotactic polypropylene (PP) was a commercial polymer supplied by Mitsui Chemicals Inc. (J3HG, $M_w = 3.5 \times 10^5 \text{ g mol}^{-1}$ and $M_n = 5 \times 10^4 \text{ g mol}^{-1}$).

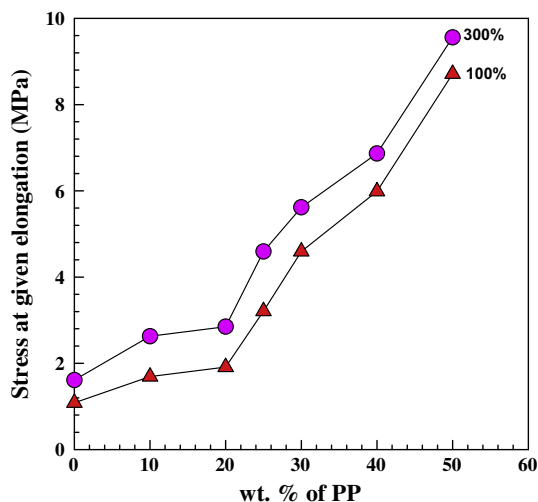


Fig. 5. Stress at given elongation as a function of PP content.

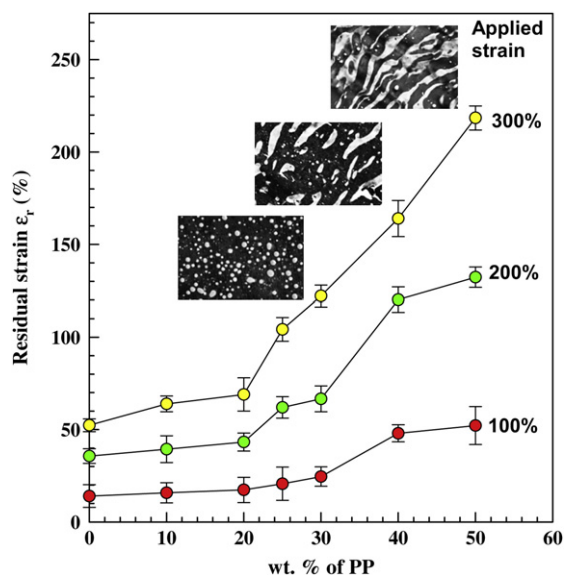


Fig. 6. Residual strain as a function of blend composition with inserted TEM pictures of the morphology related to the composition.

Ethylene–octene copolymer was a special sample prepared by Dow Chemicals. The octene content is 40 wt% (or 14.29 mol%) which means that there are about 6 ethylene units per 1 octene unit. Molecular weight M_n is 228 000 g/mol.

The PP and EOC were melt-mixed (charge 5 g) at 200 °C for 5 min at 50 rpm in a miniature Haake Minilab II mixer, two conical screws being in counter-rotating mode. Blend ratio was gradually varied across the whole range. The melt-mixed blends were extruded and then compression pressed at 200 °C to sheets.

For the transmission electron microscopy (TEM) analysis, the specimens were stained with RuO_4 vapor at room temperature for 4 h. Then, they were microtomed to an ultrathin section of about 70 nm thick using a Reichert–Jung ultracryomicrotome with a diamond knife at room temperature. The structure was observed by an electron microscope, HITACHI H-7650 (accelerating voltage 100 kV).

Micro-tensile samples were cut from the sheets, using the die of standard dimensions according to ISO 12086.

For hysteresis measurements, the tensile stress–strain curves were measured at room temperature with an Alpha Tensometer 2000 testing machine at a crosshead speed of

10 mm min^{-1} . After the pre-set strain (100%, 200% and 300%) was attained, the crosshead was returned at the same speed. Tensile testing of the specimens to rupture was carried out at a crosshead speed of 100 mm min^{-1} with tensile modulus, stress at break and yield stress being noted.

For the DSC analysis, the specimens were heated in nitrogen atmosphere (flow rate 20 mL min^{-1}) at 10 °C min^{-1} . Cooling was performed with help of a cooling unit capable of -130 °C. The temperature and heat flow of the apparatus were calibrated with indium standard. Crystallinity (X_c) was calculated with a heat of fusion of 290 J g^{-1} for perfectly crystalline polyethylene [29].

3. Results and discussion

In Fig. 1, there are three TEM pictures with increasing PP content (20, 30 and 40 wt%). At 20% of PP there are PP particles with round shape uniformly dispersed in the EOC matrix. The diameter of these round particles was in the range 0.1–1 μm . When the PP content increased to 30%, the shape of the PP particles changed. The majority of particles have elongated shape with the smaller dimension being in the range of 0.5–1 μm and the larger dimension in the range 2–10 μm . In the case of 40% of PP, the shape of the PP particles was even more elongated and the structure looked almost like a co-continuous one.

In Fig. 2, we have focused on elastic behavior during stretching in the tensile test machine. The results for the chosen pre-programmed maximum strains of 100, 200 and 300% are shown in Fig. 2a–c, respectively. Since high PP content blends do not exhibit significant elastic behavior, only blends with lower PP content were compared in this hysteresis experiment (5–50 wt% of PP). The pure EOC has fairly good elastic behavior, which can be measured as residual strain after 100% stretching. As it is shown in Fig. 2a, this value is about 14%. The origin of such good elastic behavior can be explained with the help of Fig. 3. In the case of usual amorphous rubbers (such as butadiene–styrene), good elastic properties are achieved by chemical cross-linking. However, in the case of EOC, even without chemical cross-linking the elastic properties are very good. The cross-linking is not chemical but physical, more specifically achieved by small lamellar crystallites that connect the amorphous elastic chains. To support this statement we have carried out DSC measurements of pure EOC and EOC/PP blend. The results are shown in Fig. 4.

Table 2
Mechanical properties of PP/EOC blends after elongation.

PP/EOC	Modulus at given elongation (MPa)		Residual strain ϵ_r (%)		
	M100	M300	100% applied strain	200% applied strain	300% applied strain
0/100	1.1	1.6	14.0	35.7	52.3
10/90	1.7	2.6	15.8	39.4	63.9
20/80	2.0	2.9	17.3	43.3	69.0
25/75	3.2	4.6	20.7	62.0	104.2
30/70	4.6	5.6	24.6	66.7	122.1
40/60	6.0	6.9	48.0	120.1	164.0
50/50	8.7	9.6	52.2	132.3	218.4

Clearly, the EOC exhibits a melting peak at about 48 °C with the crystallinity being about 7 wt%. Clearly, large numbers of amorphous chains (93%) are held together by a small amount of lamellar crystals that act as tie points.

From the residual strain (ϵ_r) point of view, the pure EOC has the best elastic behavior. However, in real applications other properties are important too, such as how much load the article from the blend can carry, which can be expressed as the stress at a given elongation (M100 or M300—these values are frequently used in the rubber industry), modulus at very small elongation (used mainly in plastics industry), ultimate elongation at break and tensile strength. With increasing amount of PP, the stiffness increases at the expense of elastic properties, which worsen. Fig. 2a–c look very similar except for the increase of applied strain. The values of residual strain, ϵ_r , (shown by arrow) also increase, both with increasing applied strain and with PP content. It is important to mention that these values of residual strain are immediate ones. The process of returning to its original shape continues even after releasing from the clamps and can be measured after longer times. For example, pure EOC has value of immediate residual strain of 14% (after 100% stretching) but this value decreases to 0% after 24 h. Residual strain values after 24 h for 200 and 300% of applied strain were much lower than the immediate ones and are listed in Table 1. Even though the value after 24 h is important, the accuracy of reading this value is lower than the immediate one obtained from the stress–strain curve. Therefore, in the following figures only the values of immediate residual strain are shown.

Please note that stress–strain curves in Fig. 2a–c are just typical curves that are showing one particular test. The following figures that are summarizing various properties, e.g. residual strain or modulus as a function of PP content, show the average values with error bars from 10 experiments.

From Fig. 2c it is possible to read the values of stress at elongations of 100 and 300%, referred to as M100 and M300 in the rubber industry. These stress values are plotted as a function of PP content in Fig. 5. Even though the increase

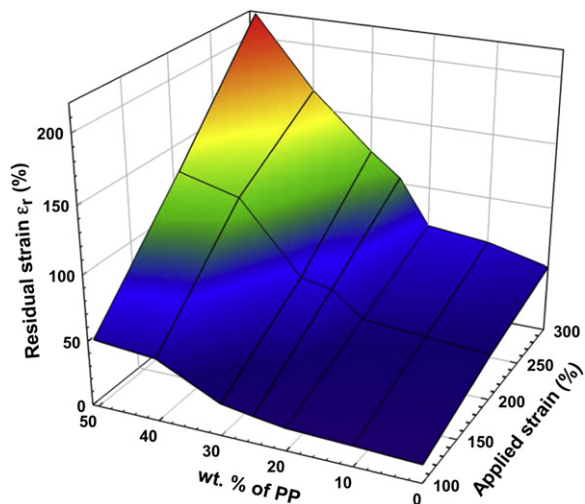


Fig. 7. 3D plot of residual strain as a function of applied strain and PP content.

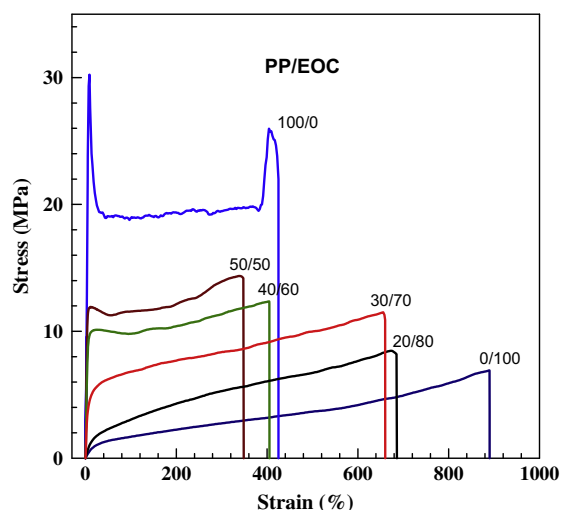


Fig. 8. Stress–strain curves of PP/EOC blends with crosshead speed 100 mm min⁻¹.

in absolute values (compare M300 and M100) is similar for all blend compositions, the increase in relative values is very different. There is about 45% increase in values from M100 to M300 for the low PP concentrations (e.g. 2.0 → 2.9 MPa for 20% PP) while the increase is only about 10% for blends with higher PP content (40 and 50%). In addition, there is only moderate increase in both M100 and M300 values in the range 0–20% of PP, while the increase is much steeper in the range 20–50% of PP. This fact is better understood with help of TEM pictures shown in Fig. 1.

In Fig. 6 there is a plot of residual strain as a function of PP content. There are three curves for three different values of applied strain. The values ϵ_r are gradually increasing with increasing applied strain. Focusing on the importance of PP content, again similar to Fig. 5, there is only moderate increase in ϵ_r for PP content in the range 0–20%, and much steeper increase in the range 20–50% of PP. In other words, the best elastic properties were found for blends with 10 and 20% of PP; the values of residual strain were close to values of pure EOC. Summary of the values presented in Figs. 5 and 6 is given in Table 2.

Table 3
Tensile properties of PP/EOC blends.

PP/EOC	Tensile modulus (MPa)	Stress at break (MPa)	Elongation at break (%)
0/100	8	5.9	860
10/90	17	6.3	655
20/80	17	8.0	646
25/75	37	7.8	627
30/70	93	11.6	602
40/60	306	11.8	316
50/50	415	11.4	85
60/40	534	11.9	17
70/30	603	12.1	5
75/25	705	18.9	17
80/20	743	19.3	7
90/10	887	24.6	6
95/5	1015	28.3	11
100/0	1102	30.8	425

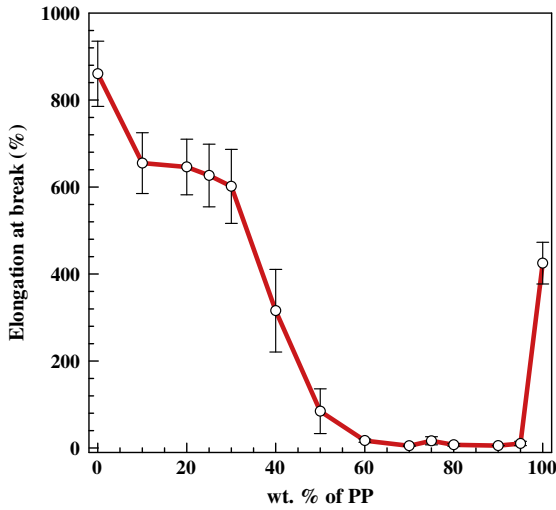


Fig. 9. Elongation at break vs. PP content.

Fig. 7 shows the 3D plot of the residual strain values as a function of PP content and also applied strain. The best elastic properties (the lowest ϵ_r value) were found for low PP content and small applied strain. The highest residual strain values were found for blends with high PP content stretched to 300% of applied strain.

Another set of experiments was focused on tensile measurement to break, as illustrated in Fig. 8. Complete results are summarized in Table 3. Pure EOC had almost 900% elongation at break and the blends with up to 30% of PP had elongation greater than 600%. The higher PP content the lower ultimate elongation together with higher modulus. The decrease in ultimate elongation is illustrated in Fig. 9. Such phenomenon was mentioned previously by Dias et al. for PP/HDPE blend where this poor elongation at break was explained by incompatibility of the two polymers [29]. Previous measurements shown in Fig. 2a–c were performed at a lower rate of 10 mm min⁻¹ and no yield points were observed for concentrations of 10–50% of PP.

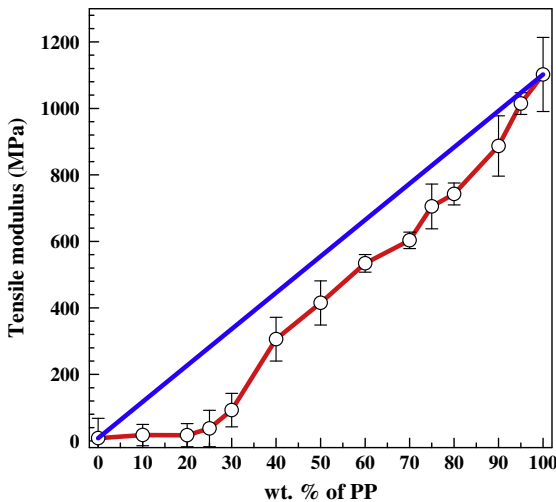


Fig. 10. Tensile modulus as a function of blend composition.

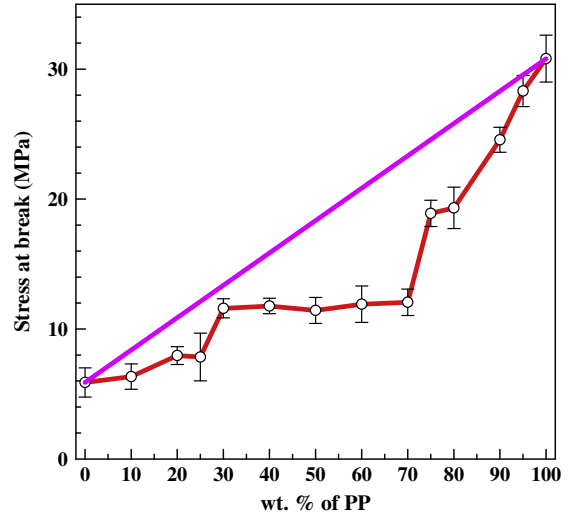


Fig. 11. Stress at break vs. PP content.

This time, the rate was set to 100 mm min⁻¹ and there were no yield points for blends 10–30% of PP, however, for concentrations 40 and 50% of PP there were very small yield points. At higher PP content the yield point was much more distinct, as shown for the example of pure PP.

Fig. 10 shows the tensile modulus as a function of PP content. It is very close to that of pure EOC when the concentration of PP is in the range 0–25%; even the blend with 30% of PP has very low modulus. In this case, PP acts as a hard filler in the soft EOC matrix. Blends with 40–95% of PP have modulus only slightly lower than one could expect from the linear mixing rule, which is shown by the line.

Another important industrially used value is stress at break. Fig. 11 shows this value for all tested blend compositions. For blends with high EOC content (10–40% of PP) and also high PP content (90–95% of PP), the stress at break

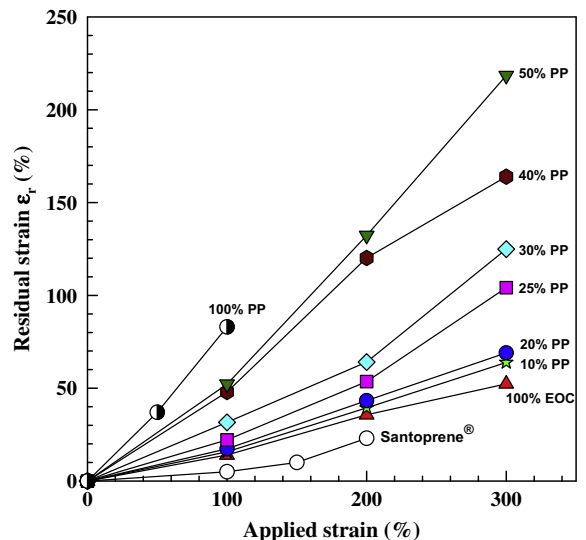


Fig. 12. Plot of residual strain vs. applied strain for PP/EOC blends.

is not very far from the ideal line. However, at concentrations 50–80% of PP the deviation is quite significant.

It is appropriate to compare the results of our blends with commercial thermoplastic elastomer (Santoprene® #201-73) on one side and pure PP on the other side, as shown in Fig. 12 where the residual strain is plotted as a function of applied strain. The values of ϵ_r for PP/EOC blends are not very far from Santoprene® when the PP content is low, while for high PP content the values are closer to pure PP. Optimized dynamic vulcanization would definitely improve the elasticity, but this will be the subject of a future paper.

4. Conclusions

EOC/PP blends exhibit fairly good elastic behavior when the PP content is low (0–30 wt%). Also, ultimate elongation is excellent for these blends. The EOC crystals (only 7 wt%) act as tie points for amorphous chains (93 wt%). With increasing PP content the modulus increases at the cost of worse elastic properties; the PP particles change shape from circular to elongated and then the structure resembles a co-continuous one. The residual strain values were found to be close to commercial thermoplastic elastomer Santoprene® #201-73.

Acknowledgement

This work has been supported by the Ministry of Education of the Czech Republic as a part of the project No. VZ MSM 7088352102.

References

- [1] H. Lee, D.H. Kim, Y. Son, Effect of octene content in poly(ethylene-co-1-octene) on the properties of poly(propylene)/poly(ethylene-co-1-octene) blends. *Journal of Applied Polymer Science* 103 (2) (2007) 1133–1139.
- [2] N.C. Nayak, D.K. Tripathy, Effect of aluminium silicate filler on morphology and physical properties of closed cell microcellular ethyleneoctene copolymer. *Journal of Materials Science* 37 (7) (2002) 1347–1354.
- [3] B. Swierz-Motysia, B. Jurkowska, M. Rajkiewicz, A preliminary study on the new thermoplastic vulcanizates. *Polimery* 52 (3) (2007) 203–209.
- [4] R.R. Babu, N.K. Singha, K. Naskar, Dynamically vulcanized blends of polypropylene and ethylene–octene copolymer: comparison of different Peroxides on mechanical, thermal, and morphological characteristics. *Journal of Applied Polymer Science* 113 (3) (2009) 1836–1852.
- [5] A.L.N. Da Silva, M.C.G. Rocha, F.M.B. Coutinho, R.E.S. Bretas, M. Farah, Evaluation of rheological and mechanical behavior of blends based on polypropylene and metallocene elastomers. *Polymer Testing* 21 (6) (2002) 647–652.
- [6] A.L.N. Da Silva, M.C.G. Rocha, F.M.B. Coutinho, R. Bretas, C. Scuracchio, Rheological and morphological properties of blends based on ethylene–octene copolymer and polypropylene. *Polymer Testing* 19 (4) (2000) 363–371.
- [7] A.L.N. Da Silva, M.C.G. Rocha, F.M.B. Coutinho, R.E.S. Bretas, C. Scuracchio, Rheological and thermal properties of binary blends of polypropylene and poly(ethylene-co-1-octene). *Journal of Applied Polymer Science* 79 (9) (2001) 1634–1639.
- [8] A.L.N. Da Silva, M.C.G. Rocha, F.M.B. Coutinho, R. Bretas, C. Scuracchio, Rheological, mechanical, thermal, and morphological properties of polypropylene/ethylene–octene copolymer blends. *Journal of Applied Polymer Science* 75 (5) (2000) 692–704.
- [9] T. McNally, P. McShane, G.M. Nally, W.R. Murphy, M. Cook, A. Miller, Rheology, phase morphology, mechanical, impact and thermal properties of polypropylene/metallocene catalysed ethylene 1-octene copolymer blends. *Polymer* 43 (13) (2002) 3785–3793.
- [10] A.L.N. Silva, M.C.G. Rocha, F.M.B. Coutinho, Study of rheological behavior of elastomer/polypropylene blends. *Polymer Testing* 21 (3) (2002) 289–293.
- [11] S. Mohanty, S.K. Nayak, Dynamic-mechanical and thermal characterization of polypropylene/ethylene–octene copolymer blend. *Journal of Applied Polymer Science* 104 (5) (2007) 3137–3144.
- [12] Y. Pang, X. Dong, K. Liu, C.C. Han, E. Chen, D. Wang, Ductile–brittle transition controlled by isothermal crystallization of isotactic polypropylene and its blend with poly(ethylene-co-octene). *Polymer* 49 (19) (2008) 4259–4270.
- [13] H. Bai, Y. Wang, B. Song, Y. Li, L. Liu, Effect of nucleating agent on the brittle–ductile transition behavior of polypropylene/ethylene–octene copolymer blends. *Journal of Polymer Science: Part B: Polymer Physics* 46 (6) (2008) 577–588.
- [14] J.-R. Ying, S.-P. Liu, F. Guo, X.-P. Zhou, X.-L. Xie, Non-isothermal crystallization and crystalline structure of PP/POE blends. *Journal of Thermal Analysis and Calorimetry* 91 (3) (2008) 723–731.
- [15] O. Prieto, J.M. Perena, R. Benavente, M.L. Cerrada, E. Perez, Effect of composition and molecular weight on the crystallization behavior of blends of iPP and a metallocenic ethylene/1-octene copolymer. *Macromolecular Chemistry and Physics* 203 (12) (2002) 1844–1851.
- [16] K. Meng, X. Dong, X.H. Zhang, C.G. Zhang, C.C. Han, Shear-induced crystallization in a blend of isotactic poly(propylene) and poly(ethylene-co-octene). *Macromolecular Rapid Communications* 27 (19) (2006) 1677–1683.
- [17] M.L. Cerrada, O. Prieto, J.M. Perea, R. Benavente, E. Pérez, Blends of isotactic polypropylenes and a plastomer: crystallization and viscoelastic behavior. *Macromolecular Symposia* 198 (1) (2003) 91–101.
- [18] X. Yan, X. Xu, L. Zhu, Analysis of brittle–ductile transition of polypropylene/ethylene–octene copolymer blends by scanning electron microscopy and small angle laser light scattering. *Journal of Materials Science* 42 (20) (2007) 8645–8651.
- [19] X. Xu, X. Yan, T. Zhu, C. Zhang, J. Sheng, Phase morphology development of polypropylene/ethylene–octene copolymer blends: effects of blend composition and processing conditions. *Polymer Bulletin* 58 (2) (2007) 465–478.
- [20] X. Xu, T. Zhu, X. Van, C. Zhang, Temporal evolution of phase morphology of polypropylene/poly(ethylene octene) elastomer binary polymer blends by phase contrast microscope. *Journal of Applied Polymer Science* 104 (5) (2007) 2778–2784.
- [21] X. Yan, X. Xu, T. Zhu, C. Zhang, N. Song, L. Zhu, Phase morphological evolution and rheological properties of polypropylene/ethylene–octene copolymer blends. *Materials Science and Engineering A* 476 (1–2) (2008) 120–125.
- [22] H. Lu, Y. Hu, M. Li, L. Song, Clay intercalation and influence on flammability and crystallization behaviors of POE-based nanocomposites. *Polymer Composites* 29 (12) (2008) 1358–1363.
- [23] Y. Liu, M. Kontopoulou, Effect of filler partitioning on the mechanical properties of TPO/nanosilica composites. *Journal of Vinyl and Additive Technology* 13 (3) (2007) 147–150.
- [24] J.R. Austin, M. Kontopoulou, Effect of organoclay content on the rheology, morphology, and physical properties of polyolefin elastomers and their blends with polypropylene. *Polymer Engineering and Science* 46 (11) (2006) 1491–1501.
- [25] M. Xiaoyan, L. Guozheng, L. Haijun, H. Yun, Novel intercalated nanocomposites of polypropylene, organic rectorite, and poly(ethylene octene) elastomer: morphology and mechanical properties. *Journal of Applied Polymer Science* 97 (5) (2005) 1907–1914.
- [26] M. Maiti, S. Sadhu, A.K. Bhowmick, Ethylene–octene copolymer (engage)-clay nanocomposites: preparation and characterization. *Journal of Applied Polymer Science* 101 (1) (2006) 603–610.
- [27] C.G. Ma, Y.L. Mai, M.Z. Rong, W.H. Ruan, M.Q. Zhang, Phase structure and mechanical properties of ternary polypropylene/elastomer/nano-CaCO₃ composites. *Composites Science and Technology* 67 (14) (2007) 2997–3005.
- [28] M. Bailly, M. Kontopoulou, Preparation and characterization of thermoplastic olefin/nanosilica composites using a silane-grafted polypropylene matrix. *Polymer* 50 (11) (2009) 2472–2480.
- [29] P. Dias, Y.J. Lin, B. Poon, H.Y. Chen, A. Hiltner, E. Baer, Adhesion of statistical and blocky ethylene–octene copolymers to polypropylene. *Polymer* 49 (12) (2008) 2937–2946.
- [30] W.-Y. Guo, B. Peng, Rheology, morphology, and mechanical and thermal properties of blends of propylene based plastomer and ethylene/1-octene copolymer. *Journal of Elastomers and Plastics* 40 (1) (2008) 61–76.

PAPER 2

A study on electrical and thermal conductivities of ethylene-octene copolymer/expandable graphite composites

Petr Svoboda*, Rajesh Theravalappil, Sameepa Poongavalappil, Jarmila Vilcakova,
Dagmar Svobodova, Pavel Mokrejs, Antonin Blaha

*Centre of Polymer Systems, Tomas Bata University in Zlin, Nam.TG Masaryka
5555, 760 01, Zlin, Czech Republic.*

* Corresponding author. Tel. 420–576 031 335, fax. 420–577 210 172.

E-mail address: svoboda@ft.utb.cz (P. Svoboda)

Abstract

A series of ethylene-octene copolymer (EOC) composites have been prepared by melt-mixing with different weight ratios of expandable graphite filler (0-50% by weight). Electrical conductivity [both alternating current (AC) and direct current (DC)] and thermal conductivity studies were carried out. Effect of filler loading and frequency on electrical conductivity was studied. DC conductivity has increased from $1.51 \times 10^{-13} \text{ S cm}^{-1}$ to $1.17 \times 10^{-1} \text{ S cm}^{-1}$. Percolation threshold by DC and also AC methods was observed at about 16 vol. % of the filler. Real part of permittivity was found to be decreasing with increase in frequency while conductivity was increasing. Thermal conductivity was also found to be increasing gradually from 0.196 to $0.676 \text{ W m}^{-1} \text{ K}^{-1}$ which is about 245% increase. Graphite not only increases the electrical and thermal conductivities but at and above 40 wt. %, also acts as a halogen-free, environmental friendly flame retardant. Shore-A hardness of EOC/graphite composites shows that even with high graphite loading, the hardness is increased from about 50 to 68 only so that the rubbery nature of the composite is not affected very much.

Key words: EOC; expandable graphite; electrical conductivity; percolation threshold; thermal conductivity.

Introduction

Polymer composites with conducting fillers serve as electrical or thermal conductors and have wide range of applications in the electric and electronic fields.

These composites have an advantage of conductivity of a filler and favorable properties of polymer material together. They are widely used in many areas like electrodes, separators, electromagnetic shielding and anti-static coating [1, 2]. The fillers generally subjected for conductivity studies are carbon fibers [3, 4], multi-wall carbon nanotubes (MWCNT) [5], natural fibers e.g. sisal fibers [6], expanded graphite [7], carbon black [8] and graphene [9].

Ethylene-octene copolymer (EOC) is a new type of copolymer developed by The Dow Chemical Company through constrained geometry catalyst technology (CGCT) under the trade name ENGAGE[®]. It is being considered for use in diverse applications such as cushioning agents, gaskets, and is particularly good alternative for sealing application due to its structural regularity and non-toxic composition. Several researchers have studied the conductivity properties of EOC composites using different fillers such as carbon black, polyaniline, and multi-wall carbon nanotubes [10-12]. Conducting polymer composites (CPC) with elastomeric polymer matrices have applications in the field of sensors, e.g. temperature sensors [13] and strain sensors [14].

Charge transport in polymer composite materials has been the object of many researches in the past. Conducting mechanism in composites containing conductive particles can be described by percolation theory [15]. The volume fraction of fillers above which the continuous conducting paths are created is known as percolation threshold. At this level, a continuous chain of particles in the matrix results in a considerable increase in conductivity of several orders. Conductivity above percolation threshold increases sharply and composites start behaving like semiconductors [16-19].

Permittivity is the ability of a material to store charge when used as a dielectric material. Capacitance and conductance as a function of frequency can be measured by dielectric analysis which can be then utilized to calculate real part (ϵ') and imaginary part (ϵ'') of permittivity and the dielectric loss factor ($\tan \delta$) [20].

Extensive studies have been performed on conductivity of numerous composites with different polymers as matrix and various fillers. Several researchers prepared composites by the incorporation of halogen-free flame retardant expandable graphite for the improvement of flame retardancy and thermal stability [21-24]. Expandable graphite as a conducting filler has been studied only few times [25, 26]. Only few researchers performed the conductivity studies using EOC as a matrix [10, 12]. In this paper, electrical and thermal conductivities of

EOC/expandable graphite composites have been studied. Also, flame retardancy according to UL-94 (Underwriters Laboratories) horizontal test was evaluated.

Experimental

Materials

Ethylene-octene copolymer was Engage 8842 supplied by Dow Chemicals. The octene content was 45 wt. %, density = 0.8595 g cm^{-3} and melt flow index (MFI) = 1.02 dg min^{-1} (at $190 \text{ }^\circ\text{C}$ /2.16 kg).

Expandable graphite flakes were Grafguard 160-50N, used as received from Graftech Inc., Ohio, Cleaveland, USA. Mean particle size was $350 \text{ }\mu\text{m}$ and density was about 2 g cm^{-3} .

Composite and sample preparation

EOC and Grafgurad 160-50N were melt-mixed in a Brabender Plasti-corder PL2000 mixing machine with a mixing volume of 50 cm^3 at $100 \text{ }^\circ\text{C}$ at mixing speed 50 rpm for 10 minutes. Graphite was preheated in a hot air oven at $100 \text{ }^\circ\text{C}$ for 12 h to remove any absorbed moisture. Graphite content was: 5, 10, 15, 20, 25, 30, 35, 40, 45, 50 wt. % or 2, 5, 7, 10, 13, 16, 19, 22, 26, 30 vol.%, respectively. The melt-mixed composites were then compression molded to 2 mm thick sheets at $110 \text{ }^\circ\text{C}$. From this sheet two discs were cut out: for the electrical conductivity measurement the disc had diameter 15 mm and for the thermal conductivity measurement it was 50 mm. Samples for flammability tests were cut out of the sheet according to UL-94 standard with sample dimensions being $125 \times 13 \times 2 \text{ mm}$. For shore-A hardness measurements the discs had diameter 50 mm and thickness 6 mm.

Scanning Electron Microscopy (SEM)

Morphology of the expandable graphite filler and composites was studied by using SEM technique. SEM analysis was carried out using Vega II LMU (Tescan, Czech Republic) with a beam acceleration voltage set at 10 kV.

Direct current (DC) conductivity

The current-voltage dependencies were measured in the two-point setup using electrodes of cylindrical shape (13 mm in diameter and covered by a layer of gold) with a programmable electrometer (Keithley 6517 A, USA). The DC conductivity was calculated from the current–voltage dependence in the range of 1–20 V. Current-Voltage characteristics were measured in DC field. Specific electrical conductivity, σ_{DC} , can be expressed as follows:

$$\sigma_{DC} = \frac{I}{U} \cdot \frac{d}{A} \quad (1)$$

where, I is the electrical current, U is the voltage, A is area of electrodes and d is the thickness of the sample.

Four-point method (Van der Pauw) [27] was used for the measurement of samples with conductivity higher than 10^{-3} S cm⁻¹. A main advantage of four-probe measurements is the elimination of contact resistance [28]. All the properties were measured at room temperature (22-25 °C).

Dielectric properties and alternating current (AC) conductivity

Dielectric characteristics involving the frequency dependence of the real part (dielectric constant, ϵ') and imaginary part of the complex permittivity (dielectric loss, ϵ'') in the frequency range of 1 MHz – 3 GHz were determined with an Radio Frequency (RF) Impedance Analyzer (Agilent E4991A, USA) using capacitive method (on a dielectric material test fixture which comes furnished with the device). After inputting the sample thickness the device automatically calculates and yields frequency dependence of complex permittivity ϵ^* . In the range of 10 Hz-100 KHz, dielectric characteristics were measured by using Hioky 3522 (LCR Hi Tester, Japan). The dielectric constant was calculated from the measured capacitance.

AC conductivity, σ_{AC} , was calculated from imaginary part of complex permittivity, ϵ'' , which was directly obtained from the instrument, following the equation (2):

$$\sigma_{AC} = 2\pi f \cdot \epsilon_0 \cdot \epsilon'' \quad (2)$$

where, ϵ_0 is permittivity of vacuum and f is frequency.

Thermal conductivity

Thermal conductivity of EOC/graphite composites was measured according to Fitch (1935) [29] where the sample is sandwiched between a constant temperature heat source and a brass cylinder as heat sink insulated on all faces but one, as shown in Figure 1. The advantage of this approach is most of all short time of measurement and also the simplicity of the procedure and also the simplicity of the measuring instrument. During the quasisteady heat conductivity measurement, the temperature at certain place changes with time. The common procedure involves a case when the heat flows only in one direction. Then temperature depends only on time and one coordinate. This instrument is

usually used for the measurement of thermal conductivity of thin sheets or slabs from various plastics and rubber and also for leather.

The principle of measuring instrument and the procedure is explained below. Initially the central brass cylinder (CBC) with diameter 5cm is annealed to reach $t_2=45$ °C with the help of another hollow brass cylinder that was connected to a water thermostat by rubber hoses. The water thermostat's accuracy was 0.1 °C. This takes about 6 min. Then the 45 °C cylinder is quickly removed, measured sample with diameter 5cm and thickness about 2mm is placed on the top of the CBC and on the top of measured sample another hollow brass cylinder connected to another water thermostat with temperature $t_1=25$ °C is placed. On the top a 100g weight was placed. The heat is being transferred from the CBC through the sample to colder brass cylinder (25 °C). The temperature of the CBC is decreasing rapidly. The data acquisition of the decreasing temperature of the CBC is being done with the help of a thermocouple (type copper-constantan) that was connected to a National Instruments data acquisition equipment (NI USB-9211A, Portable USB-Based DAQ (Data Acquisition) for Thermocouples) that was connected to a computer by USB. Software LabVIEW Signal Express 2.5 was used for temperature data acquisition. Sampling period was set to 5s. The measurement took about 25 min. The non-linear analysis (exponential decay) of the time-temperature curve was performed.

Mathematical model for the measurement

For the derivation of mathematical model describing dependence of the temperature of the CBC on time we start with following heat balance.

$$-K \frac{dt}{d\tau} = \frac{S\lambda(t - t_1)}{\delta} + B(t - t_1) \quad (3)$$

Where,

$$t(\tau=0) = t_2 = 45 \text{ °C}$$

K is the heat capacity of the CBC, central brass cylinder (J K^{-1})

S is the sample area (m^2)

λ is the thermal conductivity ($\text{W.m}^{-1}.\text{K}^{-1}$)

t is acquired temperature of the CBC (°C)

t_1 is the temperature of hollow brass cylinder 25 (°C)

t_2 is initial temperature of CBC (°C)

δ is the thickness of the sample (m)

B is the coefficient accounting for a heat loss ($J.s^{-1}.K^{-1}$)

τ is the time (s)

B can be calculated according to

$$B = \alpha S_z \quad (4)$$

Where α is heat transfer coefficient ($W.m^{-2}.K^{-1}$) and S_z is the heat loss area (m^2).

Right side of Equation (3) represents heat flow through the mass of the measured sample. The heat loss caused by natural flow of the air around the measuring instrument is accounted for.

We start with energy balance. Left side of Eq. (3) corresponds to immediate heat output of the central brass cylinder from initial $t_2=45$ °C to the equilibrium temperature $t_1=25$ °C. Thermal energy that is leaving the CBC is realized by two ways. Larger part occurs by conduction heat transfer through the measured sample. Smaller part is heat loss to the surrounding environment that is caused by natural air flow and also by radiation. This part of the equation is determined by so called “blind experiment” when instead of measured sample we place material with very small thermal conductivity. We have used expanded polystyrene with $\lambda=0.035$ W/mK. The important is a good contact of the measured sample with both brass cylinders. In case of hard samples like PP we have to use special thermally conductive paste (aluminum powder in silicone oil). In our case of CNT/silicone composites we did not have to use this special conductive paste because the samples were soft and the contact was perfect.

By solving Eq. (3) we get

$$t = t_1 - (t_1 - t_2) * e^{-(A_1+A_2)\tau} \quad (5)$$

Where for A_1 and A_2 constants are given by Eq. (6) and (7).

$$A_1 = \frac{S\lambda}{\delta K} \quad (6)$$

$$A_2 = \frac{B}{K} \quad (7)$$

Practical calculation goes as follows. Eq. (5) can be simplified for the non-linear regression (exponential decay):

$$y = y_0 + ae^{(-bx)} \quad (8)$$

From a non-linear regression we get coefficient b. For example for pure EOC we got $b=0.002382$ (from Figure 2).

The heat loss from the instrument obtained by blind experiment is $A_2 = 0.000368 \text{ s}^{-1}$. Thermal capacity of the central brass cylinder was $K_1 = 94.107 \text{ J K}^{-1}$. Area of measured cylinder was $S = 1.9635 \cdot 10^{-3} \text{ m}^2$.

Then the thermal conductivity can be calculated as shown by Eq. (9) and (10).

$$A_1 = b - A_2 = 0.002382 - 0.000368 = 0.002014 \quad (9)$$

$$\lambda = \frac{A_1 \delta K_1}{S} = \frac{0.002014 * 0.002305 * 94.107}{\frac{\pi 0.05^2}{4}} = 0.196 \text{ Wm}^{-1}\text{K}^{-1} \quad (10)$$

Flammability test

Horizontal flammability test was carried out according to the UL-94 standard. Burner with yellow-tipped blue flame of 20 ± 1 mm height was used for the test. Samples were held horizontally at an angle of 45° and ignited using the flame for 30 ± 1 seconds. Samples had two marks; one at 25 mm and another at 100 mm. Test was conducted for three specimens in each category.

Shore-A hardness

Hardness of the EOC/expandable graphite composites has been measured using Bareiss Shore-A hardness tester (Model HHP-2001).

Results and discussion

Morphology of composites

Flakes-like structure of the expandable graphite filler is clearly shown in Figure 3a. Morphology of the composites, displayed in Figure 3b, 3c and 3d, helps us to understand the distribution of expandable graphite flakes in the polymer matrix. There are three micrographs of composites shown here: one below percolation threshold (3b), one around (3c) and the third one (3d) above the

percolation threshold. One can observe increasing amount of graphite particles in the composite (3b→3d), with uniform dispersion of the particles which implies thorough mixing.

DC conductivity (σ_{DC})

Conductivity of polymer composites with conducting fillers is greatly affected by filler loading level and distribution or filler alignment in the matrix. Figure 4 shows the dependence of DC conductivity on graphite level. It is very clearly visible from the plot that a sharp increase in the conductivity at particular filler level called percolation threshold. At and above this level, free movement of charge carriers makes the system more conductive or in other words, continuity between the conducting graphite flakes is created. Below percolation threshold, for example, at 5% graphite level, the conductivity is only $1.5 \times 10^{-13} \text{ S cm}^{-1}$. Here, conductive paths were not developed and the conductivity may be due to that of ionic conductivity of the polymer composite. From the graph, one can estimate that the percolation threshold lies around 30 wt. % (or 16 vol. %) of graphite loading, where conductivity shows a sharp increase. For a mathematical model system of conducting spheres, randomly distributed in a non-conducting matrix, percolation at 16–17 vol.% was calculated [30]. And our value of percolation level is in good agreement with this model. Above percolation threshold, amount and distribution of filler increases and thus conductivity becomes easier. Small value of the deviations reveals good homogeneity of polymer composite systems, which is also supported by the SEM micrographs of the composites.

The relation of conductivity, σ with volume fraction of the filler can be explained by the power law model of conductivity [15] which is given as:

$$\sigma = \sigma_0 (\phi - \phi_c)^t \quad (11)$$

where, σ_0 is the conductivity of the filler ($1.33 \times 10^4 \text{ Scm}^{-1}$, in the case of graphite flakes), ϕ is the volume fraction of the filler, ϕ_c is the critical volume fraction and t is the universal exponent determining the power of the electrical conductivity increase above ϕ_c . The plot of $(\log \sigma - \log \sigma_0)$ versus $\log(\phi - \phi_c)$ is shown as an inset in the Figure 4. Slope of this curve gives the value of t . Calculated value of t from previous research was found to be in the range of 1.5 - 2.0 [31], in our case $t=1.77$, which is in good agreement with the literature.

AC conductivity (σ_{AC})

Dielectric properties of EOC/graphite composites were measured in an alternating electric field. Dependence of AC conductivity on frequency is shown in Figure 5. According to Eqn. (1), AC conductivity, σ_{AC} , is proportional to imaginary part of permittivity and frequency. As the frequency increases, AC conductivity also increases, according to Equation (2). For lower concentrations (20, 25, 30 wt.%) the AC conductivity is increasing with frequency, therefore conductivity is provided by polarization current of fixed dipoles. AC conductivity in the low frequency region have some relations with DC conductivity. Above percolation level (35-40 wt.%), at low frequencies, the plateau relates to the values of DC conductivity, which is in good agreement with results determined by DC conductivity measurements. Similar observations were made by other researchers also [32].

AC conductivities of all compositions at four selected frequencies, 10^3 , 10^6 , 10^7 and 10^9 Hz, are shown in Figure 6. As the frequency increases, percolation behaviour in the 30-35 wt. % graphite range is not so prominently seen like in the case of low frequencies and almost disappears at high frequencies. At high frequencies, rather than percolation, there is a gradual increase in AC conductivity with increasing graphite content. It shows the effect of frequency on the AC conductivity. In the case of composites with 10 – 50 wt.% of graphite, at low frequency, conductivity increases from 10^{-11} to 10^{-2} Scm^{-1} ; we can observe an increment of 9 orders. But at higher frequency, this rise ranges only from 10^{-3} to 1 Scm^{-1} , only of 3 orders.

Dielectric constant (ϵ')

As shown in Figure 7, for filler content 0-30 wt. %, ϵ' value is equal to around 10^1 and for filler content above 30 wt. %, ϵ' value is around 10^7 at the frequency 10^1 Hz and it is illustrated that as the filler content increases, ϵ' value also increases. As the frequency increases, permittivity decreases. This can be attributed to the interfacial polarization (IP) of the filler. At low frequencies, all types of polarization contribute to the resulting value of permittivity, in our case predominantly interfacial polarization, typical for systems containing phases of different specific conductivity. IP arises in electrically heterogeneous materials such as composites and known as the Maxwell-Wagner-Sillars (MWS) effect [20]. The IP leads to an increase in ϵ' due to the motion of virtual charges, which get trapped at the interface of components of a multiphase material of different conductivity [33]. Similar observations have been

made by Paul and Thomas [6]. Permittivity as a function of graphite content is shown in Figure 8. As in the case of conductivity, percolation behavior at low frequencies (10^3 Hz) is more prominent than at higher frequencies.

Thermal conductivity (λ)

Thermal conductivity as a function of graphite content is given in Figure 9. As it can be seen from the figure, thermal conductivity increases as the filler content increases. Thermal conductivity of pure EOC matrix was found to be $0.196 \text{ W m}^{-1}\text{K}^{-1}$ while a 30 wt.% graphite loading increased the value almost 100% to $0.393 \text{ Wm}^{-1}\text{K}^{-1}$ and for 50 wt.%, the λ value was $0.676 \text{ W m}^{-1}\text{K}^{-1}$ i.e. about 245% increase. Uniform dispersion of the filler has high influence on the increase in thermal conductivity as in the case of electrical conductivity. Since graphite is good conductor of heat and electricity, the increase in graphite level will result in an increase in electrical and thermal conductivity of the EOC/graphite composites.

Flammability testing

Flammability test (Horizontal Burning - HB classification) was carried out according to the UL-94 standard. Composites with graphite loading less than 40 wt. % burnt all the way up to the holder. Only samples with filler loading 40, 45 and 50 wt. % did not burn to the holder, the flame self-extinguished. Photograph of these three specimens is given in Figure 10. The EOC/graphite composites can be classified as HB according to the UL-94 standards since their burning rates did not exceed 75 mm min^{-1} , the maximum burning rate was found to be 47 mm min^{-1} .

Shore-A hardness

Composites of soft matrix polymers with conducting fillers are being used as strain or pressure sensors [34]. Thus hardness of these composites has practical importance. Shore-A hardness of the graphite/EOC composites has been measured and it was found to be increasing with increasing graphite content. See Figure 11. Shore-A hardness of pure EOC matrix was 50 while addition of 5% graphite increased the value to 55. Even the addition of 50 wt. % of graphite resulted in a hardness value of only 68. This shows that hardness of EOC/expandable graphite composites did not increase markedly with the addition of graphite filler, or in other word higher loadings of graphite did not hamper the rubbery nature of the EOC matrix. This is important in case of applications involving sensors when the electric conductivity is changing with pressure [34]. This will be the subject of our future study.

The softness of the composite was important also for the measurement of thermal conductivity. Very hard samples such as polypropylene (PP) might not have flat surface (especially after injection molding). Rough surface creates an air gap between the sample and the conducting metal. When the sample is soft, there is no such air gap, rendering perfect contact which assures proper thermal conductivity measurement.

Conclusions

Both AC and DC conductivities of EOC/graphite composites were found to be increasing with increase in graphite content. Percolation threshold has been observed at about 16 vol. % in both cases (DC and AC conductivities). Thermal conductivity of the composites showed a trend of increment with addition of graphite filler, but no percolation threshold was observed. Horizontal flame test according to the UL-94 standard proved the role of expandable graphite filler as an environmentally friendly halogen-free flame retardant. EOC composites with graphite content higher than 40 wt. % (or 22 vol. %) showed self-extinguishing behavior during horizontal flame test. Higher loadings of expandable graphite filler did not cause serious reduction in rubbery nature of the EOC/expandable graphite composites which could be potentially used in applications like pressure or temperature sensors. In summary these composites possess good electrical and thermal conductivities together with significant flame retardancy at higher loadings without extreme increase in hardness values.

Acknowledgments

This work has been supported by the Ministry of Education of the Czech Republic as a part of the project No. VZ MSM 7088352102, Operational Programme Research and Development for Innovations co-funded by the European Regional Development Fund (ERDF) and national budget of Czech Republic within the framework of the Centre of Polymer Systems project (reg.number: CZ.1.05/2.1.00/03.0111) and also by the Internal Grant Authority (IGA/23/FT/11/D) of Tomas Bata University in Zlin.

References

1. V.S. Mironov, J.K. Kim, M. Park, S. Lim, W.K. Cho, *Polym. Test.*, **26**, 547–555 (2007).
2. Q. Zhang, H. Xiong, W. Yan, D. Chen, M. Zhu, *Polym. Eng. Sci.*, **48**, 2090 - 2097 (2008).
3. Q. Chen, Y. Xi, Y. Bin, M. Matsuo, *J. Polym. Sci. Pol. Phys.*, **46**, 359-369 (2008).
4. J. Vilcakova, P. Saha, O. Quadrat, *Eur. Polym. J.*, **38**, 2343-2347 (2002).
5. W.-y. Wang, G.-h. Luo, F. Wei, J. Luo, *Polym. Eng. Sci.*, **49**, 2144-2149 (2009).
6. A. Paul, S. Thomas, *J. Appl. Polym. Sci.*, **63**, 247-266 (1997).
7. R.K. Goyal, S.D. Samant, A.K. Thakar, A. Kadam, *J. Phys. D. Appl. Phys.*, **43**, 1-7 (2010).
8. N.M. Renukappa, Siddaramaiah, R.D.S. Samuel, J.S. Rajan, J.H. Lee, *J. Mater. Sci.- Mater. El.*, **20**, 648-656 (2009).
9. H. Kim, A.A. Abdala, C.W. Macosko, *Macromolecules*, **43**, 6515–6530 (2010).
10. S. Bhadra, N.K. Singha, D. Khastgir, *Polym. Eng. Sci.*, **48**, 995-1006 (2008).
11. S. Hom, A.R. Bhattacharyya, R.A. Khare, A.R. Kulkarni, M. Saroop, A. Biswas, *Polym. Eng. Sci.*, **49**, 1502-1510 (2009).
12. J.-C. Huang, H.-L. Huang, *J. Polym. Eng.*, **17**, 213-229 (1997).
13. W.-P. Shih, L.-C. Tsao, C.-W. Lee, M.-Y. Cheng, C. Chang, Y.-J. Yang, K.-C. Fan, *Sensors*, **10**, 3597-3610 (2010).
14. S.A. Mansour, *eXPRESS Polym. Lett.*, **2**, 836-845 (2008).

15. S. Kirkpatrick, *Rev. Mod. Phys.*, **45**, 574-588 (1973).
16. Y.R. Hernandez, A. Gryson, F.M. Blighe, M. Cadek, V. Nicolosi, W.J. Blau, Y.K. Gun'ko, J.N. Coleman, *Scripta Mater.*, **58**, 69-72 (2008).
17. M.H. Al-Saleha, U. Sundararaj, *Carbon*, **47**, 2-22 (2009).
18. W. Zhang, A.A. Dehghani-Saniij, R.S. Blackburn, *J. Mater. Sci.*, **42**, 3408-3418 (2007).
19. R. Strumpler, J. Glatz-Reichenbach, *J. Electroceram.*, **3**, 329-346 (1999).
20. H. Hammami, M. Arous, M. Lagache, A. Kallel, *J. Alloy. Compd.*, **430**, 1-8 (2007).
21. X.Y. Meng, L. Ye, X.G. Zhang, P.M. Tang, J.H. Tang, X. Ji, Z.M. Li, *J. Appl. Polym. Sci.*, **114**, 853-863 (2009).
22. X.L. Chen, J. Yu, S.J. Lu, H. Wu, S.Y. Guo, Z. Luo, *J. Macromol. Sci. Part B-Phys.*, **48**, 1081-1092 (2009).
23. C.-H. Chen, W.-H. Yen, H.-C. Kuan, C.-F. Kuan, *Polym. Composite.*, **31**, 18-24 (2010).
24. C.-L. Chiang, S.-W. Hsu, *J. Polym. Res.*, **17**, 315-323 (2010).
25. B.J. Qu, R.C. Xie, *Polym. Int.*, **52**, 1415-1422 (2003).
26. H. Fukushima, L.T. Drzal, B.P. Rook, M.J. Rich, *J. Therm. Anal. Calorim.*, **85**, 235-238 (2006).
27. L.J. Van der Pauw, *Philips Res. Rep.*, **13**, 1-9 (1958).
28. F.G.d.S. Jr., B.G. Soares, J.C. Pinto, *Eur. Polym. J.*, **44**, 3908-3914 (2008).

29. J.E. Lozano, *Fruit Manufacturing: Scientific Basis, Engineering Properties and Deteriorative Reactions of Technological Importance*, Springer Science Business Media LLC., New York, (2006).
30. H. Scher, R. Zallen, *J. Chem. Phys.*, **53**, 3759-3761 (1970).
31. N.K. Srivastava, V.K. Sachdev, R.M. Mehra, *J. Appl. Polym. Sci.*, **104**, 2027-2033 (2007).
32. M. Pelíšková, J. Vilčáková, R. Moučka, P. Sába, J. Stejskal, O. Quadrat, *J. Mater. Sci.*, **42**, 4942-4946 (2007).
33. F. Kremer, A. Schonhals, *Broadband Dielectric Spectroscopy*, Springer-Verlag, Berlin Heidelberg, (2003).
34. S. Bhadra, N.K. Singha, D. Khastgir, *Curr. Appl. Phys.*, **9**, 396–403 (2009).

Figure captions

Figure 1. Schematic diagram of the apparatus used for thermal conductivity measurement.

Figure 2. Thermal conductivity measurement: raw data. Temperature as a function of time for EOC/graphite composites with various graphite content. Initial temperature was 45 °C and equilibrium temperature was 25 °C. Sample had diameter 50 mm and thickness about 2 mm.

Figure 3. SEM micrographs of (a) Expandable graphite and EOC/expandable graphite composites with (b) 20, (c) 30 and (d) 40 wt. % of filler.

Figure 4. Dependence of DC conductivity on graphite content.

Figure 5. AC conductivity vs. frequency of EOC/graphite composites.

Figure 6. AC conductivity as a function of graphite content at different frequencies.

Figure 7. Real part of permittivity as a function of frequency.

Figure 8. Permittivity as a function of graphite content at different frequencies.

Figure 9. Thermal conductivity as a function of graphite content.

Figure 10. Samples after horizontal flame testing.

Figure 11. Shore-A hardness as a function of graphite content.

Figures

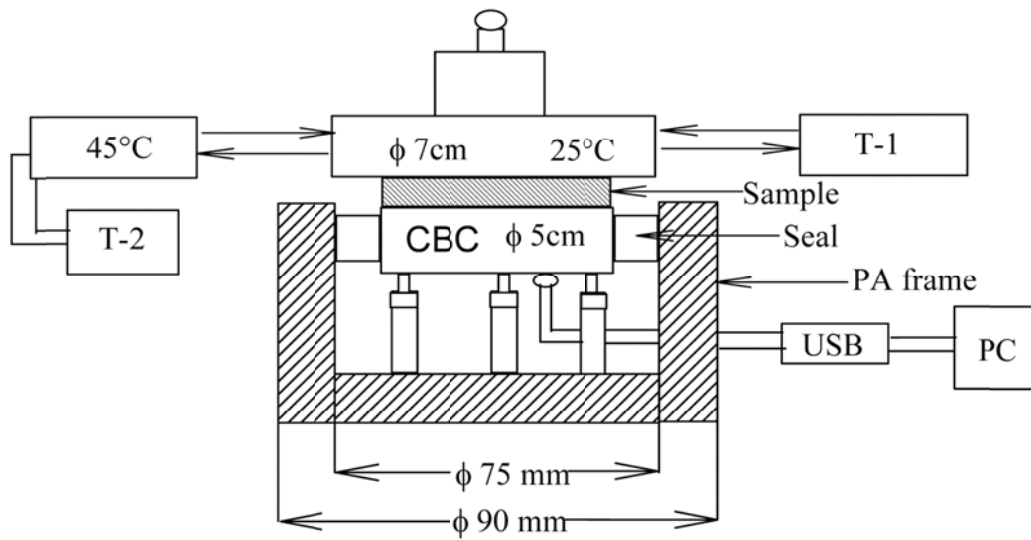


Figure 1. Schematic diagram of the apparatus used for thermal conductivity measurement.

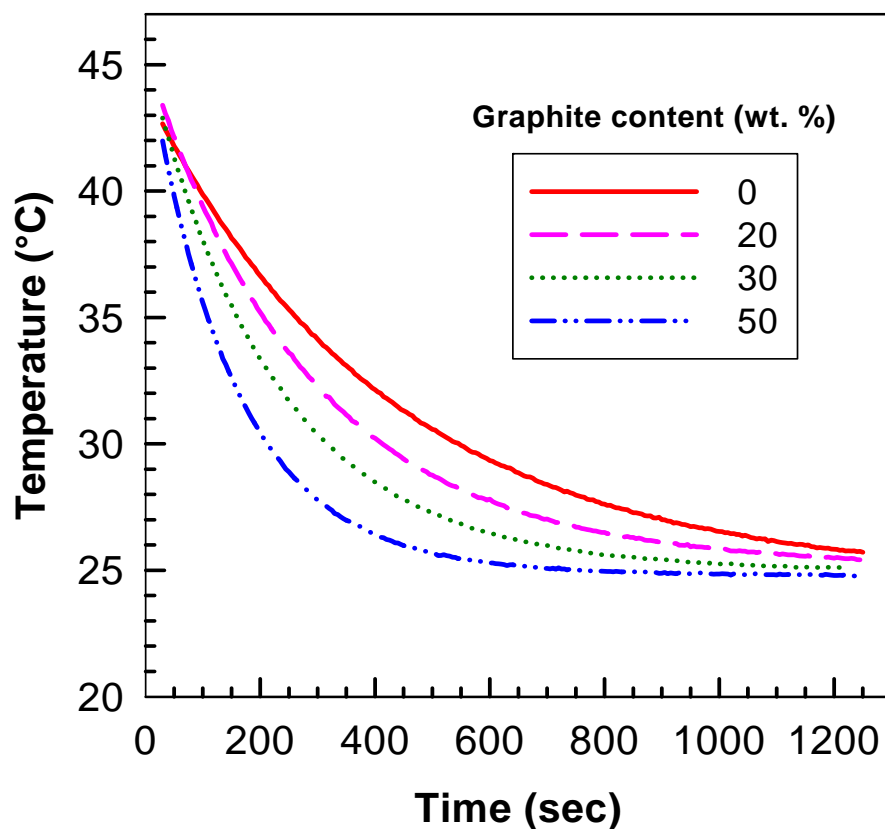


Figure 2. Thermal conductivity measurement: raw data. Temperature as a function of time for EOC/graphite composites with various graphite content. Initial temperature was 45 °C and equilibrium temperature was 25 °C. Sample had diameter 50 mm and thickness about 2 mm.

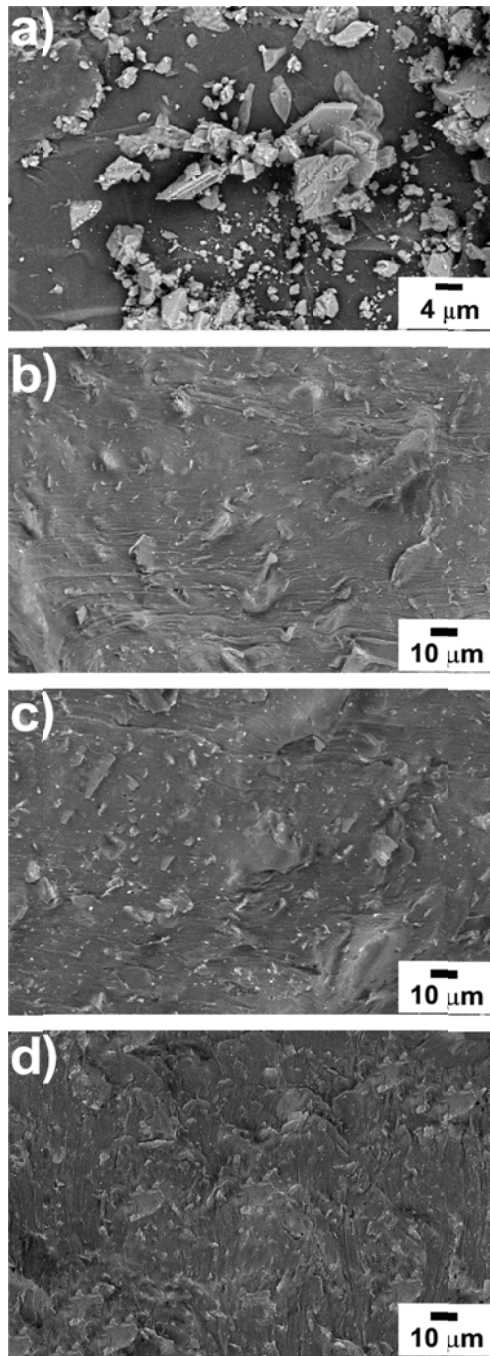


Figure 3. SEM micrographs of (a) Expandable graphite and EOC/expandable graphite composites with (b) 20, (c) 30 and (d) 40 wt. % of filler.

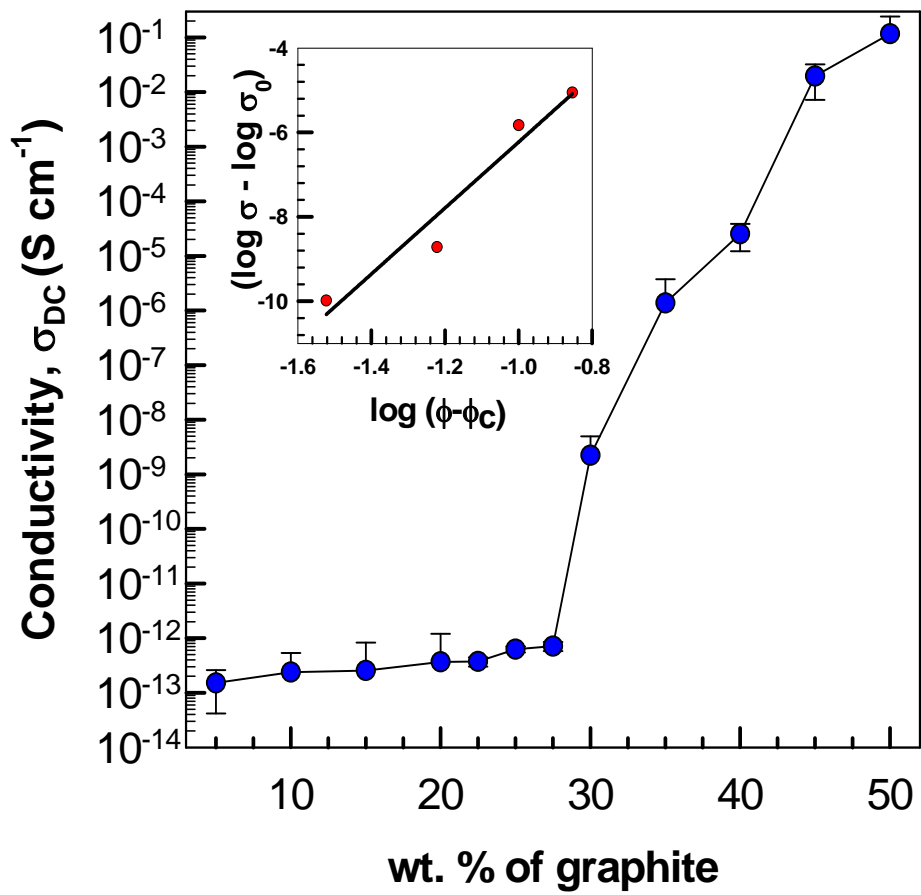


Figure 4. Dependence of DC conductivity on graphite content.

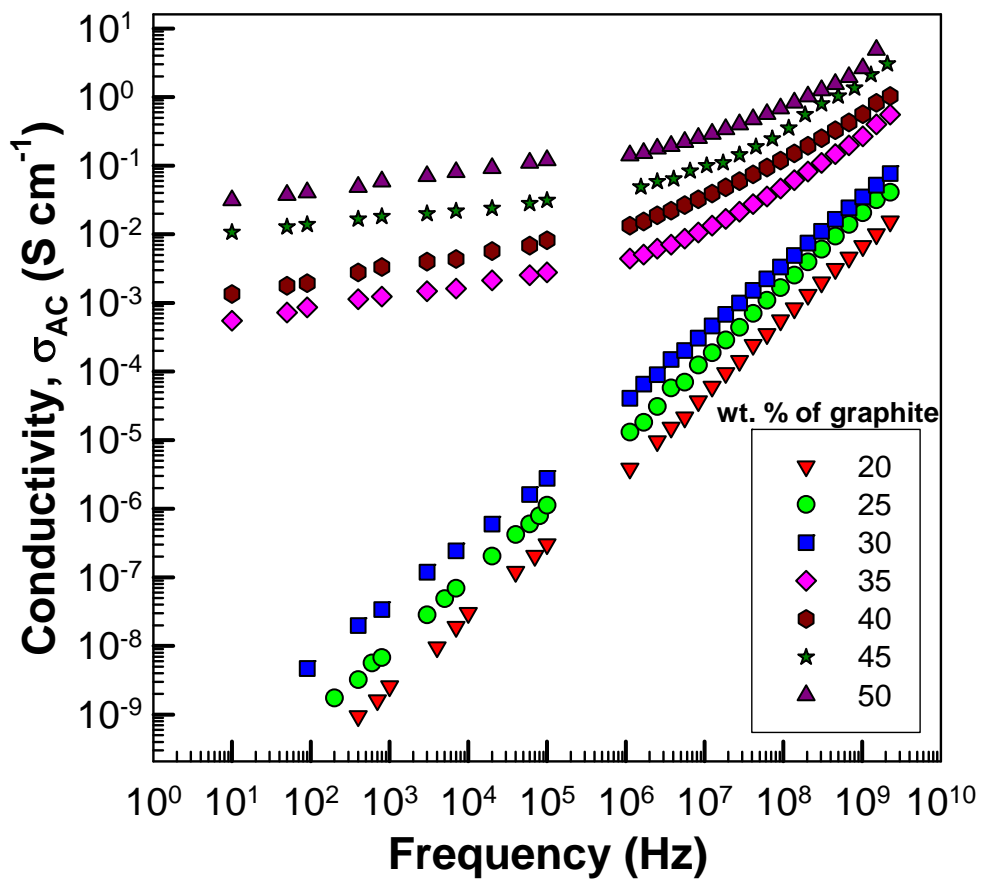


Figure 5. AC conductivity vs. frequency of EOC/graphite composites.

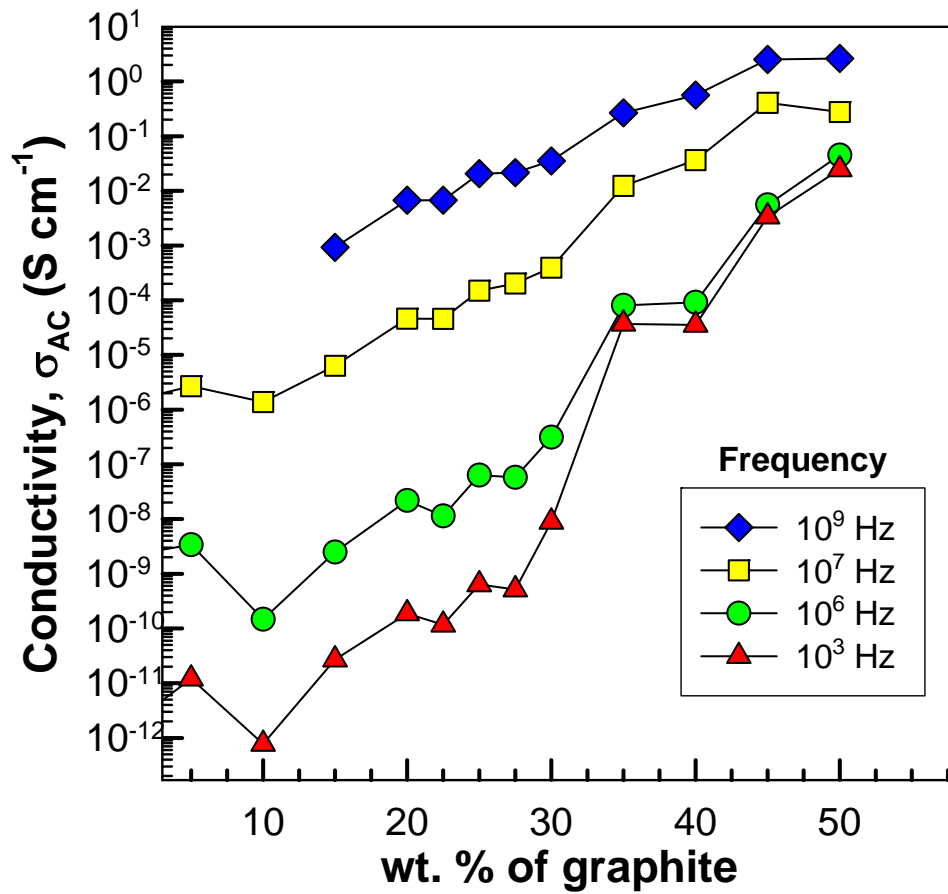


Figure 6. AC conductivity as a function of graphite content at different frequencies.

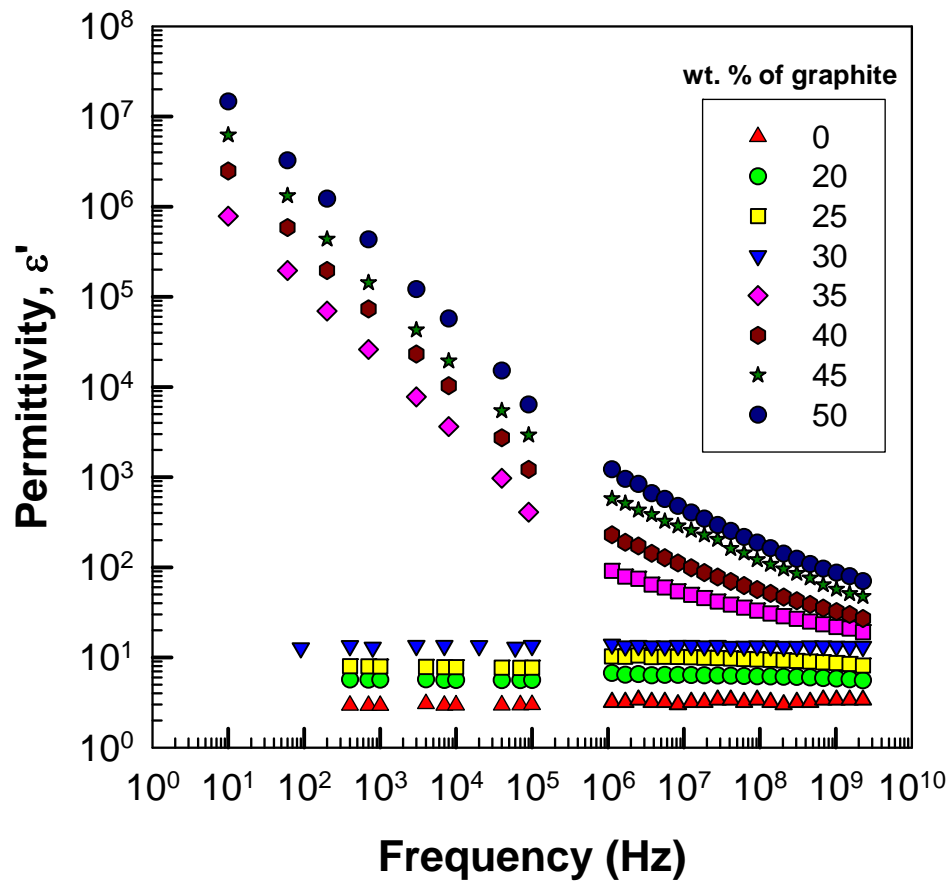


Figure 7. Real part of permittivity as a function of frequency.

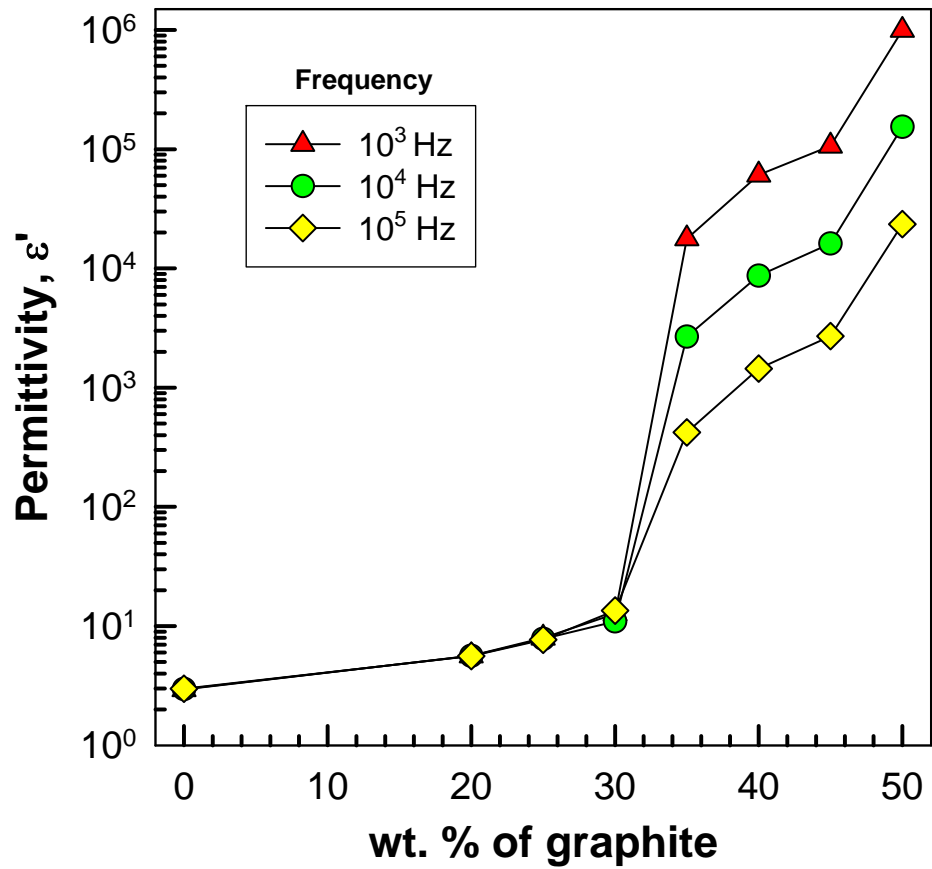


Figure 8. Permittivity as a function of graphite content at different frequencies.

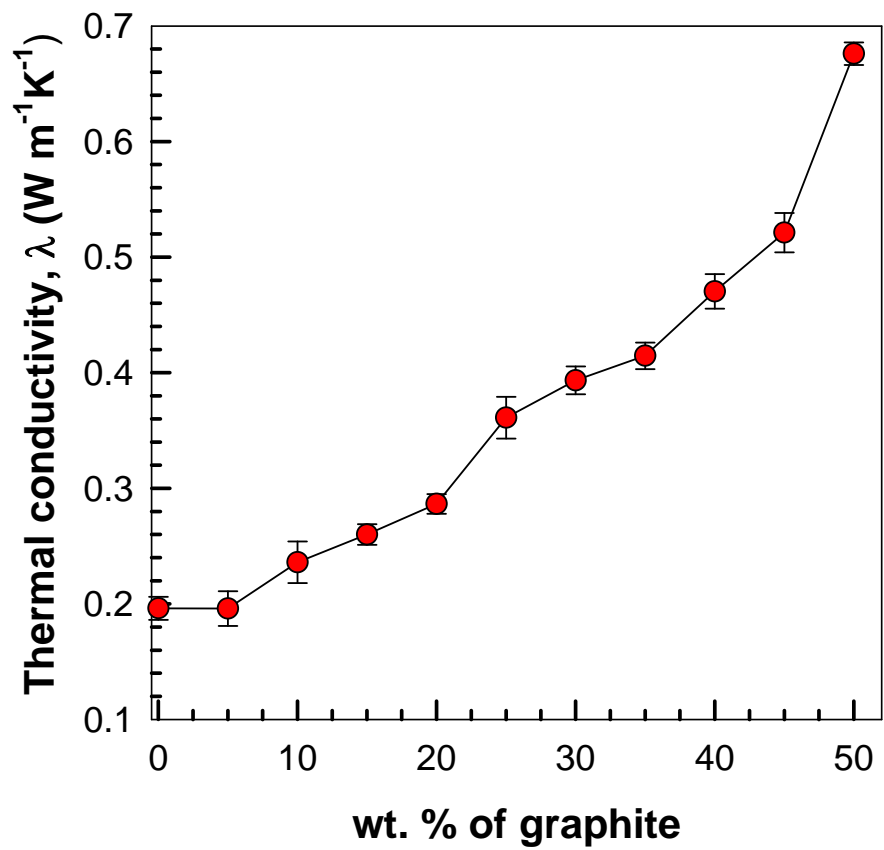


Figure 9. Thermal conductivity as a function of graphite content.

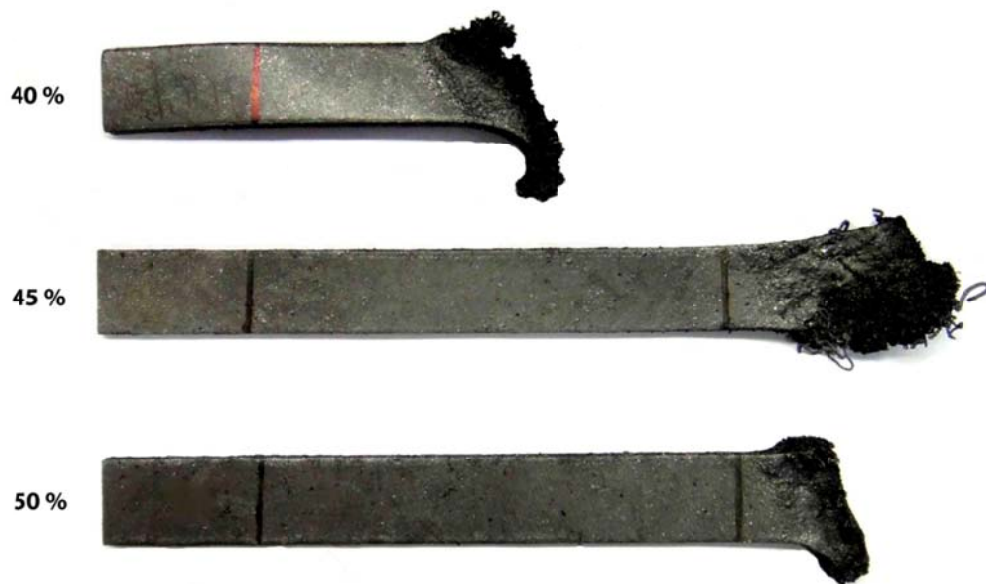


Figure 10. Samples with 40, 45 and 50 wt. % of graphite after horizontal flame testing.

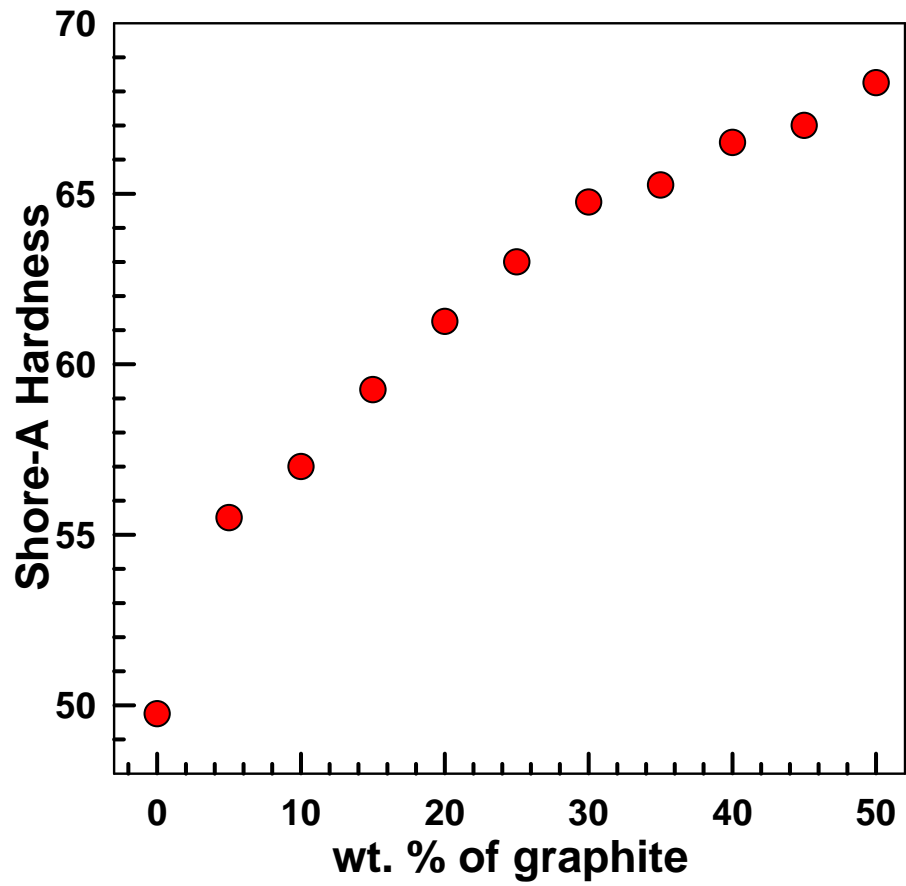


Figure 11. Shore-A hardness as a function of graphite content.

PAPER 3

Creep and dynamic mechanical analysis studies of peroxide cross-linked ethylene-octene copolymer

Rajesh Theravalappil^a, Petr Svoboda^{a*}, Sameepa Poongavalappil^a, Dagmar Svobodova^b

^a*Centre of Polymer Systems, Faculty of Technology, Tomas Bata University in Zlin, Nam.T.G.Masaryka 5555, 760 01 Zlin, Czech Republic*

^b*Faculty of Humanities, Tomas Bata University in Zlin, Mostni 5139, 760 01 Zlin, Czech Republic*

* Corresponding author. Tel.+ 420–576 031 335, fax. +420–577 210 172.

E-mail address: svoboda@ft.utb.cz (P. Svoboda)

Abstract

Ethylene-octene copolymer (EOC, with 45 wt.% of octene) was cross-linked by di-cumyl peroxide (DCP). Differential scanning calorimetry (DSC) revealed a very low (50 °C) melting temperature. The network density was evaluated by gel content. While 0.2-0.3 wt.% of peroxide leads only to the molecular weight increase (samples completely dissolved in xylene), 0.4-0.6 wt.% of peroxide caused a network formation. High temperature creep was measured at 70, 120 and 200 °C at three stress levels. At 200 °C and above 0.6 wt.% of peroxide, degradation due to chain scission was observed by rubber process analyzer (RPA) and was again supported by creep measurements. Residual strain at 70 °C was found to be improving with the increasing peroxide level. Dynamic mechanical analysis (DMA) revealed a strong influence of peroxide content on storage modulus and tan(delta), especially in 30-200 °C temperature range.

Key words: creep, cross-linking, DMA, ethylene-octene, peroxide.

Introduction

Polymers are being used in many widespread areas starting from commodity applications to high-engineering applications. Their properties in long-run are thus very important. Property enhancement of these polymers can be achieved through

many techniques like filler addition, blending and cross-linking. One of the important mechanical properties related to polymers which are being used under constant stress in exposed conditions is creep. Creep is the time-dependant behavior of the material under stress and reveals the usability of a polymer in long term application. Many researchers have shown their interest in creep behavior due to its practical importance in the applications for water/oil tanks, GRP (Glass fiber-reinforced Polymer) pipes ^[1], extruded composite profiles ^[2] and bottles/containers ^[3]. High temperature creep test is being used in foam industry, where the polyolefin foam is used e.g. for camping mats.

Slobodian et al.^[4] studied the effect of multiwall carbon nanotube (MWCNT) fillers and temperature on the creep behavior of polystyrene. Other researchers studied the effect of other fillers on creep behavior using different polymer matrices.^[5,6] Tomlins et al.^[7] investigated the influence of temperature on creep behavior of polyvinyl chloride (PVC). A.H-Ulloa et al.^[8] carried out their research on the creep behavior of high density polyethylene (HDPE) after aging in different media.

EOC is a newly developed member of the class polyolefin elastomers (POE) being supplied under the brand name ENGAGE™ by Dow Chemical Co.^[9] Mechanical and rheological properties of EOC blends and composites have been studied by several researchers.^[10-12] Many researches have been carried out on the peroxide cross-linking of EOC, so far.^[13-18] Babu et al. used the peroxide cross-linked EOC for the preparation of thermoplastic vulcanizates (TPVs) with polypropylene.^[19, 20]

To the authors best knowledge, only few articles deal with the creep behavior of EOCs. Namely, Patham and Jayaraman^[21] examined the effect of co-monomer content on creep recovery of EOCs. Kamphunthong and Sirisinha studied the creep behavior of silane-water cross-linked EOC.^[22] Creep and stress relaxation studies of irradiation cross-linked EOC was carried out by Maksimov et al.^[23] and Drozdov and Christiansen carried out the creep test at room temperature.^[24]

Relatively little or no attention has been paid to the evaluation of the creep behavior of peroxide cross-linked EOCs, especially at temperatures above the melting point of pure EOC. In this article, effects of different stress levels and temperatures on creep behavior are discussed.

Experimental

Ethylene-octene copolymer (ENGAGE 8842) with octene content 45 wt.% was supplied by Dow Chemical Co. ENGAGE 8842 possess a density of 0.8595 g cm⁻³ and melt flow index (MFI) of 1.02 dg min⁻¹ (at 190 °C /2.16 kg). Its Melting temperature (T_m) has been determined by DSC and found to be about 50 °C.

Perkadox BC-40B-PD (DCP) having active peroxide content of 40% has been used as the peroxide for cross-linking, supplied by Akzo Nobel. Its half-life time (t_{1/2}) at 138 °C is 1 h and specific gravity at 23 °C is 1.53 g cm⁻³. The influence of peroxide level on cross-linking and mechanical properties was investigated for concentrations 0.50, 0.75, 1.00, 1.25, 1.50 and 1.75 wt.%. The active peroxide content was then 0.2, 0.3, 0.4, 0.5, 0.6 and 0.7 wt.% respectively.

Irganox 1010 with chemical name tetrakis-(methylene-(3,5-di-(tert)- butyl-4-hydrocinnamate)) methane was used as the antioxidant. This was supplied by Ciba, Switzerland. Density of Irganox 1010 is 1.15 g cm⁻³. The antioxidant content was kept constant throughout the experiment; 0.40 wt.%.

Mixing of EOC, peroxide and Irganox 1010 was carried out in a Brabender Plasti-corder PL2000 mixing machine with mixing volume of 50 cm³ at 100 °C at mixing speed 50 rpm for 10 minutes. Compounded batches were stored in a freezer at -18 °C to avoid pre-mature cross-linking during storage.

Cross-linking time and temperature of EOC were optimized using Rubber Process Analyzer (RPA 2000, Alpha Instruments). Testing conditions were maintained at an angle of 0.5° and a frequency of 100 CPM (1.667 Hz).

Sheets for mechanical testing (creep, Dynamic Mechanical Analysis -DMA and residual strain) were prepared via simultaneous cross-linking and compression molding at 170 °C for 15 min.

The gel content, which is a direct measure of extent of cross-linking, of the cross-linked EOC was determined according to ASTM D2765-01 standard. About 0.3 g of cross-linked sample was wrapped in a 120 mesh stainless steel cage and extracted in refluxing xylene containing 1% of antioxidant (Irganox 1010) for 6 h. The sample was then dried in a vacuum oven at 55°C and weighed. % gel content was calculated according to Equation (1):

$$\text{Gel content} = \frac{\text{Final weight of sample}}{\text{Initial weight of sample}} \times 100 \quad (1)$$

DMA analysis was carried out in a IT Keisoku-seigyo (DVA-200S) machine in the temperature range -100 to 200 °C and the heating rate was 5°C /min. The analysis was carried out in cyclic tensile strain mode with the frequency of 10Hz.

Tensile creep experiments were conducted according to ISO 899 standard. For this, tensile samples were cut out of the cross-linked EOC sheets. Creep test was carried out in Memmert UFE 400 oven with a glass window and digital temperature control. Each creep experiment was recorded using the SONY SLT-A33 camera capable of HD 1920x1080 video capture (25 frames/sec). This video was later analyzed at proper time intervals. Effects of different temperatures (70, 120 and 200 °C) and of various stress levels (0.077, 0.123 and 0.210 MPa) on creep behavior of peroxide cross-linked EOC was studied.

Residual strain after 100% elongation was determined by stretching the samples to 100% and holding them there for 5 min at 70 °C. After that, samples were cooled to room temperature, released, and then the residual strain values were noted.

Results and discussions

In Table 1, effect of peroxide level on gel content of the cross-linked EOC samples is shown. Except the case of EOC with 0.2 and 0.3 wt.% of peroxide, gel content increased with peroxide level. In the cases of 0.2 and 0.3, the zero gel content shows that, cross-linking has led only to the increase in molecular weight, but the network did not form. As can be seen from Table 1, there is a sharp increase (from 0 to 54 %) in the gel content at 0.3 to 0.4 wt.% of peroxide, followed by a gradual increase at 0.5, 0.6 and 0.7 wt.% of peroxide. We can conclude that the network density increases with higher peroxide levels.

We intended to measure creep behavior above the melting temperature of EOC. Therefore, T_m of pure EOC has been measured using DSC and was found at about 50 °C. DSC thermogram of pure EOC is shown in Figure 1. Above this temperature, the sample strength comes only from cross-linking while below T_m the crystals play an important role. The crystals act as tie points for amorphous chains (physical cross-linking).

Figure 2 shows the elongation behavior of cross-linked EOCs under a constant stress of 0.077 MPa at 70 °C. Curves for 0.2 and 0.3 wt.% of peroxides show very fast creep, almost like elongational flow, where there is no effect of cross-linking. Just with 0.3 wt.% of peroxide, longer molecules were formed which

affects the shape of the curve. Gel content results can be read together to strengthen this claim. At the same time, EOC with 0.4 wt.% shows almost linear dependence of elongation on time where the effect of cross-linking is higher than that of previous cases. EOC with 0.5 wt.% of peroxide shows a creep flow behavior where cross-linking is much more prominent. The elongation value is approaching almost constant value in time (at this low temperature, 70 °C). The specimen behaves like a solid, highly elastic matter.

Figure 3 depicts the elongation behavior of the EOCs at a higher temperature, 200 °C at a stress of 0.077 MPa. We have observed a creep flow for EOCs with 0.4, 0.5 and 0.6 wt.% of peroxides at lower temperatures. But, at higher temperatures, even EOCs with higher peroxide levels (0.4 and 0.5 wt.%) show a pure flow. And, only EOC with 0.6 wt.% of peroxide shows a creep flow. In the case of 0.6, it shows creep flow up to about 220 s (where separated by a line on the curve) and then undergoes degradation flow, where elongation increases sharply. Degradation was verified by RPA measurement at 200 °C. The s' (elastic torque) curve shows a decreasing trend after reaching the maximum. This is shown in Figure 4.

In Figure 5, effect of different stress levels on tensile creep compliance of EOC with 0.4 wt.% of peroxide at 120 °C is shown. As the load increases, cross-linked EOC samples are more vulnerable to creep behavior. When the stress is 0.077 MPa, samples undergo creep slower than at 0.210 MPa.

Figure 6 shows the effect of temperature on creep behavior. With increasing temperature, the creep takes place faster and faster.

While Figure 5 and 6 have time axes in logarithmic form, Figure 7 has the time axis in linear form. When the time axis is in linear form one can evaluate the slope of the creep compliance curve after omitting the initial part of the curve when the heating of the sample to desired temperature is taking place. Then the slope of the creep compliance curve has been analyzed to study the effect of different factors on creep behavior of peroxide cross-linked EOC. An example of slope calculation for EOC with three different peroxide content (0.2, 0.3 and 0.4 wt.%) at 70 °C and 0.77 MPa stress is given in Figure 7. Combined effect of temperature and peroxide content on the creep compliance curve is shown in the 3D plot in Figure 8. It can be observed from the figure that with increasing peroxide level, the cross-link network (or cross-link density) is higher which results in decreased creep. This trend is more pronounced at higher temperature. After reaching certain peroxide concentration the creep becomes much smaller (almost negligible in given time frame) so the 3D plot

plane can be divided to flat area (towards the high peroxide levels) and a “mountain” or “hilly” area (towards the lower peroxide levels and higher temperatures). At 70 °C, the transition point from flat to hilly area is at about 0.4 wt.% of peroxide while at 200 °C, it is at around 0.5%. With increasing temperature the creep is more prominent especially at lower peroxide levels. Above 0.5 wt.%, the creep is very low compared to that of at lower peroxide levels. So the increase of creep is not so visible at e.g. 0.7 wt.% of peroxide.

Residual strain after 100% elongation at 70 °C was noted and the values are given in Table 1. Samples with 0.0 - 0.3 wt.% of peroxide broke at 70 °C. There is very small extent of crosslinking in these samples, so the samples did not survive 5 minutes stretching to 100% elongation at 70°C (which is above T_m of EOC). EOCs with 0.4, 0.5 and 0.6 wt.% of peroxides only withstood for 5 min at 70 °C and their residual strain (ϵ_r) values were noted as 84%, 69% and 38% respectively. We can conclude that the sample cross-linked with 0.6 wt.% peroxide shows excellent elastic behavior at elevated temperature. In discussion about Figure 4 we have mentioned degradation for samples with 0.6 wt.% of peroxide at 200 °C. Sample with 0.7 wt.% of peroxide most likely undergoes degradation (chain scission) during crosslinking even at 150°C. That could be the possible explanation of the 0.7 sample failure.

The results of DMA analysis are illustrated in Figure 9-12. Figure 9 shows the temperature dependence on storage modulus of cross-linked EOC samples. As per the gel content analysis, there was no considerable gel formed for EOCs with 0.2 and 0.3 wt.% of DCP. But there is a clear difference observed in storage modulus of these samples. The pure EOC sample withstood only up to 80 °C while EOC with 0.2 and 0.3 wt.% of DCP survived to 120 and 160 °C respectively. From 0.4 to 0.6 wt.% of peroxide level, there is a small but gradual increase in the storage modulus with increased cross-linking. The highest storage modulus for 0.7 wt.% was recorded to 180 °C and then it dropped at higher temperatures. This can be attributed to the possible degradation due to chain scission. This claim can be supported by the RPA result which is shown in Figure 4. Dependence of storage modulus on peroxide level is shown in Figure 10. It can be concluded that the storage modulus increases with the increasing peroxide content, except the case of 0.7 wt.%, above 180 °C.

In Figures 11-12, the effect of peroxide content on $\tan\delta$ is shown. In the temperature range 30-200 °C, an increase in temperature results in an increase in $\tan\delta$ value for all samples. Interesting behavior was also found in -100 to 0 °C

temperature range. There is a very clear peak indicating the position of glass transition temperature being at $-42\text{ }^{\circ}\text{C}$. The peroxide level did not influence the position of T_g . As illustrated in Figure 12, with increasing peroxide content the $\tan\delta$ value decreases except the case of EOC with 0.7 % of peroxide. From the $\tan\delta$ measurements, it is clear that increase in peroxide level beyond 0.6 wt.% of peroxide do not support the improvement of elastic properties.

Conclusions

Influence of temperature and peroxide level on the high temperature mechanical properties including creep, elastic properties and DMA studies of peroxide cross-linked EOC has been studied in this article. Peroxide levels between 0.2-0.3 wt.% caused the increase in molecular weight only, but a full network was not created. The melting temperature being only $50\text{ }^{\circ}\text{C}$, as revealed by the DSC measurement, exposed the vulnerability of this ethylene-octene copolymer in even slightly warm environment. Therefore, cross-linking is absolutely necessary for majority of applications. This goal can be achieved by the cross-linking using di-cumyl peroxide in the range 0.4-0.6 wt.% and was found to be very effective. This effectiveness was confirmed by creep test at various temperatures, at various loads, by high temperature residual strain values and also by DMA. Measurement of creep behavior at high temperatures was found to be an excellent tool for evaluation of cross-link density and possibilities of applications at elevated temperatures. A higher peroxide concentration (0.7 wt.%) does not bring any further improvement. Most likely chain-scission reaction starts to play an important role at peroxide levels above 0.6 wt.% and temperatures above $180\text{ }^{\circ}\text{C}$.

Acknowledgements

This work has been supported by the Ministry of Education of the Czech Republic as a part of the project No. VZ MSM 7088352102, Internal Grant Agency (IGA/23/FT/11/D) and also by Operational Programme Research and Development for Innovations co-funded by the European Regional Development Fund (ERDF) and national budget of Czech Republic within the framework of the Centre of Polymer Systems project (reg.number: CZ.1.05/2.1.00/03.0111).

References

- [1]. RM Guedes, A. Sa and H.Faria, *Polym. Composite*. **2010**, *31*, 1047.
- [2]. M. Bengtsson, K. Oksman and NM Stark, *Polym. Composite*. **2006**, *27*, 184.
- [3]. R. Elleuch and W. Taktak, *J. Mater. Eng. Perform.* **2006**, *15*, 111.
- [4]. P. Slobodian, D. Králová, A. Lengálová, R. Novotný and P. Sáha, *Polym. Composite*. **2010**, *31*, 452.
- [5]. V. Devasenapathi, P. Monish and S.B. Prabu, *Int. J. Adv. Manuf. Tech.* **2009**, *44*, 412.
- [6]. Y. Xu, Q. Wu, Y. Lei and F. Yao, *Bioresource Technol.* **2010**, *101*, 3280.
- [7]. P.E. Tomlins, B.E. Read and G.D. Dean, *Polymer* **1994**, *35*, 4376.
- [8]. A. Habas-Ulloa, J.-R.M. D'Almeida and J.-P. Habas, *Polym. Eng. Sci.* **2010**, *50*, 2122.
- [9]. S. Bensason, J. Minick, A. Moet, S. Chum, A. Hiltner and E. Baer, *J. Polym. Sci. Polym. Phys.* **1996**, *34*, 1301.
- [10]. G. Liu, X. Zhang, C. Liu, H. Chen, K. Walton and D. Wang, *J. Appl. Polym. Sci.* **2011**, *119*, 3591.
- [11]. M.U. Wahit, A. Hassan, Z.A.M. Ishak and T. Czigány, *eXPRESS Polym. Lett.* **2009**, *3*, 309.
- [12]. K. Sirisinha and W. Kamphunthong, *Polym. Test.* **2009**, *28*, 636.
- [13]. S. Akbar, E. Beyou, P. Chaumont and P. Cassagnau, *Mater. Chem. Phys.* **2009**, *117*, 482.
- [14]. K. Sirisinha and D. Meksawat, *J. Appl. Polym. Sci.* **2004**, *93*, 1179.
- [15]. A. Msakni, P. Chaumont and P. Cassagnau, *Polym. Eng. Sci.* **2006**, *46*, 1530.
- [16]. S.-M. Lai, J.-L. Liu, S.-H. Hu, C.-H. Huang, S.-J. Wang and S.-C. Chien, *J. Appl. Polym. Sci.* **2009**, *113*, 3791.
- [17]. H.-J. Tai, *Polym. Eng. Sci.* **1999**, *39*, 1577.
- [18]. A. Msakni, P. Chaumont and P. Cassagnau, *Rheol. Acta* **2007**, *46*, 933.
- [19]. R.R. Babu, N.K. Singha and K. Naskar, *J. Appl. Polym. Sci.* **2010**, *117*, 1578.
- [20]. R.R. Babu, N.K. Singha and K. Naskar, *J. Appl. Polym. Sci.* **2009**, *113*, 1836.
- [21]. B. Patham and K. Jayaraman, *J. Rheol.* **2005**, *49*, 989.
- [22]. W. Kamphunthong and K. Sirisinha, *J. Appl. Polym. Sci.* **2008**, *109*, 2347.
- [23]. R.D. Maksimov, V. Kalkis, T. Ivanova and E. Plume, *Mech. Compos. Mater.* **2002**, *38*, 199.
- [24]. A.D. Drozdov and J.D. Christiansen, *Int. J. Eng. Sci.* **2006**, *44*, 205.

Table 1. Gel content and residual strain (at 70 °C) values of cross-linked EOC samples.

Peroxide content (wt.%)	Gel content (%)	Residual strain at 70 °C (%)
0.0	0	-
0.2	0	-
0.3	0	-
0.4	53.97	84.61
0.5	57.89	69.23
0.6	79.87	38.46
0.7	85.86	-

Captions to Figures

Figure 1. DSC thermogram of pure EOC showing T_m and T_c .

Figure 2. Plot of elongation vs. time of cross-linked EOCs at 70 °C and stress of 0.077 MPa.

Figure 3. Plot of elongation vs. time of cross-linked EOCs at 200 °C and stress of 0.077 MPa.

Figure 4. s' curve of EOC with 0.6 wt.% of peroxide cross-linked at 200 °C.

Figure 5. Tensile creep curves at different stress levels for EOC with 0.4 wt.% of peroxide level at 120 °C.

Figure 6. Tensile creep curves at different temperatures for EOC with 0.4 wt.% of peroxide level at 0.077 MPa stress.

Figure 7. Slope calculation of the creep compliance vs. time curves of EOC with different peroxide levels at 70 °C and 0.077 MPa.

Figure 8. Influence of temperature and peroxide content on creep compliance curve at 0.077 MPa.

Figure 9. Storage modulus as a function of temperature for EOC cross-linked with various levels of DCP.

Figure 10. Storage modulus as a function of peroxide content measured at various temperatures.

Figure 11. $\tan\delta$ as a function of temperature for EOC cross-linked with various levels of DCP from DMA analysis.

Figure 12. $\tan\delta$ as a function of peroxide content measured by DMA at various temperatures.

Figures

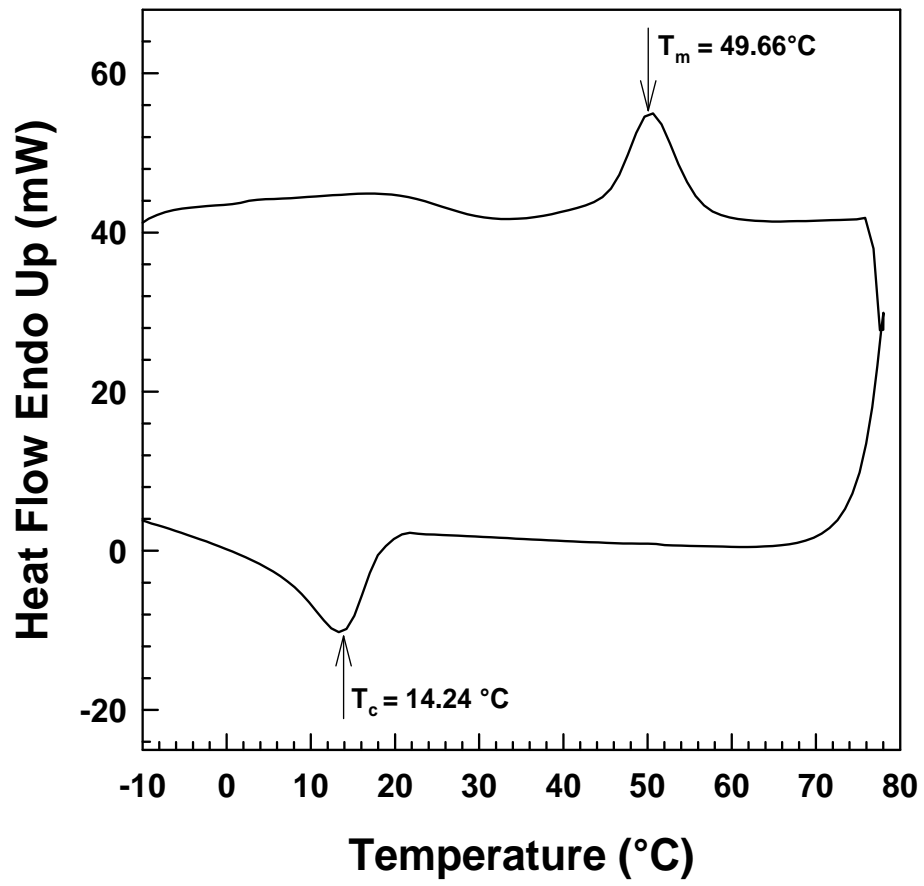


Figure 1. DSC thermogram of pure EOC showing T_m and T_c .

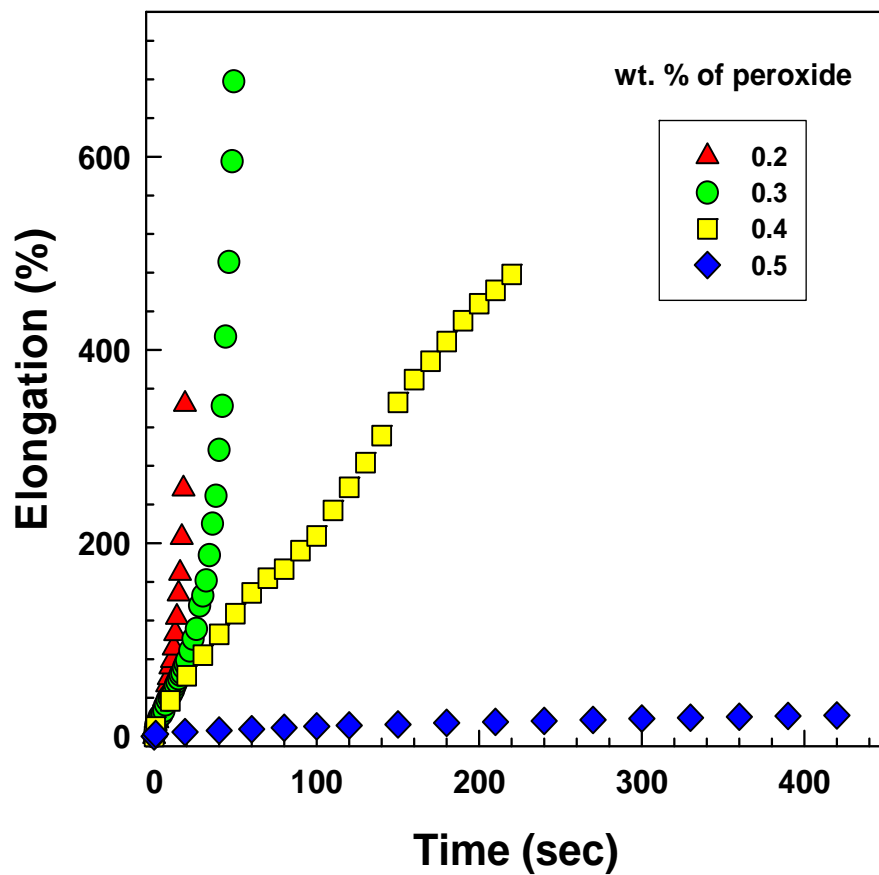


Figure 2. Plot of elongation vs. time of cross-linked EOCs at 70 °C and stress of 0.077 MPa.

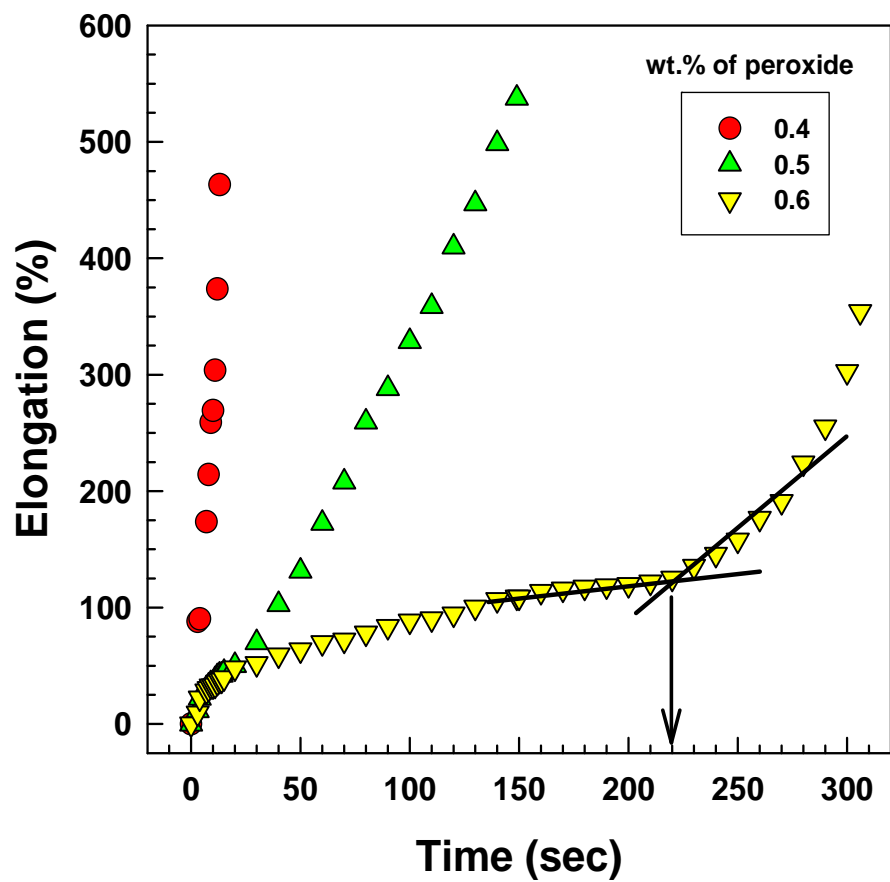


Figure 3. Plot of elongation vs. time of cross-linked EOCs at 200 °C and stress of 0.077 MPa.

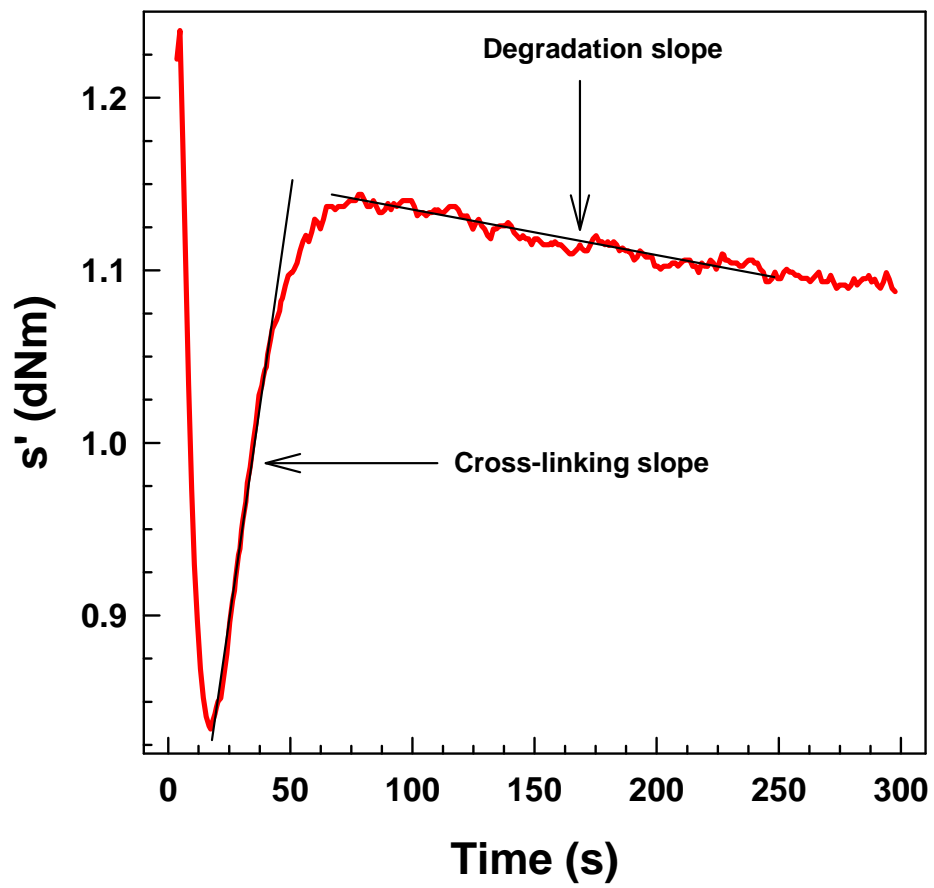


Figure 4. s' curve of EOC with 0.6 wt.% of peroxide cross-linked at 200 °C.

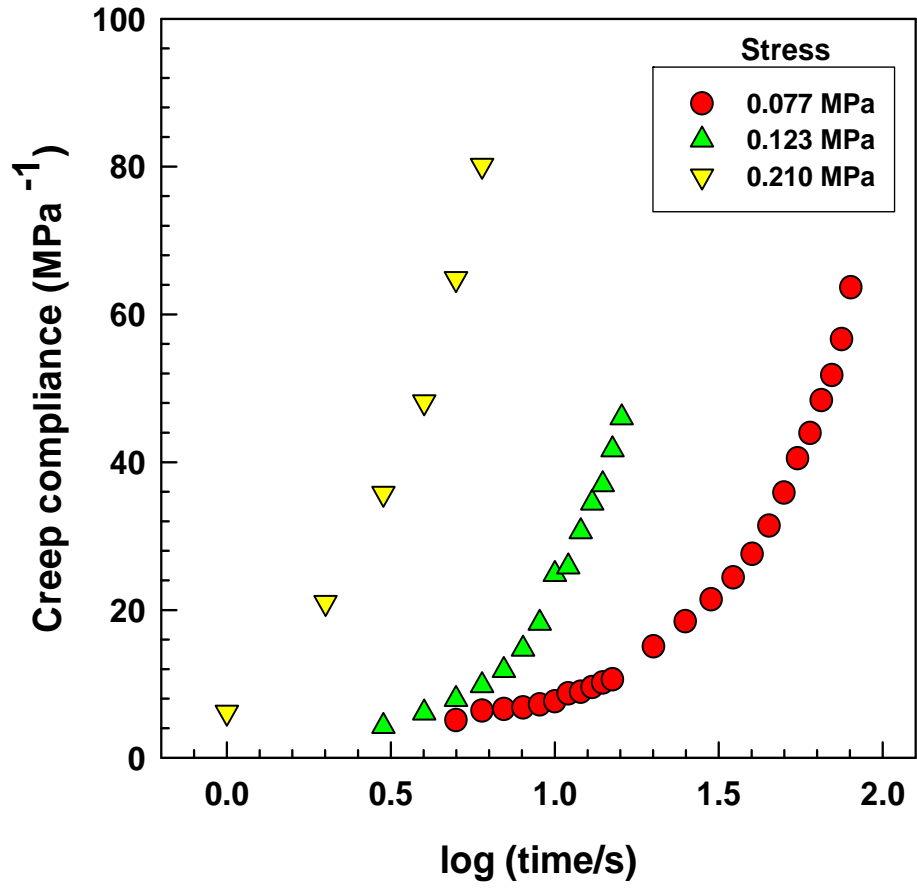


Figure 5. Tensile creep curves at different stress levels for EOC with 0.4 wt.% of peroxide level at 120 °C.

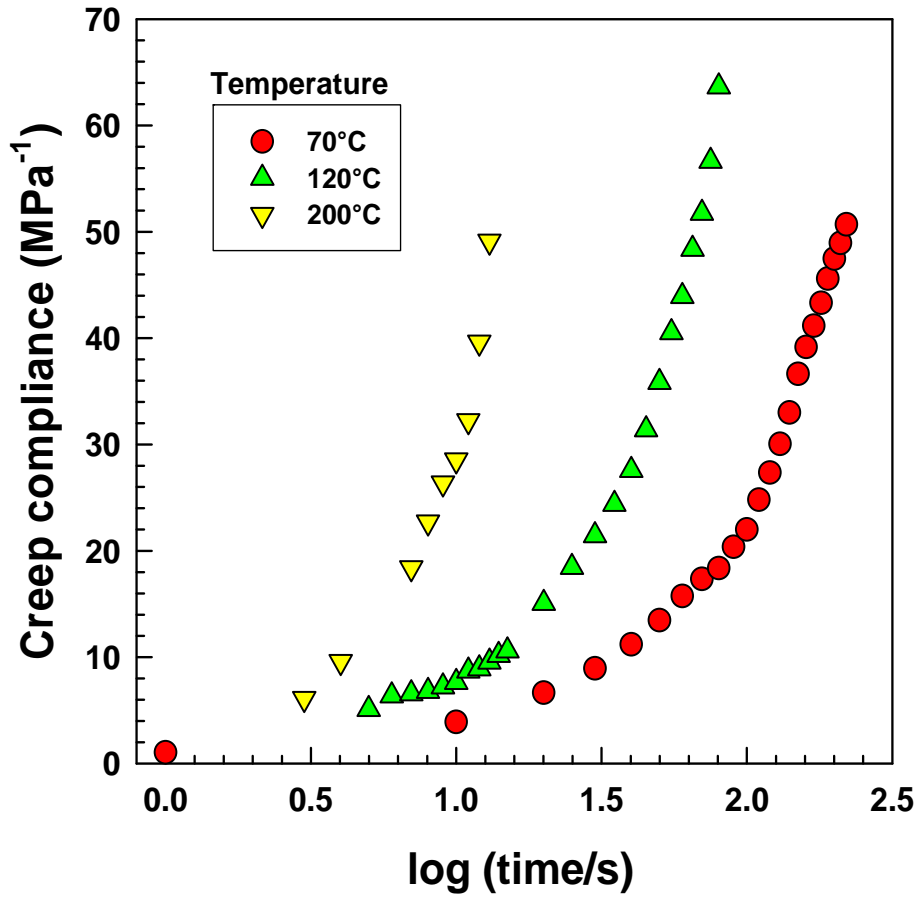


Figure 6. Tensile creep curves at different temperatures for EOC with 0.4 wt.% of peroxide level at 0.077 MPa stress.

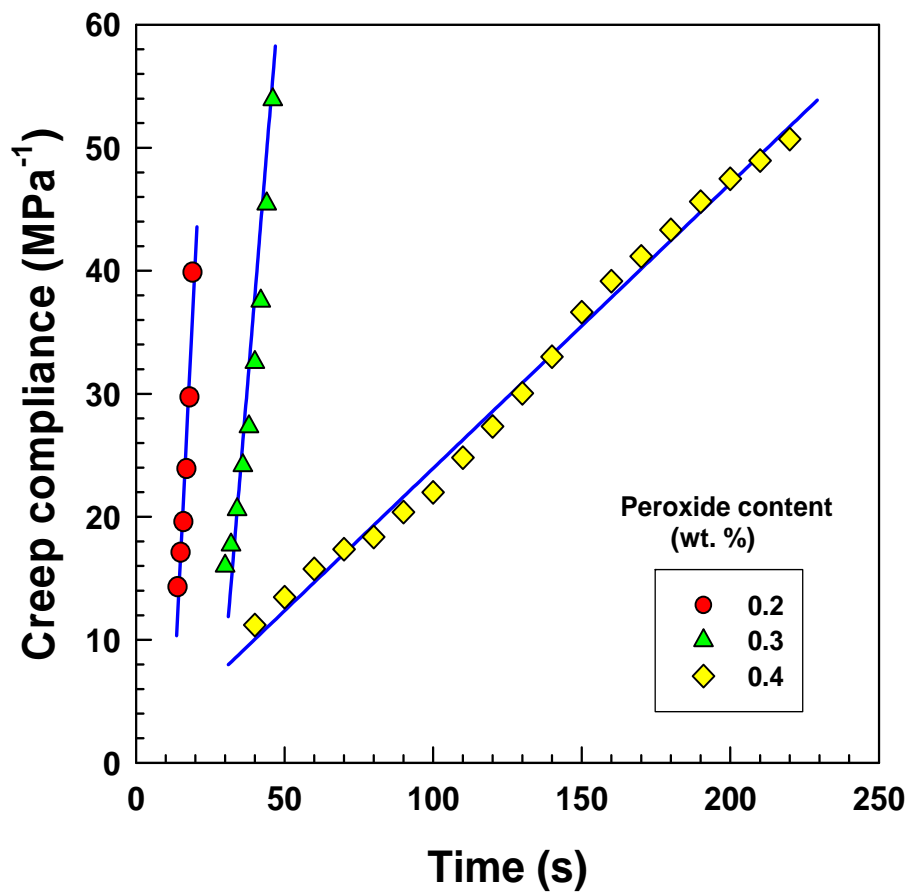


Figure 7. Slope calculation of the creep compliance vs. time curves of EOC with different peroxide levels at 70 °C and 0.077 MPa.

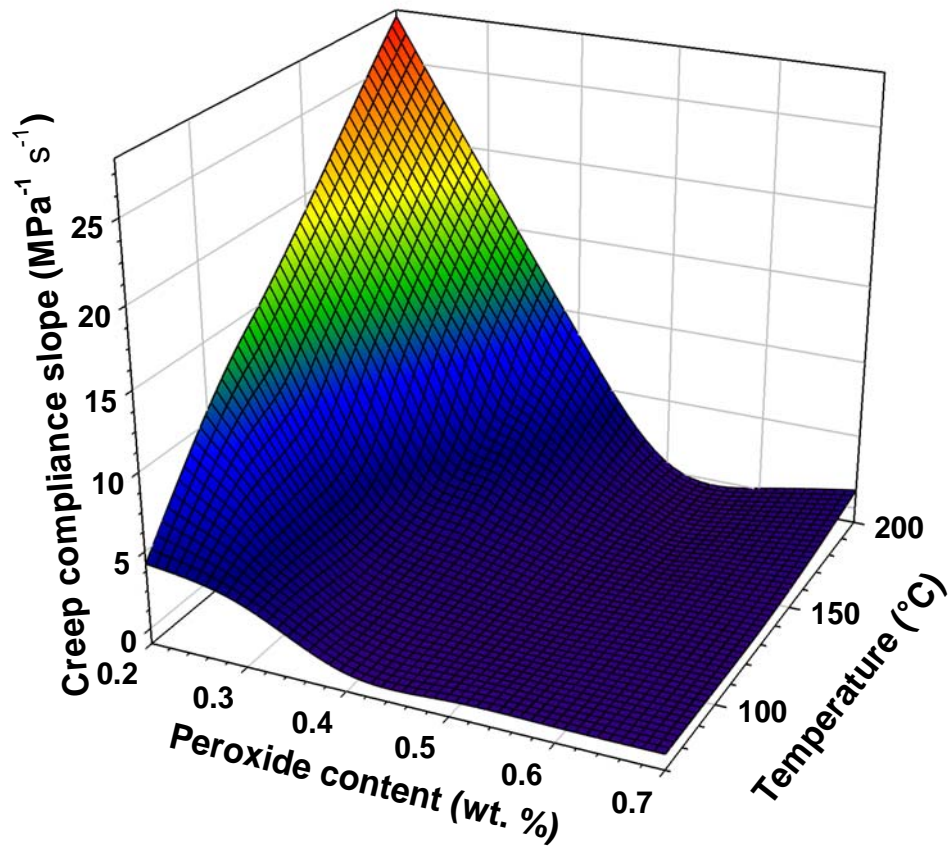


Figure 8. Influence of temperature and peroxide content on creep compliance curve at 0.077 MPa.

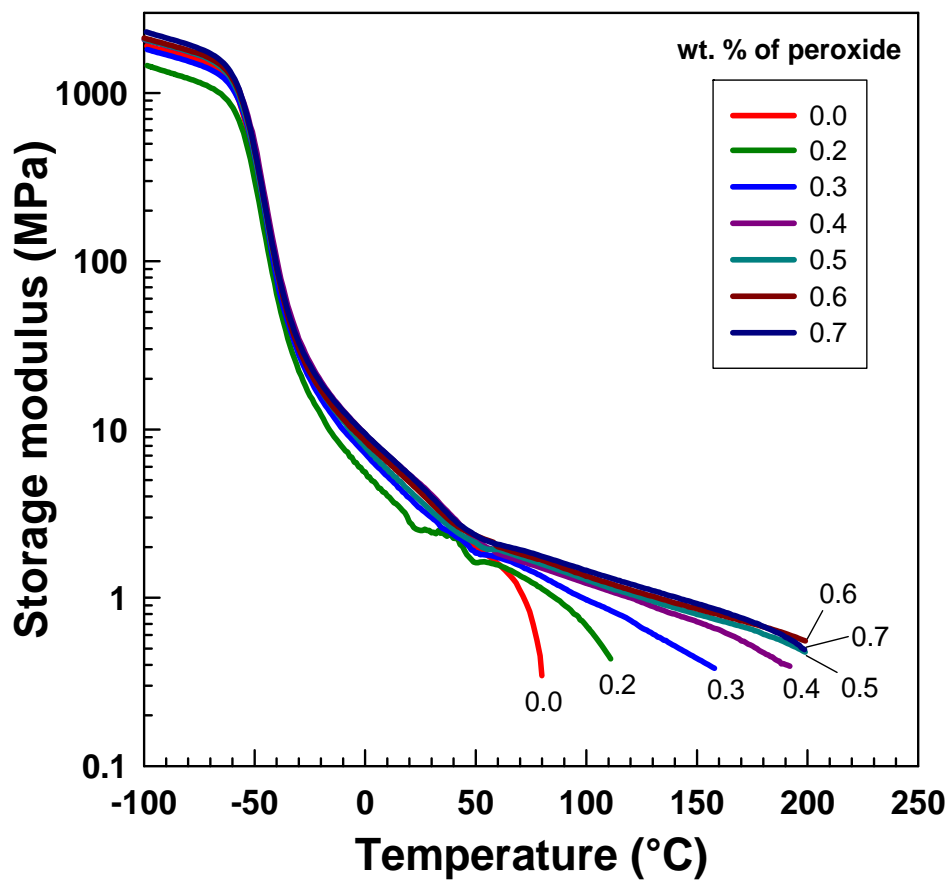


Figure 9. Storage modulus as a function of temperature for EOC cross-linked with various levels of DCP.

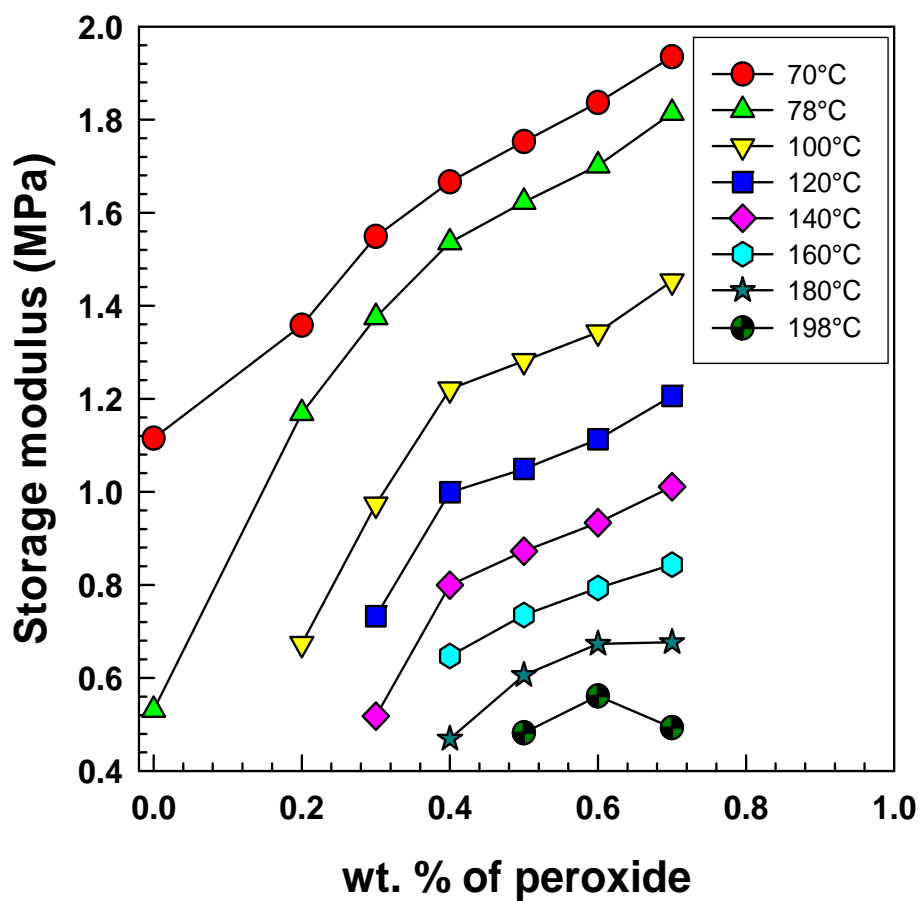


Figure 10. Storage modulus as a function of peroxide content measured at various temperatures.

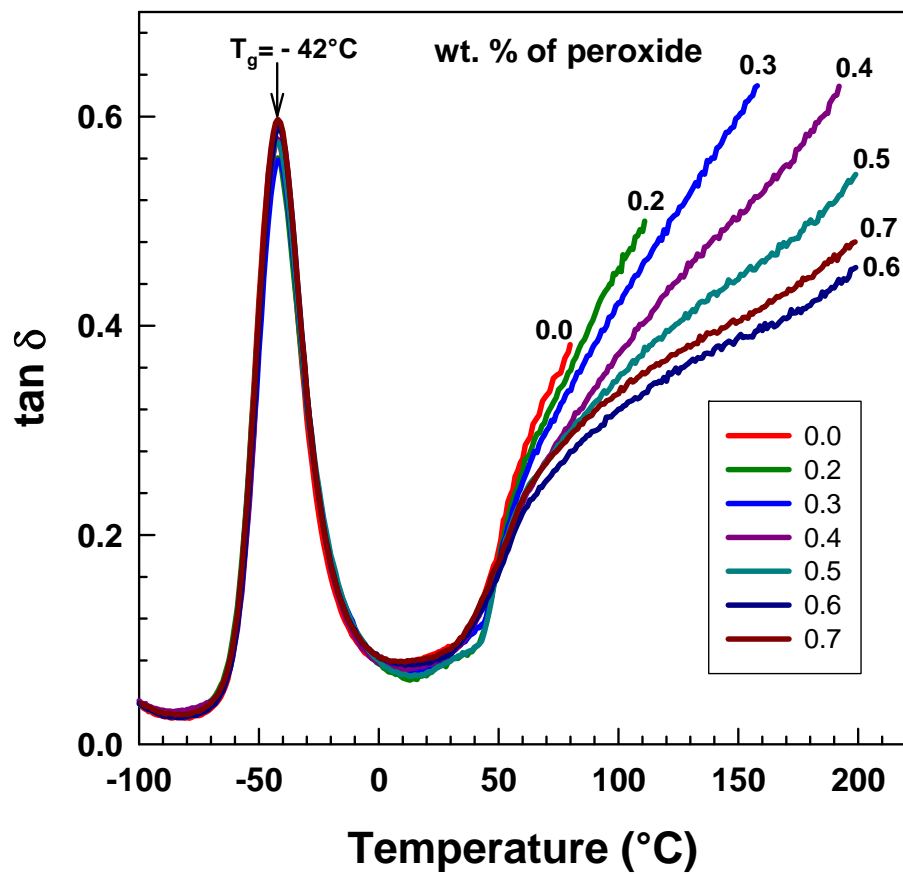


Figure 11. $\tan \delta$ as a function of temperature for EOC cross-linked with various levels of DCP from DMA analysis.

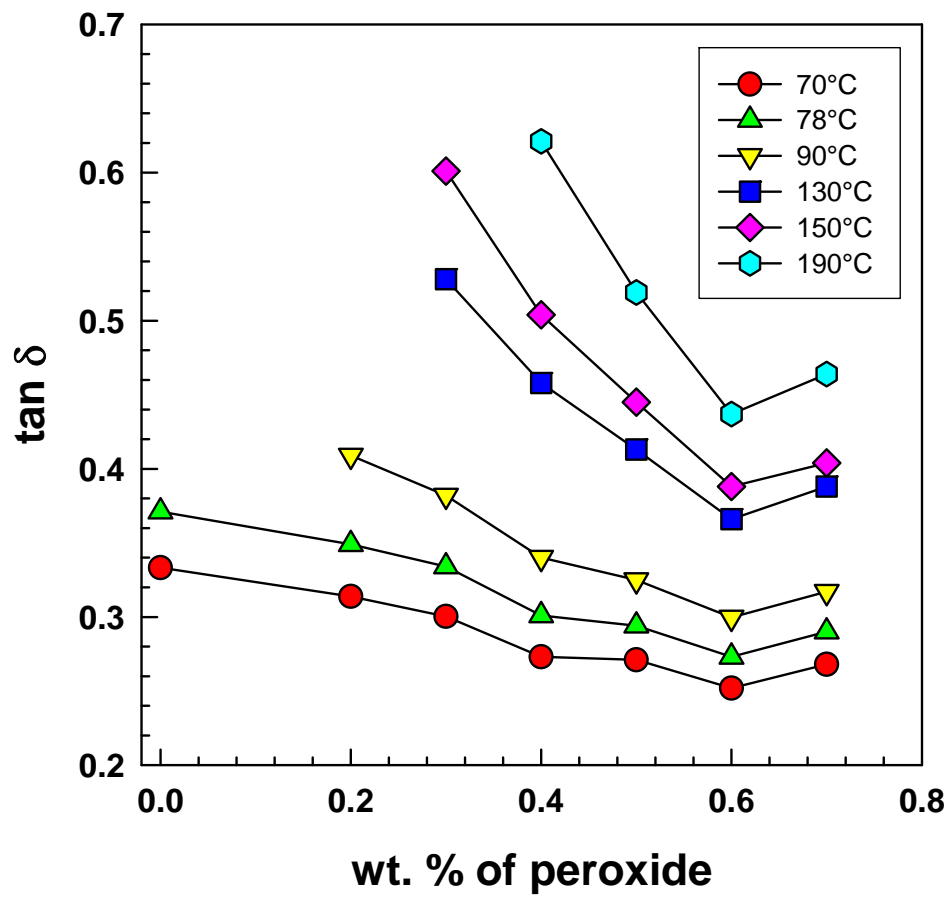
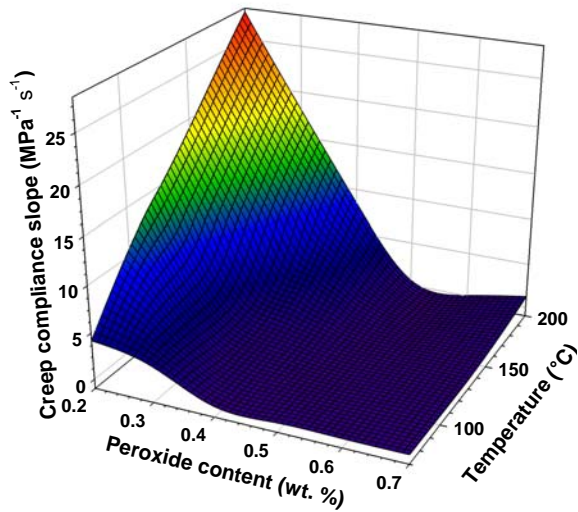


Figure 12. $\tan \delta$ as a function of peroxide content measured by DMA at various temperatures.

Table of contents

Creep and dynamic mechanical analysis studies of peroxide cross-linked ethylene-octene copolymer

Rajesh Theravalappil, Petr Svoboda, Sameepa Poongavalappil, Dagmar Svobodova



With increasing peroxide level, the cross-link density is higher which results in a lower creep. This trend is more pronounced at higher temperature. With increasing temperature the creep is more prominent especially at lower peroxide levels.

PAPER 4

Multiple roles of multiwall carbon nanotubes (MWCNT) and carbon fibers (CF) in their composites with ethylene-octene copolymer

Rajesh Theravalappil^a, Petr Svoboda^{a*}, Sameepa Poongavalappil^a, Jarmila Vilcakova^a, Dagmar Svobodova^b, Petr Slobodian^a, Robert Olejnik^a, Simona Mrkvickova^a

^a*Centre of Polymer Systems, Tomas Bata University in Zlin, Nam.TG Masaryka 5555, 760 01, Zlin, Czech Republic.*

^b*Faculty of Humanities, Tomas Bata University in Zlin, Mostni 5139, 760 01 Zlin, Czech Republic.*

* Corresponding author. Tel. 420–576 031 335, fax. 420–577 210 172.

E-mail address: svoboda@ft.utb.cz (P. Svoboda)

Abstract:

Conducting polymer composites (CPC) were prepared from ethylene-octene copolymer (EOC) matrix and carbon fibers (CF) or multiwall carbon nanotubes (MWCNT) as fillers. Their electrical and thermal conductivities, mechanical properties and thermal stabilities were evaluated. EOC/CF composites showed percolation behavior at a lower filler level (5 vol.%) than the EOC/MWCNT composites (8 vol.%). Alternating current (AC) conductivity and real part of permittivity (dielectric constant) of these composites was found to be frequency-dependent. Dimensions and electrical conductivities of individual fillers have a great influence on conductivities of the composites. EOC/CF composites possessed higher conductivity than the MWCNT-composite at all concentrations, due to the higher length and diameter of CF filler. Both electrical and thermal conductivities were observed to be increasing with filler level. Tensile modulus and thermal stabilities of these composites were found to be increasing with increase in filler content. Improvement in conductivities and mechanical properties was achieved without extreme increase in the hardness of the composites, which is a very essential property as far as the candidature for sensors, is concerned. This strengthens the claim that CF and MWCNT fillers have multiple roles in their composites rather than just the role of being only conducting fillers.

1. Introduction

Thermoplastic elastomers are a special class of polymers which possess processability of a thermoplastics and rubbery nature of elastomers. They generally have two phases; hard and soft. Ethylene-octene copolymer (EOC) is one which belongs to division of polyethylene/poly(α -olefin) block copolymers [1]. Dow Chemical Co, through their constrained geometry catalyst technology (CGCT) has developed a series of EOCs having various comonomer content (here, octene) and densities. Their exceptional performances are ascribed to the good control over polymer structure, molecular weight distribution, uniform comonomer composition and rheology. They are being used in wide variety of applications such as footwear, automotive, foams, gaskets, sealants etc [2, 3]. Excellent elastic behavior of EOCs can be ascribed to small amount of crystal lamellae that hold amorphous chains together (crystals act as tie points).

Ever since the invention of carbon fibers (CF) [4] and carbon nanotubes [5], their possibility as potential conducting fillers in conducting polymer composites (CPC) has been explored. Nowadays, CPCs are attracting much attention among the academic as well as industrial sectors due to their practical importance in the electrical and electronic applications [6]. CPCs are finding applications as pressure/strain sensors [7-9], temperature sensors [10], organic vapor detectors [11], actuators [12] and also in solar cells [13].

Superior properties of carbon fillers over metal powders are that they help to improve mechanical properties also along with conductivity enhancement and do not corrode or act as catalyst for oxidative degradation of the polymer matrix. Also, a considerably smaller amount of carbon fillers imparts a good conductivity which ultimately helps to reduce total weight of the composites [14]. This makes carbon fillers (graphite, carbon fibers and carbon nanotubes) suitable candidates as conducting fillers in CPCs.

Mechanism of electrical conductivity in CPCs can be explained with help of percolation theory [15]. The volume fraction of filler above which the continuous conducting paths are created is known as percolation threshold. At and above this level, conductivity path between the filler particles forms, conductivity increases considerably in several orders and the composite starts to act as semiconductor [16]. Bauhofer and Kovacs [17] reviewed the effect of various types of carbon nanotube fillers on electrical percolation. Chang et al. proved that size and dimension of fillers have a major role on percolation threshold [18].

Permittivity is the ability of a material to store charge when used as a dielectric material. Capacitance and conductance as a function of frequency can be measured by dielectric analysis which can be then utilized to calculate real part (ϵ') and imaginary part (ϵ'') of permittivity and the dielectric loss factor ($\tan \delta$) [19].

Several researchers have explored the possibility of EOC as matrix for conducting polymer composite using various fillers [20, 21]. Flandin et al. studied the effect of various carbon fillers on conductivity of composites with EOC as matrix [22]. Palza et al. investigated the effect of oscillatory motion on alignment of CNT fillers and conductivity of their composites with EOC matrix [23]. Effect of filler dispersion degree on the Joule heating stimulated recovery behavior of EOC/carbon black filler was studied by Le and co-workers [24].

Even though some researchers put their effort on the investigation of EOC as a matrix and CF and MWCNT as fillers, less attention has been paid on to comparison of conductivities and mechanical properties of these two fillers. An EOC copolymer with high octene content exhibits high elasticity. Conductivity together with excellent elasticity of its conducting composites could find an application such as pressure or strain sensors. This was the motivation behind the present study. Influence of factors like pressure/strain, temperature and irradiation crosslinking on conductivities and other essential properties will be the subject of our future study.

2. Experimental

Ethylene-octene copolymer with 45 wt.% of octene content (ENGAGE 8842) was supplied by Dow Chemicals. The density of this EOC was 0.8595 g cm^{-3} and melt flow index (MFI) was 1.02 dg min^{-1} (at $190 \text{ }^\circ\text{C}$ /2.16 kg).

Purified MWCNT produced by acetylene chemical vapor deposition (CVD) method were supplied by Sun Nanotech Co. Ltd., China. Properties of MWCNT provided by the manufacturer are given in Table 1. Purity of MWCNT was $>90\%$. Dimensions such as diameter and length were analyzed by transmission electron microscope (TEM) also and found to be a little different from the data provided by the manufacturer. Diameter was found to be around $15 \pm 6 \text{ nm}$ and length around $3 \text{ }\mu\text{m}$. This is shown in Figure 3d. It can also be observed from the TEM picture that MWCNT consists of about 15 layers showing the multi-wall nature.

Carbon fiber (CF) with trade name VGCF® (stands for Vapor Grown Carbon Fiber) was supplied by Showa Denko K. K (Japan). Their properties are summarized in Table 1.

Composites of MWCNT and CF fillers with EOC matrix were prepared by ultrasonication method. For this, 5% solution of EOC in toluene solvent was prepared and calculated amount of fillers were added. 2, 5, 10, 15, 20, 25, 30 and 35 wt.% of fillers were added to prepare the composites. Their corresponding vol.% values are given in Table 2. The sonication process was carried out in a Dr. Hielscher GmbH apparatus (ultrasonic horn S7, amplitude 88 μm , power density 300 W/cm^2 , frequency 24 kHz) for 3 h at a temperature of 80°C. After sonication, acetone was used as a non-solvent to precipitate out the EOC/CF composite from the toluene solution. This was then dried under vacuum at 40 °C and composite sheets were prepared by compression molding.

Dimensions of MWCNT were analyzed via high-resolution transmission electron microscopy (HRTEM) using microscope JEOL JEM 2010 at the accelerating voltage of 160 kV. For this, samples were deposited on a copper grid (SPI, USA) and dried.

Morphology of the prepared EOC/MWCNT and EOC/CF composites were studied using scanning electron microscope (SEM) technique. SEM analysis was carried out using Vega II LMU (Tescan, Czech Republic) with a beam acceleration voltage set at 10 kV.

DC conductivity of composites were measured using four-point method (Van der Pauw) [25]. Circular specimens had diameter of 15 mm and thickness of 2 mm. A main advantage of four-probe measurements is the elimination of contact resistance [26]. All the properties were measured at room temperature (22-25 °C).

Dielectric characteristics involving the frequency dependence of the real part (dielectric constant, ϵ') and imaginary part of the complex permittivity (dielectric loss, ϵ'') in the frequency range of 1 MHz – 3 GHz were determined with an RF Impedance Analyser (Agilent E4991A, USA) using capacitive method (on a dielectric material test fixture which comes furnished with the device). After inputting the sample thickness the device automatically calculates and yields frequency dependence of complex permittivity ϵ^* . In the range of 10 Hz-100 kHz, dielectric characteristics were measured by using Hioky 3522 (LCR Hi Tester, Japan). The dielectric constant was calculated from the measured capacitance.

AC conductivity, σ_{AC} , was calculated from directly obtained imaginary part complex permittivity, ϵ'' , following an equation:

$$\sigma_{AC} = 2\pi f \cdot \epsilon_0 \cdot \epsilon'' \quad (1)$$

where, ϵ_0 is permittivity of vacuum and f is frequency.

Thermal conductivity of the composites was measured using an experimental setup shown in Figure 1 according to the method described by Fitch [27]. The advantage of this approach is most of all short time of the measurement and also the simplicity of the procedure and also the simplicity of the measuring instrument. During non-stationary heat conductivity measurement the temperature at certain place changes with time. The common procedure involves a case when heat flows only in one direction. Then temperature depends only on time and one coordinate.

The instrument mentioned above is usually being used for the thermal conductivity measurements of thin sheets or slabs made of rubber, plastic or leather. Central brass cylinder (CBC) is firstly annealed to a temperature of 45 °C (t_2) using another hollow cylinder connected to a water thermostat through rubber hoses. After CBC has aquired the temperature of 45 °C, hollow cyclinder at 45 °C was removed and the sample (with diameter of 5 cm and thickness of about 2 mm) whose thermal conductivity was to be measured was placed. Another hollow brass cyclinder which is maintained at 25 °C (t_1) is then placed over the sample. A 100g weight is also kept over the 25 °C brass cylinder to avoid any air gap between the sample and cylinders and to ensure firm contact. Now, the heat is being conducted from CBC to the cold cyclinder, through the sample and the decrease in temperature of CBC is measured using a thermocouple (type copper-constantan) which is connected to a National Instruments data aquisition equipment (NI USB-9211A, Portable USB-Based DAQ for Thermocouples) and to a computer via USB. Software LabVIEW SignalExpress 2.5 was used for temperature data acquisition. Sampling period was set to 5s and one measurement took about 25 min. One obtains temperature vs. Time curves that are shown in Figure 2. The non-linear regression analysis (exponential decay) of the time-temperature curve was performed by using Sigmaplot 12[®] software. Detailed mathematical analysis of the data leading to thermal conductivity values has been shown in our previous study [28].

Tensile properties were studied using a Tensometric (M350-5CT) instrument fitted with 100N loadcell. The cross-head speed was 100 mm min⁻¹. Microtensile samples were cut out from the compression molded composite sheets, with a thickness of 0.2 mm.

Sheets of thickness of 6 mm prepared via compression molding were used for the hardness test. Hardness of the composites has been measured using Bareiss Shore-A hardness tester (Model HHP-2001). The needle of the instrument

penetrated for a time duration of 15 s and the values were read directly from the instrument.

Thermogravimetric analysis was carried out using TGA Q500 (TA instruments). The samples were examined under nitrogen atmosphere. About 10 mg of sample was taken for analysis in a platinum crucible and the temperature was increasing from ambient up to 600 °C. The heating rate was kept at a constant rate of 20 °C min⁻¹.

3. Results and discussions

Morphologies of the fillers and the composites are shown in Figure 3(a-f). Uniform distribution of fillers is very clear from the Figures 3 b-c and e-f. Micrographs below and above the percolation threshold show the good dispersion of MWCNT and CF fillers that proves the better efficiency of sonicator mixing.

DC conductivities of the EOC/MWCNT and EOC/CF composites are shown in Figure 4. A composition above which the conducting phase (here, the filler) forms a continuous network in the composite and as a result of it, a sharp increase in conductivity is visible, is known as percolation threshold. We can observe from the figure that at all points of filler concentration (with an exception to the concentration below percolation threshold) EOC/CF composites show higher conductivity values than EOC/MWCNT composites. CF-composites exhibit percolation jump at 5 wt.% (5 vol.%) of filler level while MWCNT-composites at 10 wt.% (8 vol. %). Individual conductivity values of composites along with their corresponding filler content (both wt. % and vol. %) are shown in Table 2. Dimensions of the fillers, especially the length, play an important role in this case. Longer CF particles (about 10 µm) can create a clear conducting path at smaller concentration compared to MWCNT fibres that are shorter (3 µm). Also because of lower diameter (about 15 nm) MWCNT fibres bend easily (compared to CF with diameter 150 nm that remain straight). At and above 15 wt.% of fillers, the CF-composites exhibit about one order of magnitude higher DC conductivity. The reason of this behavior is probably lower electrical resistivity of pure CF, compare 0.012 Ω cm for CF to 0.12 Ω cm for MWCNT, or in other words, higher conductivity of CF, compare 83 S cm⁻¹ (CF) to 8.3 S cm⁻¹ (MWCNT). MWCNT-composites show a percolation threshold above 10 wt.% (or 8 vol.%). At low filler loadings (2, 5 and 10 wt.%), distances between filler particles are large and therefore

conducting paths are not created and the resulting conductivity is governed by the conductivity of the polymer matrix. When the filler content increases above percolation level, particles get closer and a linkage between them is formed. This results in an increase in conductivity of several orders. Lower percolation threshold of CF-composite is due to the high length and diameter of CF filler over MWCNT filler (length of 10 μm for CF and 3 μm for MWCNT fillers and diameter of 150 nm and 15 \pm 6 nm for CF and MWCNT fillers respectively) [29].

Conductivity of composites below their percolation threshold mainly comes from ionic conductivity of the polymer matrix, where continuous conductive paths are not created. Generally, according to classical percolation theory, for conducting composite systems with spherical fillers, percolation threshold lies around 16-17 vol.% [30]. But, a higher filler loading like this can cause brittleness of the composites. Simultaneous achievement of good electrical conductivity along with improved mechanical properties can be obtained by using fillers with high aspect ratio such as MWCNT and CF.

According to Kirkpatrick [15] , electrical conductivity of composites follows power law model of conductivity according to Eq. (3),

$$\sigma = \sigma_0 (\phi - \phi_c)^t \quad (2)$$

where, σ_0 is the conductivity of the filler (here, about 83.3 and 8.33 S cm^{-1} in the case of CF and MWCNT respectively), ϕ is the volume fraction of the filler, ϕ_c is the critical volume fraction and t is the universal exponent determining the power of the electrical conductivity increase above ϕ_c .

Plots of $(\log \sigma - \log \sigma_0)$ versus $\log(\phi - \phi_c)$ for the EOC/CF and EOC/MWCNT composites are shown in inset of Figure 4. Slope values of these plots give the value of t parameter. For MWCNT and CF filler composites, they were found to be 2.0 and 1.9 respectively. Vavouliotis et al. discussed that depending on the polymer matrix, the processing technology as well as the employed type of fillers critical exponents (t parameter) to vary from 1.3 to 3 [31].

Figure 5a-b shows the schematic representation of MWCNT and CF fillers below and above percolation threshold. MWCNT fillers are seen mostly curly and have smaller diameter and length compared to that of CF fillers. CF fillers are seen

rod-like and have larger dimensions. This enables them to have percolation at a lower volume percentage.

As we know, AC conductivity increases with increase in frequency according to Eq. (1). The reason for this is polarization of fixed dipoles, with the increase in frequency. AC conductivities of EOC/CF and EOC/MWCNT composites are depicted in Figures 6a-b. For composites with filler level above percolation threshold, lower frequency portion of the AC conductivity relates to the DC conductivity values which is called as DC plateau. This correlates well with DC conductivity values measured for the composites. Effect of frequency on the percolation jump is very clear from the Figure 6c. For EOC/MWCNT composites, up to 10 wt.% of MWCNT loading, conductivities were only around order of 10^{-9} S cm^{-1} . But when it reaches 15 wt.% loading, conductivity jumps six orders reaching around 10^{-3} S cm^{-1} (percolation behavior).

Dependences of real part of permittivity (ϵ' or dielectric constant) on frequency are illustrated in Figures 7a-b. Permittivity decreases with increase in frequency which can be ascribed to the interfacial polarization (IP). Composites are heterogeneous systems where fillers covered with the polymer matrix act as trapped charge carriers and there is a large difference between their dielectric constants [19]. Large local fields are created at the interface of these heterogeneous systems. This leads to an increase in the dielectric constant due to the motion of virtual charges [32]. Thus, permittivity becomes more frequency-sensitive and shows a sharp decrease with frequency. Effect of percolation threshold is visible in the case of permittivity also as in the case of conductivity, for both composites. Increase in permittivity with increase in filler level and decrease with increase in frequency are in the similar manner for both composites.

Thermal conductivities of CF and MWCNT composites are displayed in Figure 8. A regular increase in thermal conductivity can be observed in the case of both composites. From the thermal conductivity value of $0.196 \text{ Wm}^{-1}\text{K}^{-1}$ of pure EOC, CF-30% composite has significantly increased thermal conductivity to $0.808 \text{ Wm}^{-1}\text{K}^{-1}$ (312% increase). Maximum MWCNT content of 35 wt.% resulted in the increase of λ value to $0.409 \text{ Wm}^{-1}\text{K}^{-1}$ only (about 108% increase). Increase in the filler content increases the thermal conductivity as it happened in the case of electrical conductivity. However, higher values obtained for the CF-composites most likely are due to the higher diameter and total length of the CF filler when compared to that of MWCNT filler.

Mechanical properties of conducting composites are also very important when it comes to the matter of applications. Tensile stress-strain curves of both

composites are shown in Figures 9, 10 and 11. In both cases, tensile modulus increases with increasing filler loading. Stress at break initially increases and then decreases. MWCNT fillers have smaller length compared to CF and have also bend structure. CF fillers are longer than MWCNT fillers and also they may be aligned in the direction of applied tensile force. This is the reason why CF-composites show higher tensile modulus than MWCNT-composites. This can be better understood with the help of schematic diagram shows the filler shape and their distribution in Figure 5a-b. These observations point towards the role of CF and MWCNT fillers as reinforcement fillers while acting as conducting fillers also. This is an advantage that these composites could achieve improved conductivities without sacrificing mechanical properties.

Tensile properties of CF and MWCNT composites are graphically summarized in Figure 11 a-c, where dependences of tensile modulus, stress at break and elongation at break on filler content are shown. For example, there is a significant increase from 2 to 20 MPa for 30 wt. % CF. The values for MWCNT are a little bit lower than for CF. Even though, such large increase in modulus was found, the composites still remained soft and elastic (compare 20 MPa of this EOC/CF composite with hard polypropylene with modulus being around 1000 MPa). Stress at break and elongation at break exhibit similar trend. Initially with 2 wt. % of filler, there is an increase followed by steady decrease. The CF composites have higher values in both cases (stress at break and elongation at break). Very important result is elongation at break larger than 1000% for all CF composites and MWCNT composites up to 15 wt. %. Even though these composites are highly filled they did not become brittle.

Shore-A hardness of these composites was also measured. Even with higher filler levels (30 wt.% in the case of CF and 35 wt.% in the case MWCNT), shore-A hardness value did not increase excessively from the value of 49 which is corresponding to that of pure EOC (see Figure 12). It means that, these well conducting composites still possess the softness or rubbery nature which is a favorable property for the application as strain or pressure sensors.

Another important property is the thermal stability of CF and MWCNT composites. Other than pure EOC samples, only samples below and above the percolation threshold are compared here. TGA curves of the composites are illustrated in Figures 13a and b. The pure EOC shows the thermal stability up to about 266 °C, from where it starts to degrade and at about 420 °C it degrades completely. As it can be seen from the figures, onset temperatures of degradation are shifting to high temperatures as the filler level rises. For comparison, we have noted the temperature at which the 50% weight loss of the composite happens and

observed a gradual improvement. These results are summarized in Table 3. Pure EOC loses its 50% weight around at 385 °C. This point is at 405 °C and 414 °C for composites with 5 and 15 wt.% of CF filler, respectively. And for MWCNT composites with 10 wt.%, this point was at 419 °C and for 15 wt.% at 425 °C, correspondingly. MWCNT at a given concentration (15 wt.%), exhibit better thermal stability of composite compared to CF (425 vs. 414 °C). According to TGA, both CF and MWCNT survive up to 600 °C but EOC degrades completely at about 420 °C. CF or MWCNT fillers protect the matrix from degradation. Shielding efficiency of larger rod-like carbon fibres is comparatively lower than smaller MWCNT particles which have more surface area. MWCNT filler is more uniformly dispersed in the EOC matrix (see Figure 3f) and acts as a better shield than CF. This confirms the function of CF and MWCNT fillers as thermal stabilizers also. The residual weights even after the complete degradation of the matrix corresponds to that of the fillers which are not degraded even after 600 °C.

Altogether, CF-composites have shown properties superior to MWCNT-composites, except of hardness and thermal stability. The summary is given in Table 4.

4. Conclusions

Composites of ethylene-octene copolymer with two conducting fillers, carbon fiber and multiwall carbon nanotubes were prepared and their electrical and thermal conductivities and mechanical properties were studied. Composites with CF filler were found to be electrically and thermally more conductive than the MWCNT ones, due to their higher diameter and fiber length. Increase in filler content and frequency resulted in an increased AC conductivity of the composites. As frequency increases, dielectric constant (real part of permittivity) of composites was found to be decreasing due to the interfacial polarization effect. Excellent improvement in thermal conductivity (more than 300%) was observed in the case CF-composite while there was only a gradual increment in the case of MWCNT-composite (100% increase). A considerable increase in tensile modulus of composites has been observed with increase in filler content. Another favorable property which could be noted is the hardness. Even with higher filler loading levels, shore-A hardness values did not increase excessively which shows that these composites still possess good elastomeric nature which could be potentially utilized when they are being considered for applications like pressure/strain sensors. Thermal stability of both composites has been significantly improved by the addition of conducting fillers. All of these observations are pointing towards the role of CF and MWCNT fillers as multifaceted fillers, not mere conducting ones.

Acknowledgements

This work has been supported by the Operational Programme Research and Development for Innovations co-funded by the European Regional Development Fund (ERDF) and national budget of Czech Republic within the framework of the Centre of Polymer Systems project (reg.number: CZ.1.05/2.1.00/03.0111)

References

- [1] Drobny JG. Handbook of Thermoplastic Elastomers. New York: William Andrew Inc; 2007.
- [2] Bensason S, Minick J, Moet A, Chum S, Hiltner A, Baer E. Classification of homogeneous ethylene-octene copolymers based on comonomer content. *J Polym Sci Pol Phys* 1996; 34(7):1301-15.
- [3] Bhatt CU, Royer JR, Hwang CR, Khan SA. Compressive stress relaxation of metallocene-based polyolefin foams: Effect of gamma-ray-induced crosslinking. *J Polym Sci Pol Phys* 1999; 37(11):1045-56.
- [4] Koyama T, Endo M. Structure and growth process of vapor-grown carbon fibers. *Oyo Butsuri* 1973; 42(7):690-6.
- [5] Iijima S. Helical microtubules of graphitic carbon. *Nature* 1991; 354(6348):56-58.
- [6] Faez R, Schuster RH, De Paoli MA. A conductive elastomer based on EPDM and polyaniline. II. Effect of the crosslinking method. *Eur Polym J* 2002; 38(12):2459-63.
- [7] Souza FG, Orlando MTD, Michel RC, Pinto JC, Cosme T, Oliveira GE. Effect of Pressure on the Structure and Electrical Conductivity of Cardanol-Furfural-Polyaniline Blends. *J Appl Polym Sci* 2011; 119(5):2666-73.
- [8] Hwang J, Jang J, Hong K, Kim KN, Han JH, Shin K, et al. Poly(3-hexylthiophene) wrapped carbon nanotube/poly(dimethylsiloxane) composites for use in finger-sensing piezoresistive pressure sensors. *Carbon* 2011; 49(1):106-10.
- [9] Pham GT, Park YB, Liang Z, Zhang C, Wang B. Processing and modeling of conductive thermoplastic/carbon nanotube films for strain sensing. *Compos Part B-Eng* 2008; 39(1):209-16.
- [10] Sibinski M, Jakubowska M, Sloma M. Flexible Temperature Sensors on Fibers. *Sensors* 2010; 10(9):7934-46.
- [11] Slobodian P, Riha P, Lengalova A, Svoboda P, Saha P. Multi-wall carbon nanotube networks as potential resistive gas sensors for organic vapor detection. *Carbon* 2011; 49(7):2499-507.

- [12] Li C, Thostenson ET, Chou TW. Sensors and actuators based on carbon nanotubes and their composites: A review. *Compos Sci Technol* 2008; 68(6):1227-49.
- [13] Landi BJ, Castro SL, Ruf HJ, Evans CM, Bailey SG, Raffaella RP. CdSe quantum dot-single wall carbon nanotube complexes for polymeric solar cells. *Sol Energ Mat Sol C* 2005; 87(1-4):733-46.
- [14] Bhattacharya SK. *Metal-Filled Polymers: Properties and Applications*. New York: Marcel Dekker; 1986.
- [15] Kirkpatrick S. Percolation and conduction. *Rev Mod Phys* 1973; 45(4):574-88.
- [16] Vilcakova J, Saha P, Quadrat O. Electrical conductivity of carbon fibres/polyester resin composites in the percolation threshold region. *Eur Polym J* 2002; 38(12):2343-47.
- [17] Bauhofer W, Kovacs JZ. A review and analysis of electrical percolation in carbon nanotube polymer composites. *Compos Sci Technol* 2009; 69(10):1486-98.
- [18] Chang L, Friedrich K, Ye L, Toro P. Evaluation and visualization of the percolating networks in multi-wall carbon nanotube/epoxy composites. *J Mater Sci* 2009; 44(15):4003-12.
- [19] Hammami H, Arous M, Lagache M, Kallel A. Study of the interfacial MWS relaxation by dielectric spectroscopy in unidirectional PZT fibres/epoxy resin composites. *J Alloy Compd* 2007; 430(1-2):1-8.
- [20] Bhadra S, Singha NK, Khastgir D. Dielectric properties and EMI shielding efficiency of polyaniline and ethylene 1-octene based semi-conducting composites. *Curr Appl Phys* 2009; 9(2):396-403.
- [21] Hom S, Bhattacharyya AR, Khare RA, Kulkarni AR, Saroop M, Biswas A. Blends of Polypropylene and Ethylene Octene Comonomer with Conducting Fillers: Influence of State of Dispersion of Conducting Fillers on Electrical Conductivity. *Polym Eng Sci* 2009; 49(8):1502-10.
- [22] Flandin L, Chang A, Nazarenko S, Hiltner A, Baer E. Effect of strain on the properties of an ethylene-octene elastomer with conductive carbon fillers. *J Appl Polym Sci* 2000; 76(6):894-905.

- [23] Palza H, Kappes M, Hennrich F, Wilhelm M. Morphological changes of carbon nanotubes in polyethylene matrices under oscillatory tests as determined by dielectrical measurements. *Compos Sci Technol* 2011; 71(10):1361-66.
- [24] Le HH, Kolesov I, Ali Z, Uthardt M, Osazuwa O, Ilisch S, et al. Effect of filler dispersion degree on the Joule heating stimulated recovery behaviour of nanocomposites. *J Mater Sci* 2010; 45(21):5851-9.
- [25] Van der Pauw LJ. A method of measuring specific resistivity and Hall effect of discs of arbitrary shape. *Philips Res Rep* 1958; 13(1):1-9.
- [26] Jr. FGdS, Soares BG, Pinto JC. Electrical surface resistivity of conductive polymers – A non-Gaussian approach for determination of confidence intervals. *Eur Polym J* 2008; 44(11):3908-14.
- [27] Lozano JE. *Fruit Manufacturing: Scientific Basis, Engineering Properties, and Deteriorative Reactions of Technological Importance*. New York: Springer.
- [28] Svoboda P, Theravalappil R, Poongavalappil S, Vilcakova J, Svobodova D, Mokrejs P, et al. A Study on Electrical and Thermal Conductivities of Ethylene–Octene Copolymer/Expandable Graphite Composites. *Polym Eng Sci* 2011; DOI:10.1002/pen.22192.
- [29] Strumpler R, Glatz-Reichenbach J. Conducting polymer composites. *J Electroceram* 1999; 3(4):329-46.
- [30] Scher H, Zallen R. Critical density in percolation processes. *J Chem Phys* 1970; 53(9):3759-61.
- [31] Vavouliotis A, Fiamegou E, Karapappas P, Psarras GC, Kostopoulos V. DC and AC Conductivity in Epoxy Resin/Multiwall Carbon Nanotubes Percolative System. *Polym Composite* 2010;31(11):1874-1880.
- [32] Kremer F, Schonhals A. *Broadband dielectric spectroscopy*. Berlin Heidelberg: Springer-Verlag; 2003.

Figure Captions

Fig. 1 - Experimental set-up for the thermal conductivity measurement.

Fig. 2 - Raw data of thermal conductivity measurement.

Fig. 3 - TEM and SEM of fillers and composites.

a) SEM of CF filler, b) 5 wt.% CF composite, c) 20 wt.% CF composite, d) TEM of MWCNT filler, e) SEM of 10 wt.% MWCNT composite and f) SEM of 25 wt.% MWCNT composite.

Fig. 4 - DC conductivity of EOC/MWCNT and EOC/CF composites.

Fig. 5 - Schematic diagram showing size and distribution of CF and MWCNT fillers in composites.

Fig. 6 - AC conductivity of (a) EOC/CF, (b) EOC/MWCNT composites and (c) frequency dependence of composites on AC conductivity.

Fig. 7 - Frequency dependence of real part of permittivity of (a) EOC/CF and (b) EOC/MWCNT composites.

Fig. 8 - Thermal conductivity of EOC/CF and EOC/MWCNT composites.

Fig 9 - Tensile stress-strain curves of EOC/CF composites.

Fig. 10 - Tensile stress-strain curves of EOC/MWCNT composites.

Fig. 11 - Influence of filler content on (a) Tensile modulus, (b) stress at break and (c) elongation at break of EOC/CF and EOC/MWCNT composites.

Fig. 12 - Shore-A hardness of the composites.

Fig. 13 - Thermogravimetric analysis of (a) EOC/CF and (b) EOC/MWCNT composites.

List of Tables

Table 1 - Properties of MWCNT and CF fillers.

Table 2 - Content (wt. and vol.) % of fillers along with DC conductivity values of MWCNT and CF fillers in the composites.

Table 3 - Thermogravimetric analysis of EOC and its composites.

Table 4 - Overall comparison of properties of EOC composites.

Table 1. Properties of MWCNT and CF fillers.

Property	MWCNT	CF
Diameter (nm)	15±6	150
Length (µm)	3	10
Aspect ratio	200	67
Density (g cm ⁻³)	1.7	2.0
Electrical resistivity (Ω cm)	0.12	0.012
Electrical conductivity (S cm ⁻¹)	8.33	83.3

Table 2. Content (wt. and vol.) % of fillers along with DC conductivity values of MWCNT and CF fillers in the composites.

MWCNT			CF		
wt.%	vol.%	DC Conductivity (S cm⁻¹)	wt.%	vol.%	DC Conductivity (S cm⁻¹)
2	1	(3.16 ± 0.91).10 ⁻⁹	2	1	(3.48 ± 0.85).10 ⁻⁹
5	3	(3.25 ± 0.83).10 ⁻⁹	5	2	(3.54 ± 0.81).10 ⁻⁹
10	6	(4.08 ± 0.76).10 ⁻⁹	10	5	(7.54 ± 0.44).10 ⁻⁶
15	8	(4.61 ± 0.30).10 ⁻³	15	7	(1.46 ± 0.24).10 ⁻²
20	12	(6.32 ± 0.22).10 ⁻³	20	10	(3.13 ± 0.19).10 ⁻²
25	15	(1.34 ± 0.24).10 ⁻²	25	13	(1.60 ± 0.21).10 ⁻¹
30	18	(2.53 ± 0.18).10 ⁻²	30	16	(4.28 ± 0.14).10 ⁻¹
35	22	(8.62 ± 0.15).10 ⁻²			

Table 3. Thermogravimetric analysis of EOC and its composites

Sample	T _{Onset} (°C)	T _{50%} (°C)
EOC	266	385
EOC/5% CF	283	405
EOC/15% CF	295	414
EOC/10% MWCNT	309	419
EOC/15% MWCNT	331	425

Table 4. Overall comparison of properties of EOC composites

Property	Unit	wt. % of filler	EOC/CF	EOC/ MWCNT	Remarks
DC conductivity	S cm ⁻¹	25	1.60 x 10 ⁻¹	1.34 x 10 ⁻²	CF better
Percolation threshold	vol. %		3	5	
Thermal conductivity	Wm ⁻¹ K ⁻¹	25	0.60	0.37	
Tensile modulus	MPa	15	11.1	7.9	
Stress at break	MPa	15	12.6	9.1	
Elongation at break	%	15	1870	1261	
Shore-A hardness	-	30	77	75	Almost the same
Thermal Stability (onset)	°C	15	295	331	MWCNT better
Thermal stability (50% wt. loss)	°C	15	414	425	

Figures

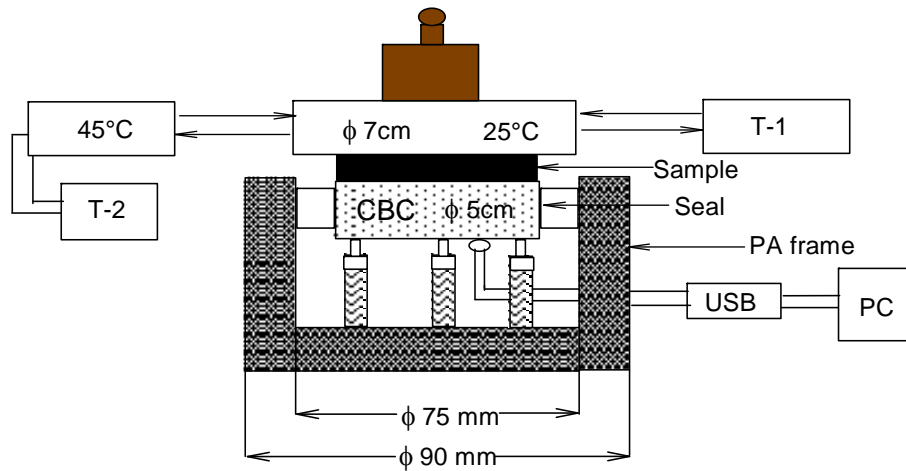


Fig. 1 - Experimental set-up for the thermal conductivity measurement.

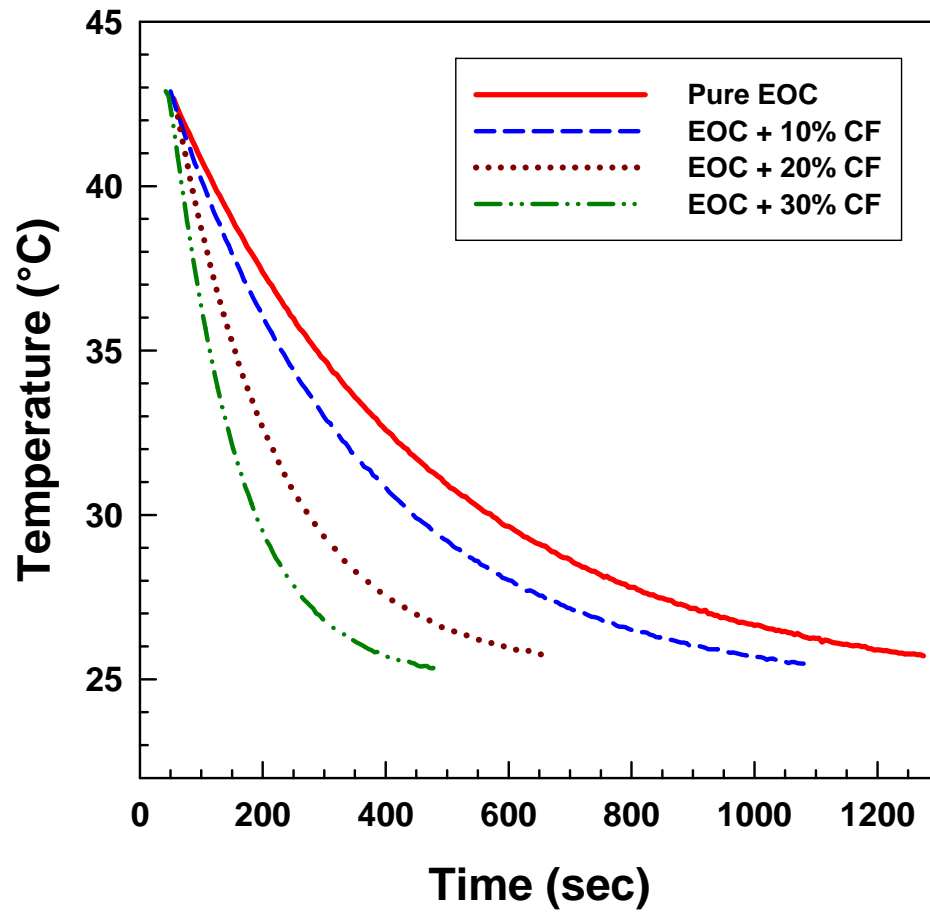


Fig. 2 - Raw data of thermal conductivity measurement.

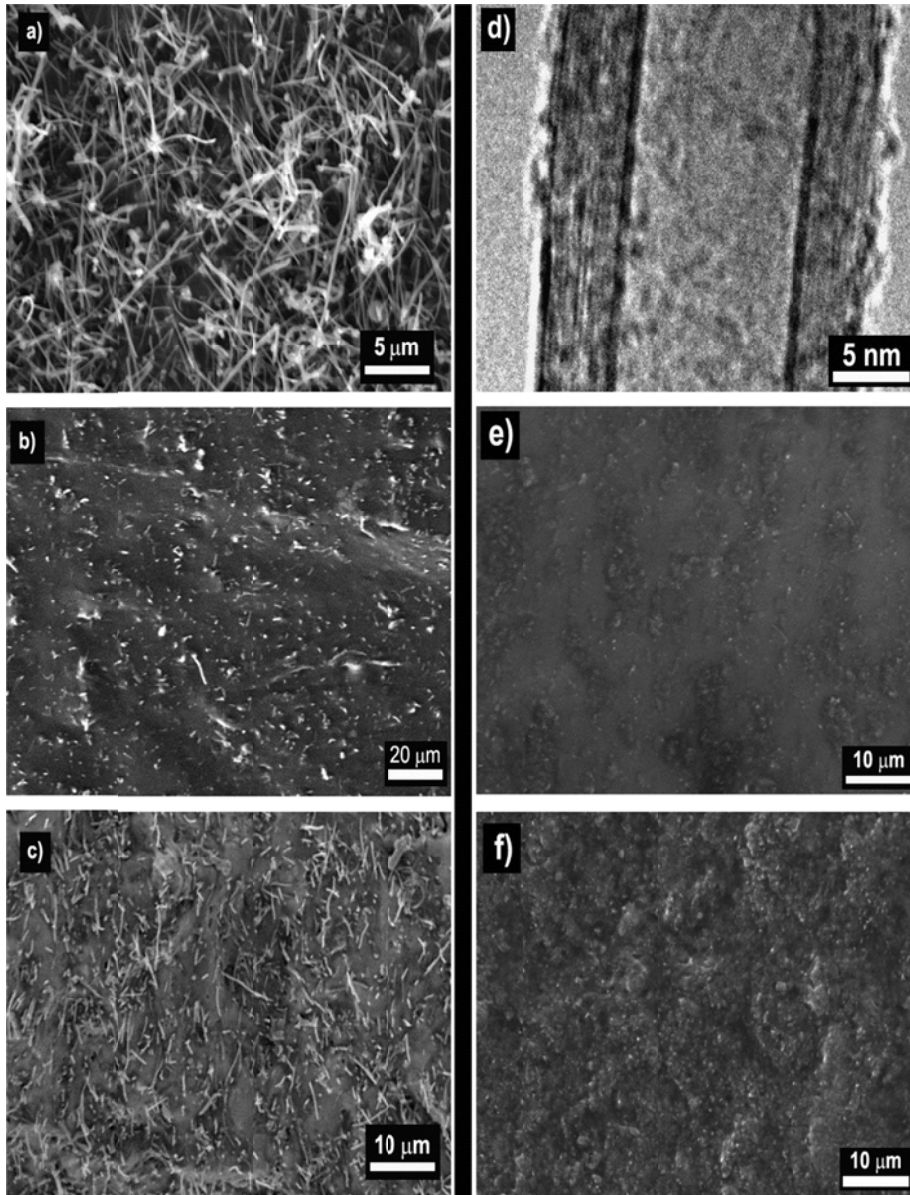


Fig. 3 - TEM and SEM of fillers and composites.

b) SEM of CF filler, b) 5 wt.% CF composite, c) 20 wt.% CF composite, d) TEM of MWCNT filler, e) SEM of 10 wt.% MWCNT composite and f) SEM of 25 wt.% MWCNT composite.

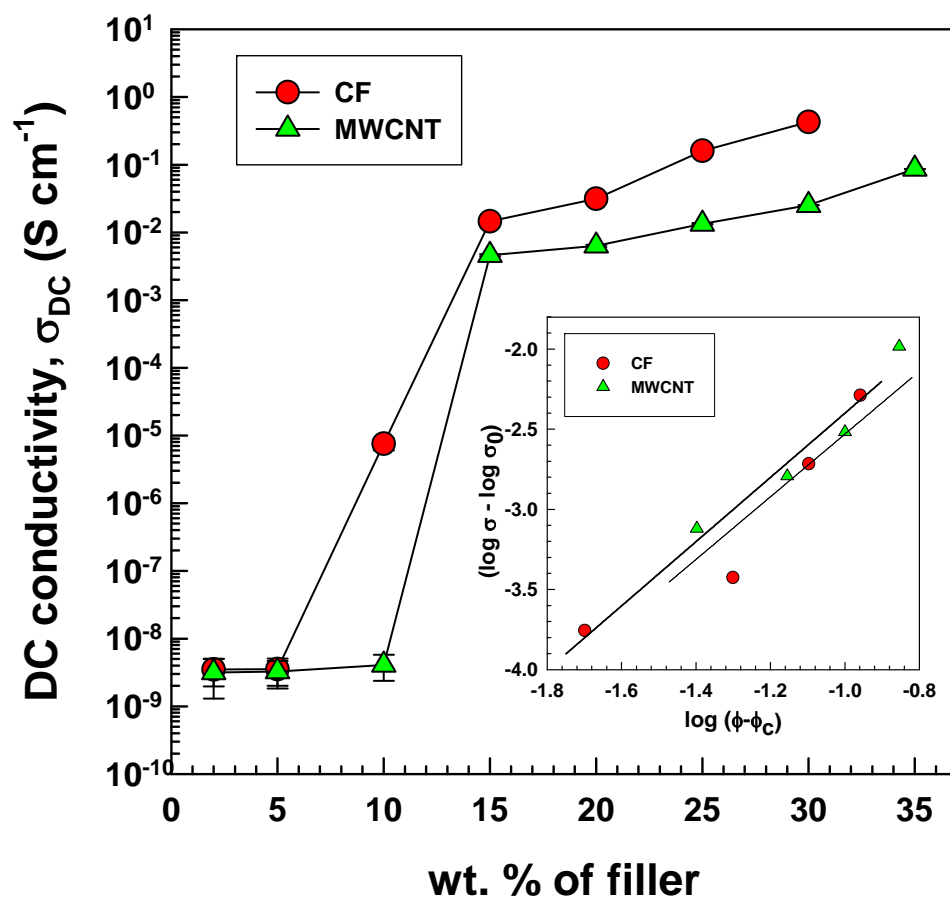


Fig. 4 - DC conductivity of EOC/MWCNT and EOC/CF composites.

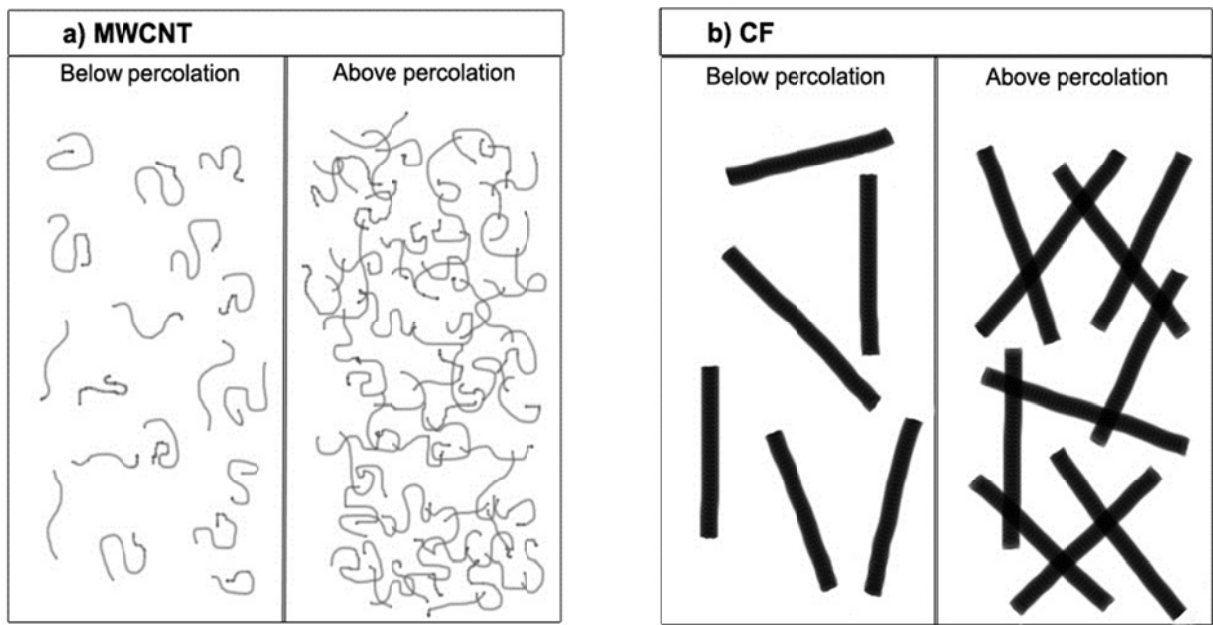


Fig. 5 - Schematic diagram showing size and distribution of MWCNT and CF fillers in composites.

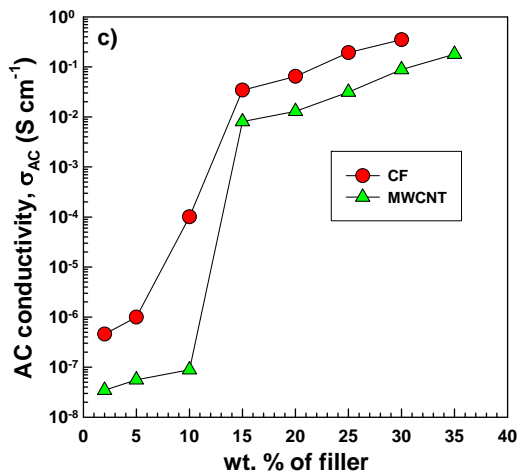
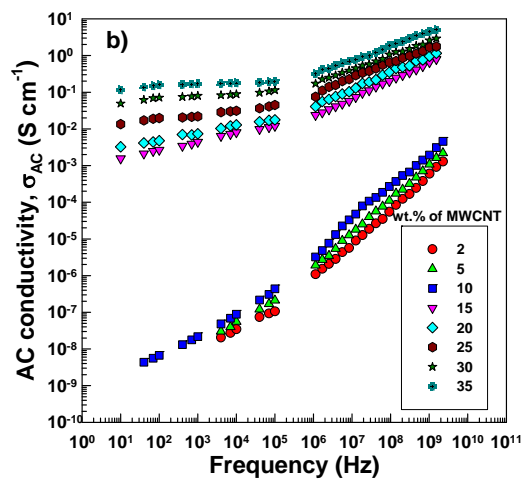
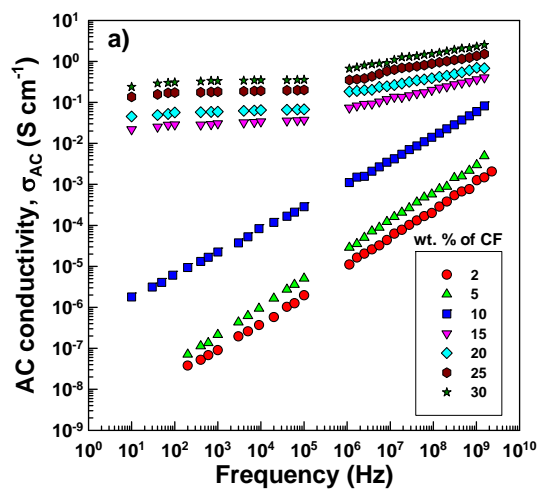


Fig. 6 - AC conductivity of (a) EOC/CF, (b) EOC/MWCNT composites and (c) AC conductivities at a frequency of 10^4 Hz.

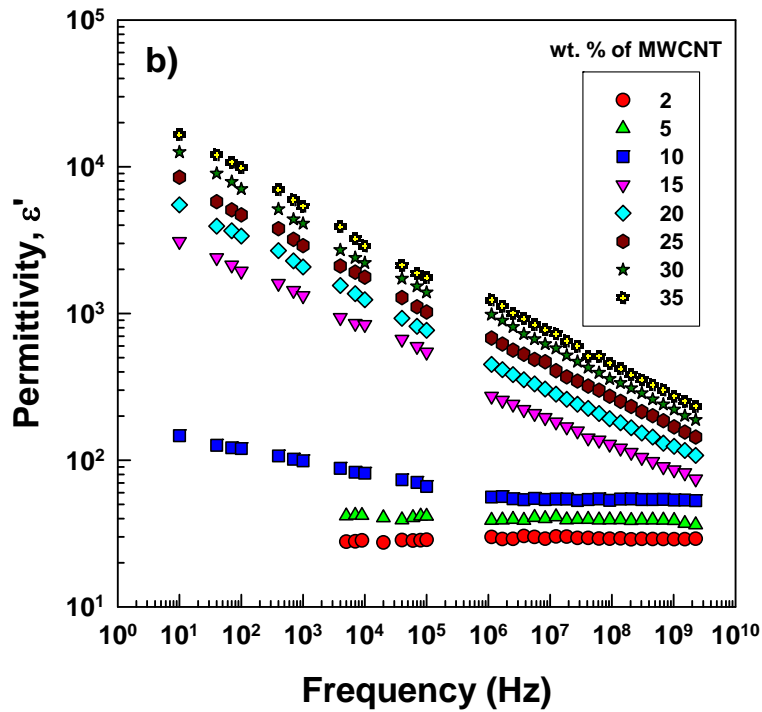
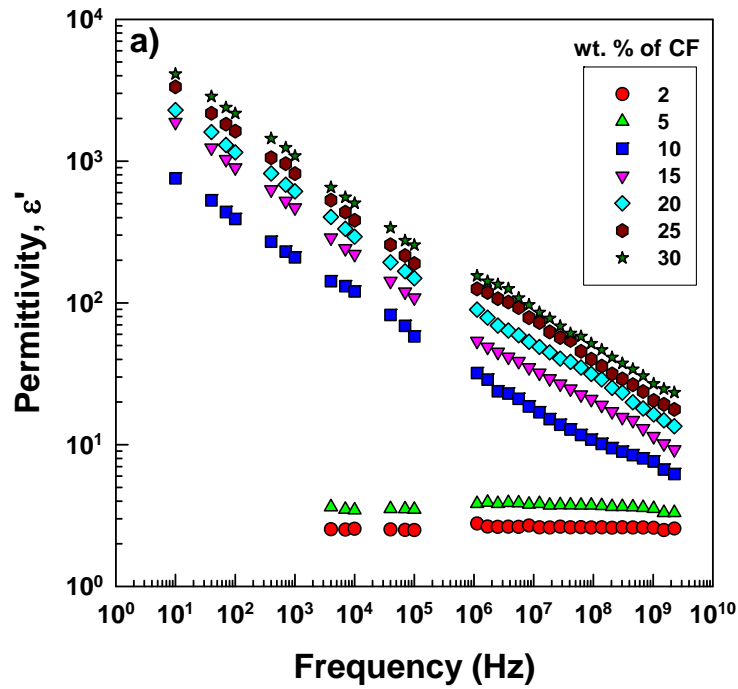


Fig. 7 - Frequency dependence of real part of permittivity of (a) EOC/CF and (b) EOC/MWCNT composites.

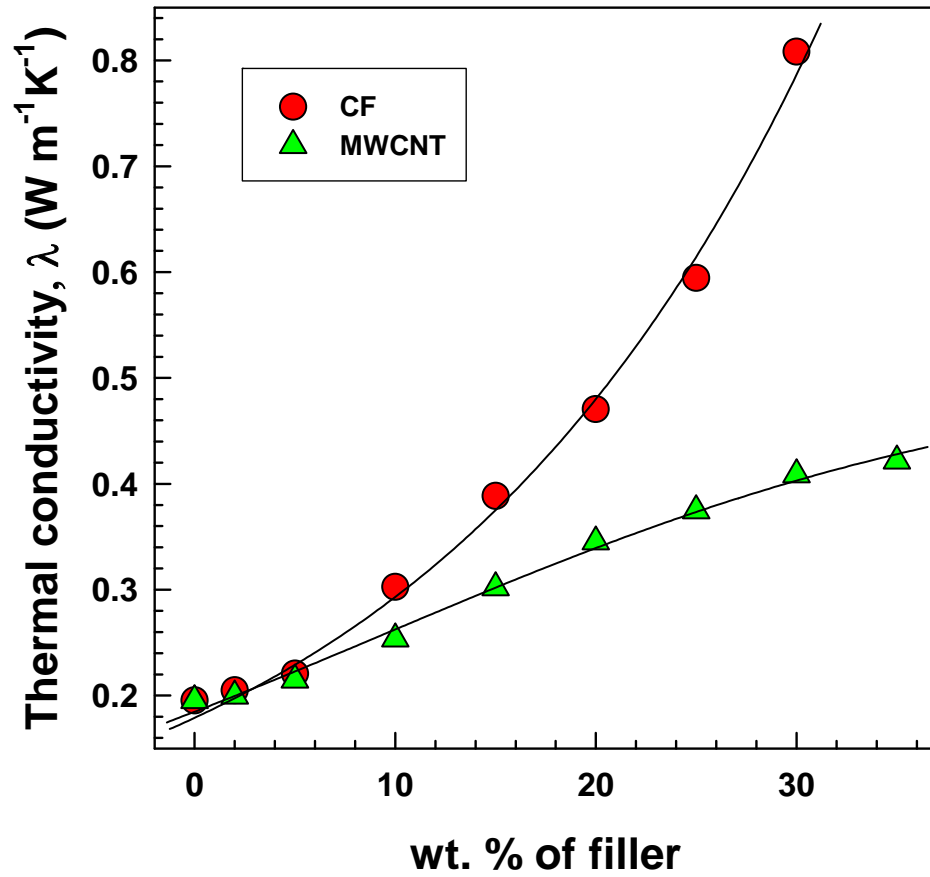


Fig. 8 - Thermal conductivities of EOC/CF and EOC/MWCNT composites.

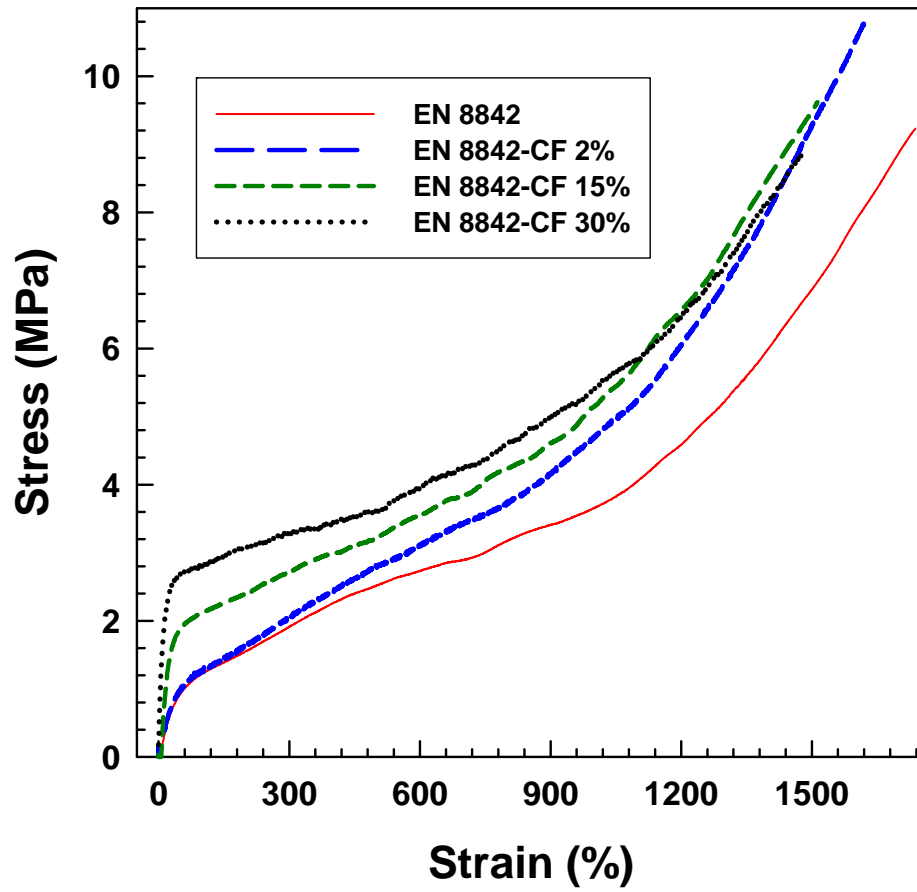


Fig. 9 - Tensile stress-strain curves of EOC/CF composites.

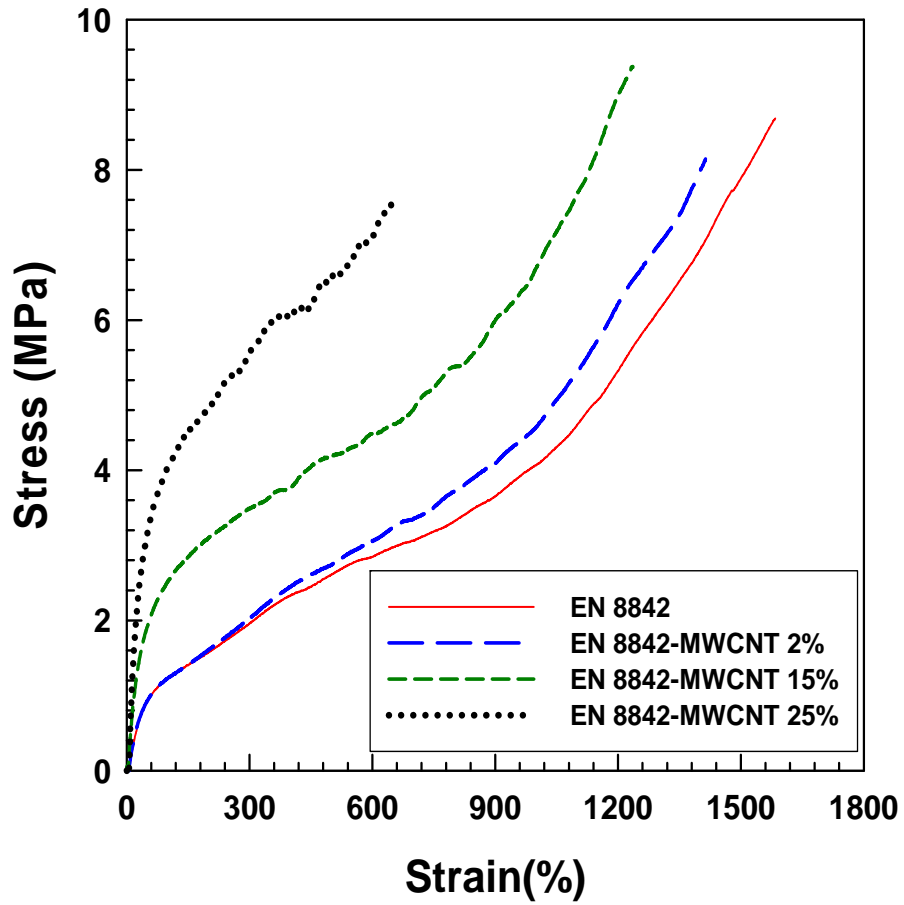


Fig. 10 - Tensile stress-strain curves of EOC/MWCNT composites.

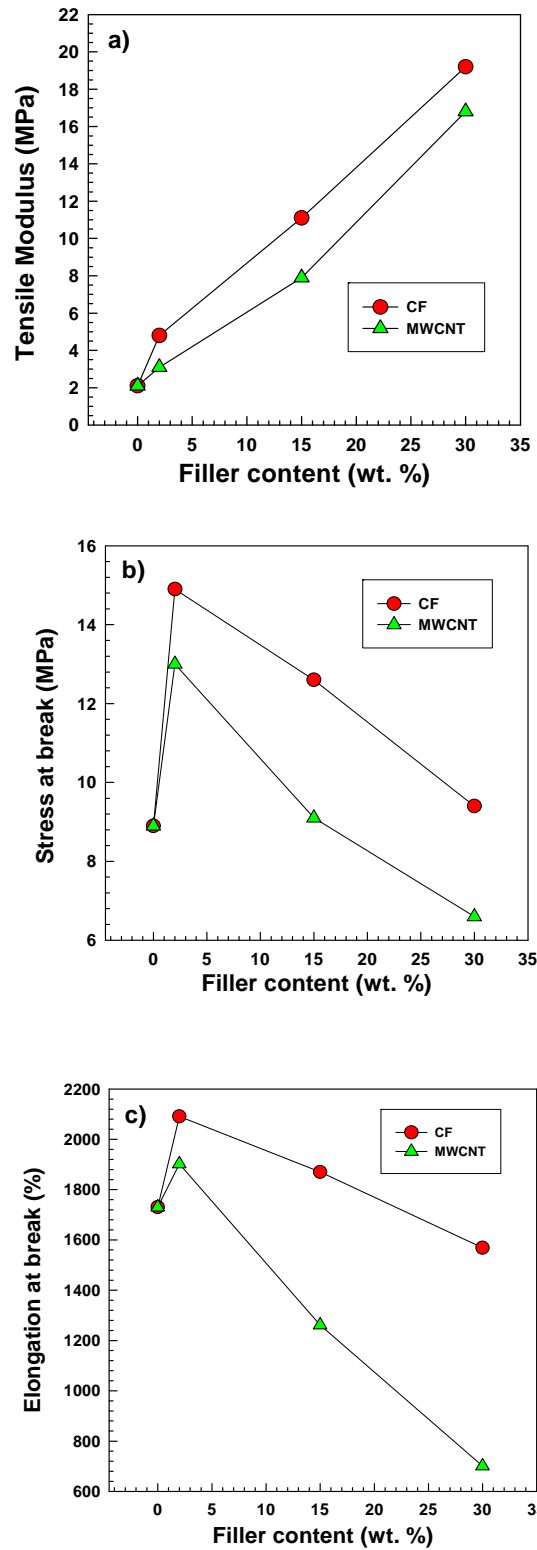


Fig. 11 - Influence of filler content on (a) tensile modulus, (b) stress at break and (c) elongation at break of EOC/CF and EOC/MWCNT composites.

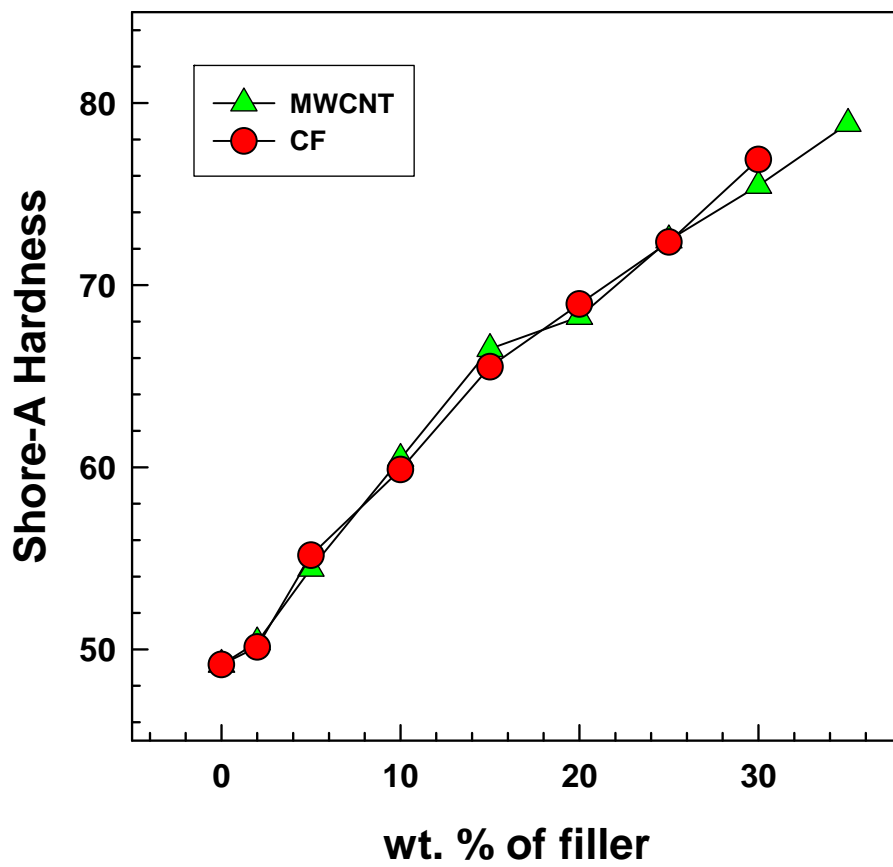


Fig.12 - Shore-A hardness of EOC/CF and EOC/MWCNT composites.

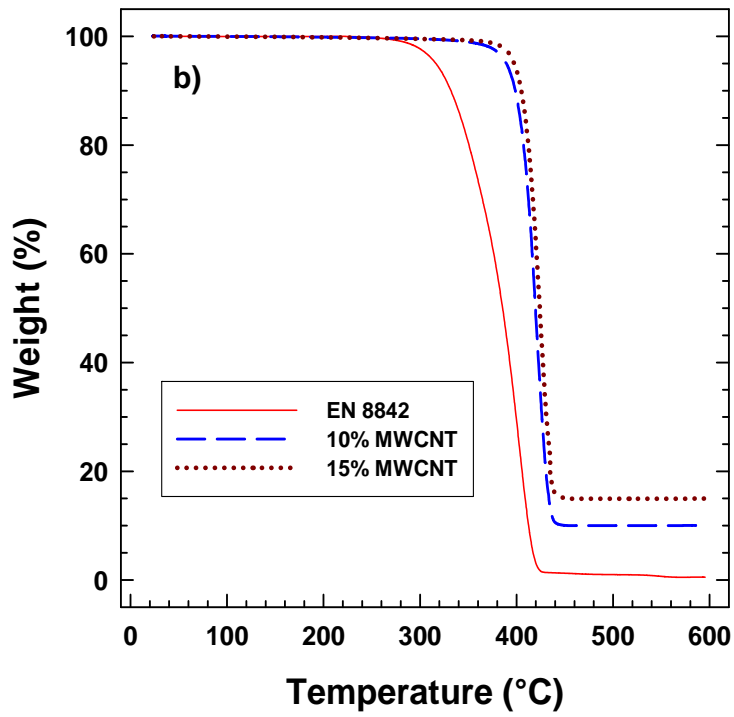
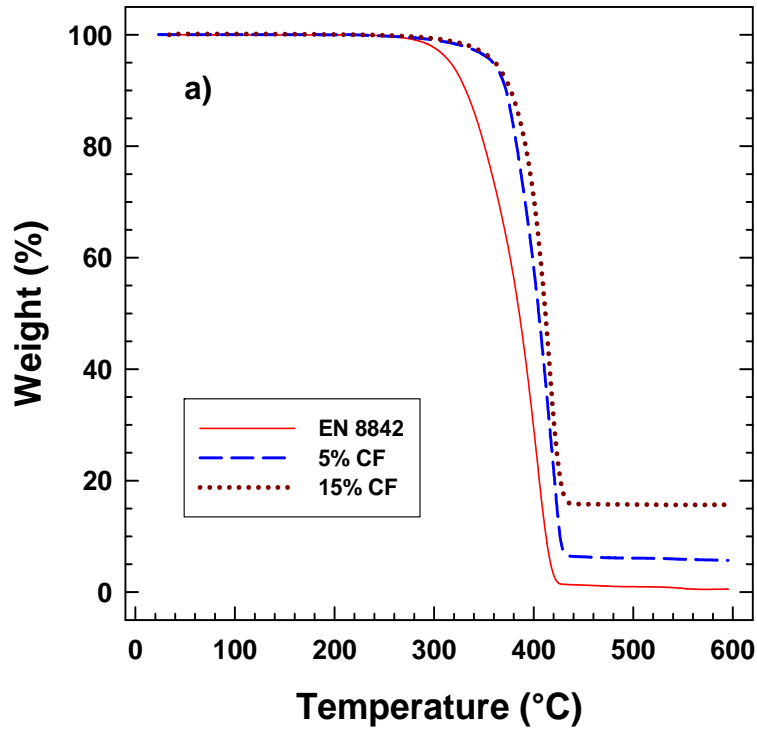


Fig. 13 - Thermogravimetric analysis of (a) EOC/CF and (b) EOC/MWCNT composites.

CURRICULUM VITAE

Personal information:

First name/ surname : Rajesh Theravalappil
Date of Birth : 26.03.1981
Nationality : Indian
Address : Theravalappil, Chalakod (PO), Payyanur (Via)
Kannur (Dt), Kerala, 670307 (PIN), India.
Email : tvrajpol@yahoo.co.in

Education

- 2008- Present, **Ph.D.** - Chemistry and Materials Technology, Department of Polymer Engineering, Faculty of Technology, Tomas Bata University in Zlin, Czech Republic.
- 2001 - 2003, Master of Science, **M.Sc.** (Polymer Science), Mysore University, Karnataka, India.
- 1998 - 2001, Bachelor of Science, **B.Sc.** (Polymer Chemistry), Kannur University, Kerala, India.

Work experience

- 2006 November - 2008 October, **Assistant Engineer**, Enercon India Ltd. (Indian Associate of Enercon GmbH, Germany), Daman, India.
- 2004 October - 2006 October, **Junior Research Fellow**, Department of Polymer Engineering, Amrita VishwaVidyapeetham, Coimbatore, India.
- 2004 May - October, **Technical Assistant**, Central Institute of Plastics Engineering and Technology (CIPET) India, under Ministry of Chemicals and Fertilisers, Mysore, India.

Achievements

- First Rank in M. Sc. (Polymer Science) Examination of Mysore University in 2003.

Publications:

Thesis

- **Rajesh. T.V.** Studies on Polycarbonate toughened Novolac type phenol-formaldehyde resin/glassfibre laminates (*M.Sc. thesis*) carried out at National Aerospace Laboratories, Bangalore, India (2003).

Journal (International)

1. **Rajesh Theravalappil**, Petr Svoboda, Sameepa Poongavalappil and Dagmar Svobodova, Creep and dynamic mechanical analysis studies of peroxide cross-linked ethylene-octene copolymer (accepted for publication in *Macromolecular Materials and Engineering*). DOI: 10.1002/mame.201100289.
2. Petr Svoboda, **Rajesh Theravalappil**, Sameepa Poongavalappil, Jarmila Vilcakova, Dagmar Svobodova, Pavel Mokrejs, Antonin Blaha, A study on electrical and thermal conductivities of ethylene-octene copolymer/expandable graphite composites (accepted for publication in *Polymer Engineering & Science*). DOI 10.1002/pen.22192.
3. Sameepa Poongavalappil, Petr Svoboda, **Rajesh Theravalappil**, Dagmar Svobodova, Vladimir Vasek, Kittisak Jantanasakulwong, Toshiaki Ougizawa, Cross-linking kinetics study and high temperature mechanical properties of ethylene-octene copolymer (EOC)/dicumyl peroxide (DCP) system, *European Polymer Journal*, Volume 47 (10), 2011, 1949-1955.
4. Petr Svoboda, Sameepa Poongavalappil, **Rajesh Theravalappil**, Dagmar Svobodova, Pavel Mokrejs, Karel Kolomaznik, Toshiaki Ougizawa, Takashi Inoue, Cross-linking of ethylene-octene copolymer (EOC) by dicumyl peroxide (DCP). *Journal of Applied Polymer Science*, Volume 121 (1), 2011, 521-530.
5. Petr Svoboda, **Rajesh Theravalappil**, Dagmar Svobodova, Pavel Mokrejs, Karel Kolomaznik, Keisuke Mori, Toshiaki Ougizawa and Takashi Inoue, Elastic properties of polypropylene/ethylene-octene copolymer blends, *Polymer Testing*, 2010, vol. 29 (6), 742-748, DOI: 10.1016/j.polymertesting.2010.05.014.

6. **Rajesh Theravalappil**, Petr Svoboda, Sameepa Poongavalappil, Jarmila Vilcakova, Dagmar Svobodova, Petr Slobodian, Robert Olejnik, Simona Mrkvickova; Multiple roles of multiwall carbon nanotubes (MWCNT) and carbon fibers (CF) in their composites with ethylene-octene copolymer (submitted to *Carbon* in January 2012).
7. Sameepa Poongavalappil, Petr Svoboda, **Rajesh Theravalappil**, Dagmar Svobodova, Tomas sedlacek; Comparison of peroxide cross-linked ethylene-octene copolymers (submitted to *Polymer Bulletin*).
8. Sameepa Poongavalappil, Petr Svoboda, **Rajesh Theravalappil**, Dagmar Svobodova, Michal Danek, Martin Zatloukal; Study on the influence of electron beam irradiation on the thermal, mechanical and rheological properties of ethylene-octene copolymer with high comonomer content (submitted to *European Polymer Journal*).

Conference contributions

- i. **Rajesh Theravalappil**, Petr Svoboda, Sameepa Poongavalappil, High temperature mechanical properties of peroxide cross-linked ethylene-octene copolymer, ANTEC 2011, May 1-5, 2011, Boston, USA (Oral presentation).
- ii. **Rajesh Theravalappil**, Petr Svoboda, Sameepa Poongavalappil, Jarmila Vilcakova. Electrical, thermal and flame properties of ethylene-octene copolymer/expandable graphite composites, ANTEC 2011, May 1-5, 2011, Boston, USA (Poster presentation).
- iii. Sameepa Poongavalappil, **Rajesh Theravalappil**, Petr Svoboda, Cross-linking Kinetics Study in Ethylene-Octene Copolymer (EOC)/Dicumyl Peroxide (DCP) System, ANTEC 2011, May 1-5, 2011, Boston, USA (Poster presentation).
- iv. Petr Svoboda, **Rajesh Theravalappil**, Keisuke Mori, Toshiaki Ougizawa, Elastic properties of polypropylene/ethylene-octene copolymer blends, 10th European Symposium on Polymer Blends, March 7-10, 2010, Dresden, Germany.
- v. **T.V. Rajesh**, K.S. Rai and R.M.V.G.K. Rao, Polycarbonate modified novalac resin/glass fibre composites, Macro '05, April 15-16, 2005, SJ College of Engineering, Mysore, India.